LBL-13185

Lawrence Berkeley Laboratory
UNIVERSITY OF CALIFORNIA

EARTH SCIENCES DIVISION

ESTIMATION OF IN-SITU THERMAL CONDUCTIVITIES FROM TEMPERATURE GRADIENT MEASUREMENTS

Viet Thai Hoang
(Ph.D. thesis)

December 1980

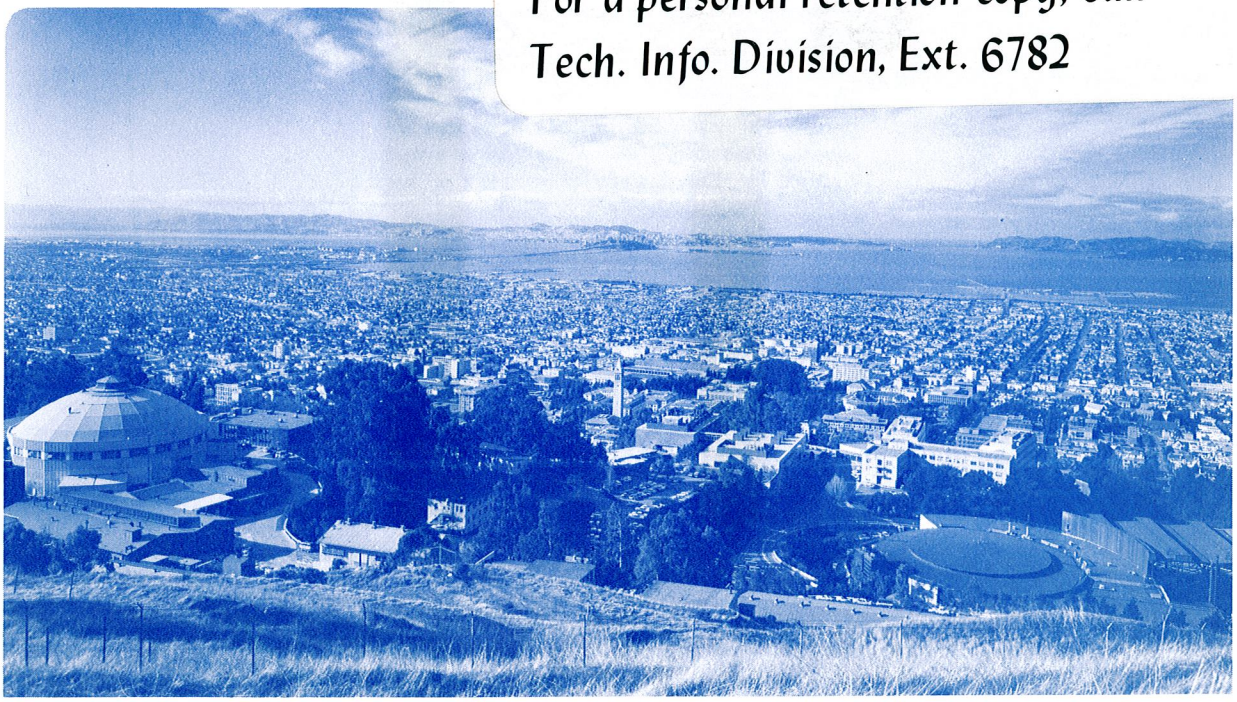

Prepared for the U.S. Department of Energy under Contract W-7405-ENG-48

LBL-13185

ESTIMATION OF IN-SITU THERMAL CONDUCTIVITIES FROM TEMPERATURE GRADIENT MEASUREMENTS

Viet Thai Hoang

Ph.D. Thesis

Earth Science Division
Lawrence Berkeley Laboratory
and
College of Engineering
University of California
Berkeley, CA 94720

This work was supported by the Office of Energy Research, Office of Basic Energy Sciences, Division of Engineering, Mathematics, and Geosciences of the U.S. Department of Energy under Contract No. W-7405-ENG-48; and by the Jane Lewis Fellowship Committee.

To my Mother and my Father.

ACKNOWLEDGEMENT

In completion of this work I have received much assistance from others during the course of this investigation.

I wish to express my deepest gratitude to all my friends and colleagues who helped and encouraged me in every difficult moment throughout my study.

I would like to thank my advisor, Professor W. Somerton, for his help and support. Thanks are also due to Dr. J. Wang and Professor G. Brimhall, my dissertation committee members, as well as Dr. C. Miller of Lawrence Berkeley Laboratory for their valuable suggestions and remarks.

I want to thank Dave White, a good friend, for his help with the laboratory work and for many constructive conversations together.

Finally I wish to acknowledge the Jane Lewis Fellowship committee for their support of this work. Additional support was provided by the Department of Energy through Lawrence Berkeley Laboratory, and the Office of Energy Research, Office of Basic Energy Sciences, Division of Engineering, Mathematics, and Geosciences of the U.S. Department of Energy under Contract No. W-7405-ENG-48.

TABLE OF CONTENTS

LIST OF TABLES

LIST OF FIGURES

ESTIMATION OF IN SITU THERMAL CONDUCTIVITIES
FROM TEMPERATURE GRADIENT MEASUREMENTS

Ph.D. Viet Thai Hoang Mechanical Engineering

[redacted]

Prof. W.H. Somerton
Chairman of Committee

ABSTRACT

A mathematical model has been developed to study the effect of variable thermal conductivity of the formations, and the wellbore characteristics, on the fluid temperature behavior inside the wellbore during injection or production and after shut-in. During the injection or production period the wellbore fluid temperature is controlled mainly by the fluid flow rate and the heat lost from the fluid to the formation. During the shut-in period, the fluid temperature is strongly affected by differences in the formation thermal conductivities. This effect is very apparent after as little as four hours of shut-in. When the well is shut-in for a longer period of time, the fluid temperature gradients approach the geothermal gradients and changes in these temperature gradients with depth is inversely proportional to changes in the formation thermal conductivities.

Based on the results of the present analysis, two methods for estimating in-situ thermal conductivity were derived. First, the line source concept is extended to estimate values of the formation thermal conductivities utilizing the fluid temperature record during the transient

period of injection or production and shut-in. The second method is applied when a well is under thermal equilibrium conditions. Values of the formation thermal conductivities can also be estimated by using a continuous temperature gradient log and by measuring the thermal conductivity of the formation at a few selected wellbore locations.

From the results of this study, in-situ values of thermal conductivity can be estimated from temperature measurements in wells. Although laboratory methods can measure thermal conductivities with accuracy as high as one per-cent, it can only represent the value of an individual specimen. A method for measuring conductivitiew in-situ which is accurate to within 5 to 10 per-cent would be more useful for many purposes than the high precision laboratory values. Values of in-situ thermal conductivity can be useful for the determination of terrestrial heat flows in the earth , heat losses from the wellbore in thermal recovery processes, and in differentiating oil-bearing or gas-bearing formations from water bearing formations. They may also be useful in the estimation of other physical properties such as type of formation, its porosity, as well as its fluid content.

CHAPTER I

INTRODUCTION

In recent years considerable interest has been generated in thermal processes of petroleum recovery, especially hot fluid injection. These processes involve the injection of heat into a reservoir in the form of steam or hot water. Every production and injection operation is accompanied by the transfer of heat between wellbore fluids and the formation around the wellbore. The resultant heat losses between the surface and the injection interval could be very important in the success or failure of these processes.

Knowledge of the subsurface thermal properties is of importance not only in the thermal recovery process but also in geothermal operations and in geophysical applications. Knowledge of thermal conductivity is an important parameter in the detection and development of geothermal fields. In the recovery of geothermal energy, the rate at which heat can be extracted from a hot reservoir is proportional to $\lambda_f/\sqrt{\alpha_f}$ where λ_f is the formation thermal conductivity, and α_f is the formation thermal diffusivity (Murphy, et al. [51]). The amount of heat flowing through the surface of the earth from the interior is a quantity which is of fundamental importance for geophysics. To determine the terrestrial heat flow in any area the temperature gradient ($\partial T/\partial z$) and the thermal conductivity (λ) of rocks in that area must be measured.

There are many methods for the determination of thermal conductivity broadly classified as laboratory methods or in-situ methods. Although laboratory methods are generally more accurate, the problem is essentially one of sampling. In many cases there are no cores available for laboratory measurements. In some instances, measurements on samples from the surface of nearby cored holes provide a reasonable estimate of conductivity. For the most part, however, conductivity variations within a given type of rock are of such magnitude that measurements should be made in the same hole as that in which temperatures are measured. Even when cores are available, the determination of thermal conductivity is not straightforward. The most common problems, reviewed by Beck, et al., [10] are:

(1) Friable rocks: Laboratory determinations of conductivity involve a considerable degree of machining and polishing. The specimens that survive this process are invariably the most competent and, usually, the most highly conducting. The bias so introduced can result in serious systematic errors.

(2) Specimen size: Another type of systematic error can result when the specimen size is not large relative to the average size of the individual crystals (Beck and Beck, [8]).

(3) Heterogeneity: On a regional scale, a core drill sample is a very narrow vertical column of rock. Variations in the relative abundances of such components as micas

and pyrite minerals can result in large conductivity variations within a single lithology unit. In contrast to (1) and (2) above, these variations will tend to produce random rather than systematic errors.

(4) Removal of the rock from its environment: It is difficult, if not impossible, to produce in the laboratory the physical conditions which exist at great depth within the earth. Moreover, with certain rocks, the process of coring and specimen preparation may produce irreversible changes in thermal conductivity as well as in other physical properties.

Some of the above problems can be minimized by using non-standard laboratory techniques, such as chips, and/or careful petrographic studies. In many cases, however, the only satisfactory solution entails the measurement of thermal conductivity in-situ. Since its introduction by Van Der Held and Van Drumen [70], use of the line source, or "probe", method of measuring thermal conductivity has become popular for low conductivity materials. However, many practical problems associated with making measurements with a heated probe can occur, such as thermal contact resistance, natural convection in the fluid induced by the heated probe, etc. This method will be discussed in detail later in this study.

In most of the studies dealing with heat flow and thermal gradients in wells, a linear geothermal gradient profile has been assumed. This assumption corresponds

to a constant thermal conductivity of the earth. However, in actual well temperature measurements there are variations in the temperature profile. This effect is most likely due to the differences in thermal conductivities in different formations of the earth or with different fluid saturations. The geothermal gradient is caused by the continuous flow of heat from the interior of the earth. The magnitude of the gradient depends upon the difference in the temperature between the surface and the heat source in the interior of the earth and upon the thermal conductivities of the materials in between. For a uniform heat flux, variations in thermal conductivities will result in variations in the temperature gradients.

In this study, based on the above concepts, a theoretical analysis of fluid temperature gradients in the wellbore, as well as temperature gradients in the surrounding formations during injection and production and after shut-in, will be made to evaluate the effects of thermal conductivities of the formation on such gradients. These results will be used to estimate the in-situ thermal conductivities of the formation.

CHAPTER II

LITERATURE REVIEW

When a temperature gradient exists in a body there is an energy transfer from the high temperature region to the low temperature region in accordance with the second law of thermodynamics. The heat transfer rate per unit area, q, is given by the empirical relation known as Fourier's equation of heat conduction,

$$q = - \lambda \text{ grad } T \quad . \qquad (2.1)$$

The positive constant of proportionality between the heat flux and the temperature gradient is called thermal conductivity and is denoted by λ.

Thermal Conductivities of Porous Rocks

Thermal conductivity of a porous material is a complex function of density, porosity, grain size and shape, cementation and mineral composition. If it is saturated with fluid, its thermal conductivity is also dependent upon the conductivities of the saturating fluid and the rock material (Somerton, [64]). In the following, the effect of constituents, porosity, and saturating fluid on thermal conductivity of rocks will be discussed.

(1) Effect of Constituents: Mineral composition affects the thermal conductivity of rocks because of different conductivity values of individual minerals, orientation of crystal axes and influence of impurities in solid solution (Anand, [2]). The major constituent of mineral

sandstone is quartz for which a fairly large number of thermal conductivity measurements have been made. Kersten [43] found that the thermal conductivity is lowest for basic minerals, increases for intermediate minerals and is highest for felsic minerals. As such, quartz has one of the highest conductivities. On the other hand, coal is among the materials which has very low conductivity. A list of thermal conductivity of materials usually found in subsurface reservoirs is presented in Tables 1, 2 and 3.

(2) Effect of porosity: From the statistical thermodynamics point of view, thermal conductivity for dielectrics is directly proportional to density as follows (Tien, et al., [68]):

$$\lambda = 1/3\ pc_v \bar{c} l \qquad (2.2)$$

where: pc_v = phonon heat capacity,

$\bar{c}$ = phonon velocity,

l = phonon mean free path.

The density of porous material is related to porosity as follows:

$$\rho = \rho_f \phi + (1.0 - \phi)\rho_s \qquad (2.3)$$

where: ρ = density of porous material,

ρ_s = density of the solid matrix,

ρ_f = density of the fluid in the pores,

ϕ = fractional porosity.

Since ϕ and ρ are directly related it can be said that λ is related to the porosity ϕ of the material, the conductivities of the solid matrix and the fluid in the pores

TABLE 1

Thermal Conductivities of Some Rocks-forming Minerals at T=23°C (Horai [36]).

Mineral	Chemical Composition	Thermal Conductivity ($W/m^{o}K$)
Quartz	SiO_2	7.70
Plagioclase	$NaAl_2Si_3O_8$-$CaAlSi_3O_8$	2.15
Orthoclase	$KAl_2Si_3O_8$	2.30
Muscovite	$(K,Na)A_{12}(OH)_2(AlSi_3O_{10})$	2.20
Calcite	$CaCO_3$	3.60
Chlorite	$(Mg,Fe,Al)_6(OH)_8((Al,Si)_4O_{10})$	4.34
Biotite	$K,(Mg,Fe)_3(OH)_2(Al,Si_3O_{10})$	2.34
Hornblende	$NaCa_2(Mg,Fe,Al)_5(OH)_2(SiAl_8O_{22})$	3.10
Magnesite	$MgCO_3$	5.85
Sphene	$CaSiTiO_5$	2.34

TABLE 2

Thermal Conductivity of Some Reservoir Rocks.

Rock Type	Density (g/cm^3)	Thermal Conductivity (W/m^oK)		Source No.
		Mean	Range	
Dolomite	2.70	4.99	3.72-5.82	17
Limestone	2.56	2.56	1.97-2.97	17
Gnieiss		3.49	2.55-3.35	17
Shale		1.76	1.34-2.34	17
Sandstone		4.12	2.39-5.86	17
Clay	1.47	0.91		17
Coal	1.05	0.24		17
Chert	2.56	4.53		36
Slate	2.76	1.99		36
Mud	1.31	0.79		17

TABLE 3

Thermal Conductivity of Some Saturant Fluids

Fluid	Thermal Conductivity (W/m^oK)	Source No.
Light oil	0.15	2
Water	0.55	2
Air	0.33	17

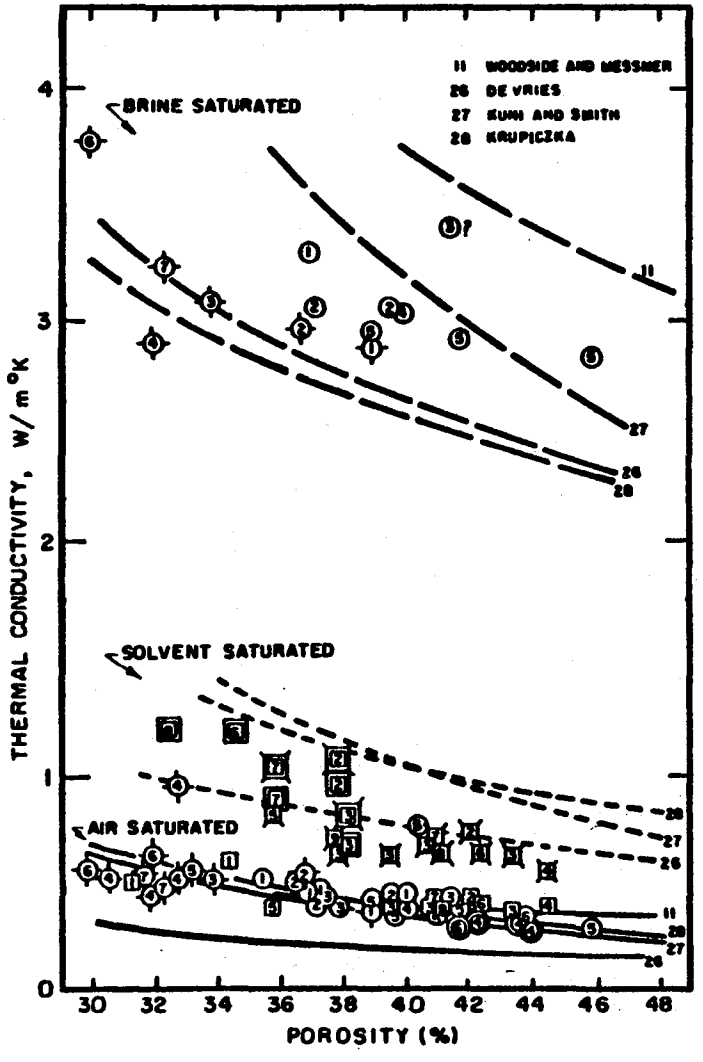

KEY TO FIGURE 1

Quartz Sands - Uniform Grain Size

	D_{50}
○ Ottawa	
①	.0239 inches
②	.0182 "
③	.0145 "
④	.0097 "
⑤	.0060 "
⑥	.0029 "
● Del Monte	

Quartz Sands - Mixed Grain Size

	D_{50}	D_{90}/D_{10}
①	.0167 inches	.677
②	.0070 "	.292
③	.0075 "	.244
④	.0077 "	.136
⑤	.0078 "	.097
⑥	.0175 "	.136
⑦	.0039 "	.136

Oil Sands

□ air saturated ▣ solvent saturated

■ containing original fluids ▣ solvent added

	Source	D_{50}	D_{90}/D_{10}
[1]	Kern River	.0231 inches	.063
[2]	Kern River	.0285 "	.097
[3]	Huntington Beach	.0082 "	.161
[4]	Midway Sunset	.0079 "	.185
[5]	Bradley Canyon	.0072 "	.100
[6]	Midway Sunset	.0070 "	.076
[7]	Bradley Canyon	.0064 "	.192
[8]	Bradley Canyon	.0057 "	.103
[9]	Bradley Canyon	.0052 "	.103

FIG. 1 THERMAL CONDUCTIVITY OF UNCONSOLIDATED SANDS
(From Somerton et al., [63])

XBL 818-3482

(Anand, [2]). Since the density of the fluid which occupies the pore spaces is less than the solid density, generally the thermal conductivity is reduced with increased porosity, Figure 1. Quantitatively, how much less the thermal conductivity of a porous material will be than the solid matrix will depend upon the amount of void spaces, the arrangement of voids, the fluid with which the voids are filled, etc.

(3) Effect of Saturating Fluid: Fairly limited amount of work has dealt with the prediction of thermal conductivity of liquid saturated rocks and has not yielded satisfactory results. The difficulty seems to lie in the fact that although liquid saturated rocks have higher conductivities than dry rocks, the amount of increase is a complex function of the amount of pore space, its character and distribution, and the conductivity of the saturating fluid (Somerton, [63]). Many measurements indicated that thermal conductivities of brine saturated samples are higher than dry samples. This is due to the fact that the thermal conductivity of water (0.59 w/m°K at 21°C) is higher than that of silicon oil (0.28w/m°K at 21°C) which in turn is higher than that of dry air (0.026w/m°K at 21°C) (Anand, [2], Figure 2).

Saturation of the wetting phase fluid has a dominant effect on the thermal conductivity of the system. The study of partially liquid saturated rocks by Somerton [64] showed that for brine-air saturation, thermal conductivity is related to the square root of brine saturation. For uncon-

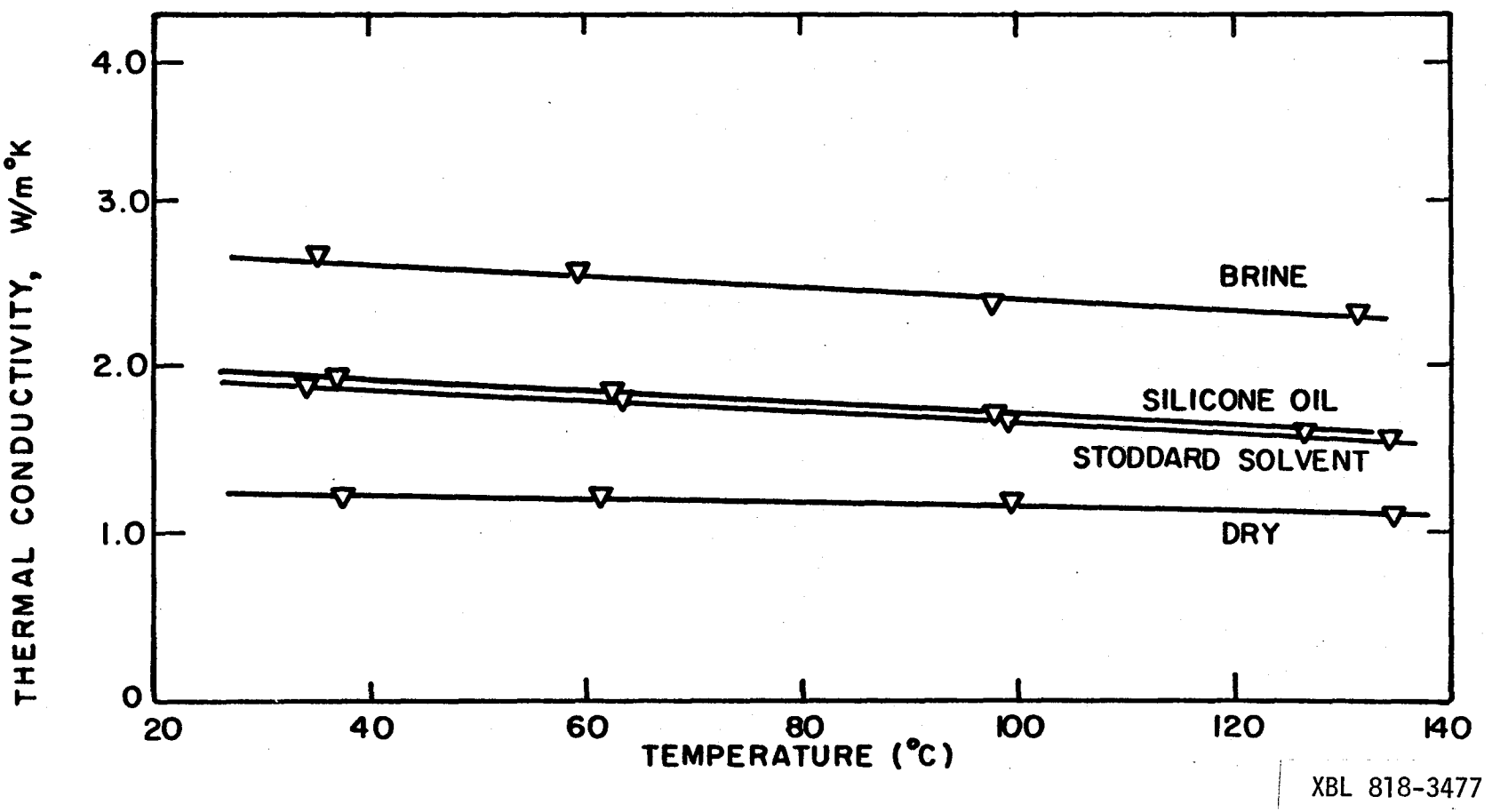

FIG. 2 THERMAL CONDUCTIVITY OF BOISE SANDSTONE
(From Anand, [2])

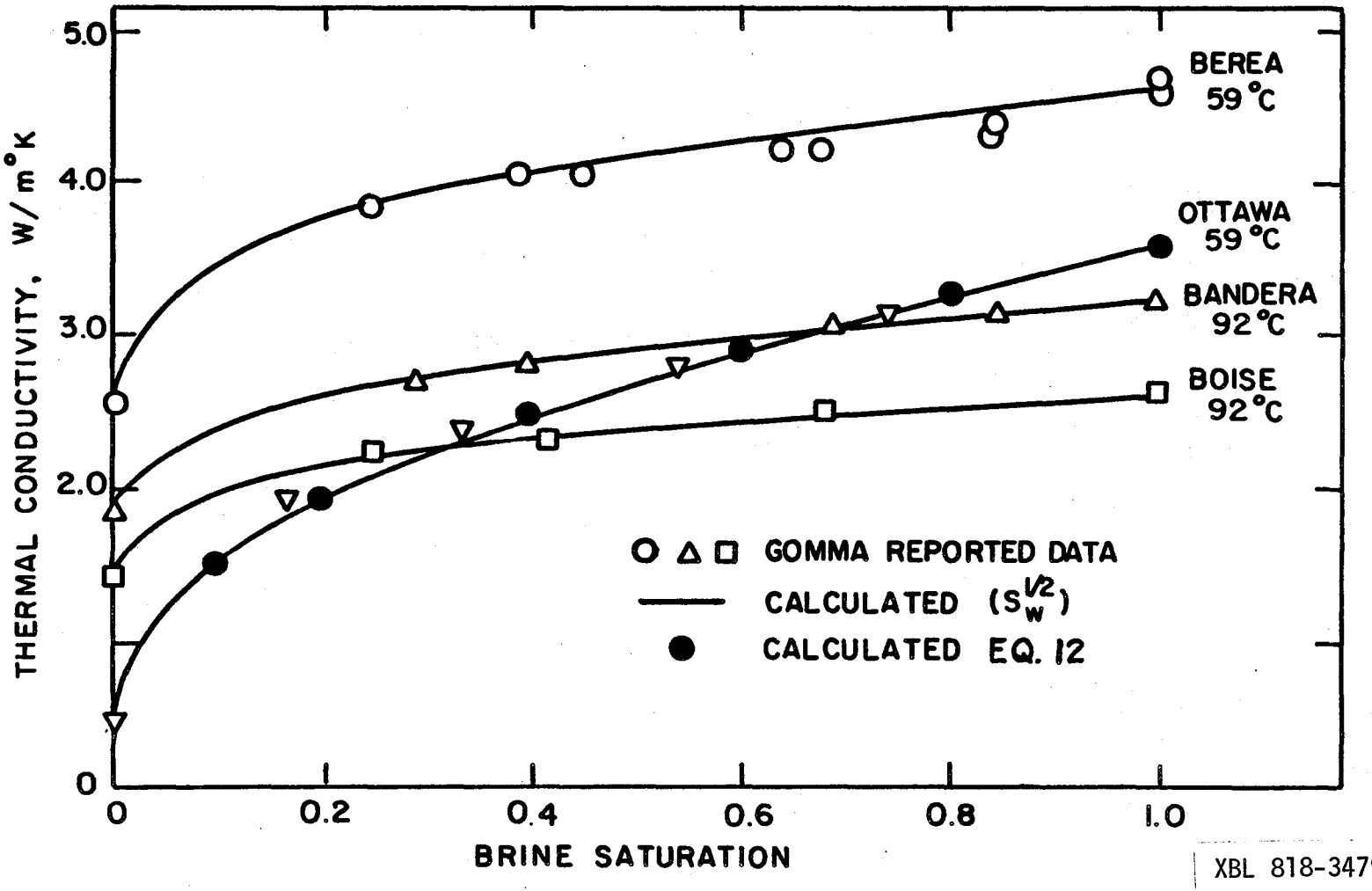

FIG. 3 THERMAL CONDUCTIVITY OF BRINE-AIR SATURATED SAMPLES
(From Somerton et al., [64])

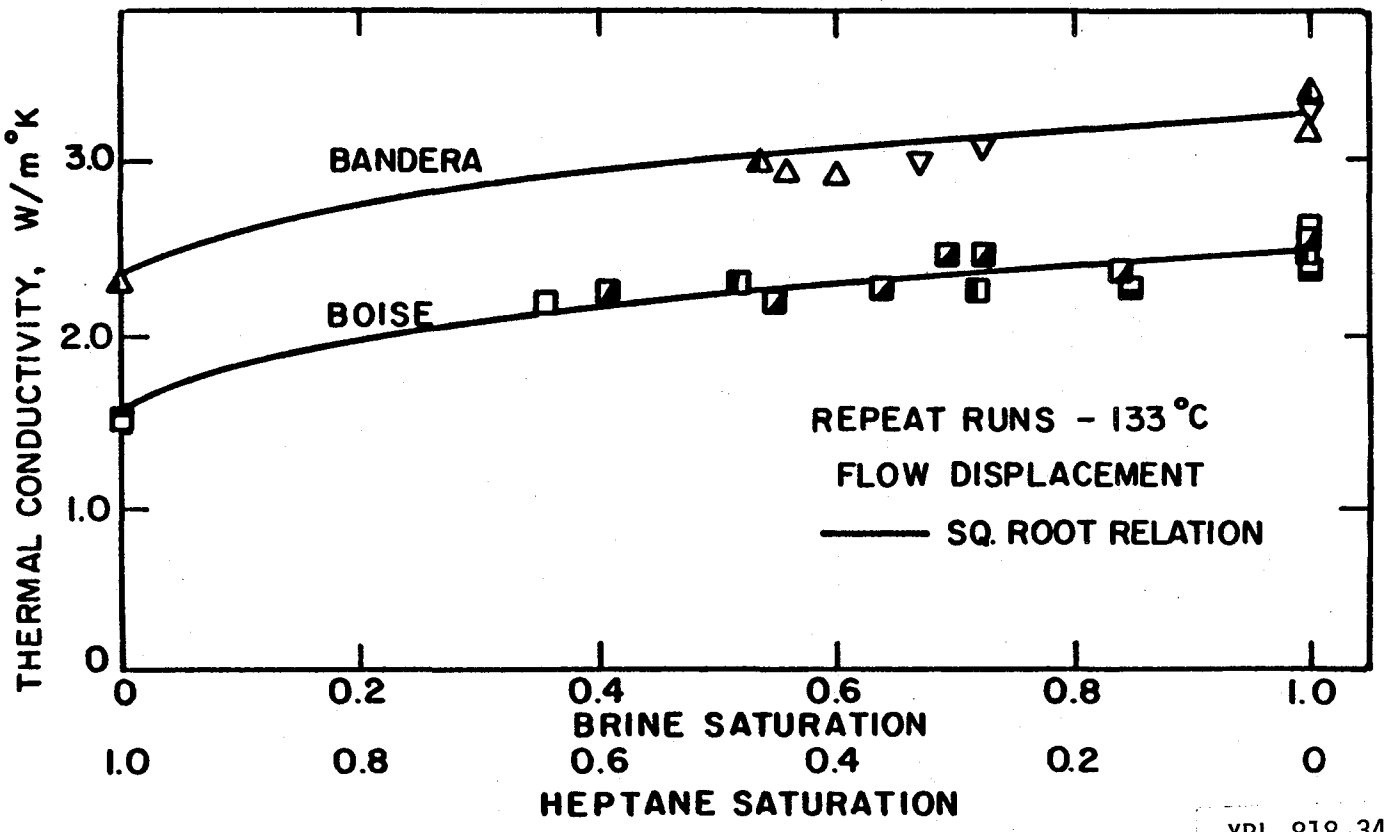

XBL 818-3476

FIG. 4 BRINE-HEPTANE SATURATION
BANDERA AND BOISE
(From Somerton et al., [64])

solidated sands saturated with air and brine and all samples tested which were saturated with two liquids, showed a relationship with square root of the wetting phase saturation (Figures 3 and 4).

Measurement of Thermal Conductivities

Because of the complexity of laboratory measurements, it is very difficult to obtain accurate thermal conductivity values, and in many circumstances laboratory methods for measuring thermal conductivity are unsatisfactory. In-situ thermal conductivity measurement has received a great deal of attention in petroleum technology, geothermal, and geophysics fields because of its important role. Some of the previous works on this subject will be reviewed in detail.

Most of the previous studies involving the determination of in-situ thermal conductivity were conducted in the geophysics field through the measurements of heat flow on land and at sea. To determine the terrestrial heat flow in any area, the temperature gradient ($\partial T/\partial z$) and the thermal conductivity (λ) of rocks in that area must be measured.

1) Probe Measuring Methods

The probe method is commonly chosen for the in-situ thermal conductivity measurements. This method involves the use of an electrically heated cylindrical probe which, to insure radial heat flow conditions at the central plane normal to its axis, has a length 20 to 30 times the diameter

of the hole into which it is inserted (Blackwell [12]). Seals at each end of the probe prevent convection losses up and down the hole (Beck, et al., [7]). A temperature sensitive element is located on the outer surface and at the mid-point of the probe. When the probe is in place and has reached the equilibrium temperature of the borehole at that location, the current is switched on and a record is made of the temperature rise versus time.

The idealized model is a perfect thermal conductor of radius, a, with constant heat supply Q per unit length per unit time immersed in a material of conductivity λ and there is assummed to be no thermal resistance at the contact surfaces. If there is thermal resistance at the surface, modifications in the theory have to be made. This problem is discussed by Carslaw and Jaeger [16]. Theory of the probe method has been given by Blackwell [11], Jaeger [38] and De Vries and Peck [23] and it was reviewed extensively by Beck [5].

The data obtained by the probe test can be reduced by one of three methods. The first is the method commonly used for all probe types of probe measurements. It consists of plotting the natural logarithm of the time, t, versus the temperature, T, and finding the slope of the logarithm asymptote. The thermal conductivity, λ, can be found from the equation:

$$T(t) = (Q/4\pi\lambda)\ \ln(t) + B0\ (1/t)\ , \qquad (2.4)$$

where B is a constant, and the terms $0(1/t)$ are negligible

for long times. The time to reach the asymptotic section of the curve depends on the radius of the borehole involved, the thermal constants of the rocks surrounding the hole, and the thermal contact resistance of the fluid layer between the probe and wall of the borehole.

The second method of interpreting probe test results (Blackwell, [11]) involves the determination of the thermal contact resistance by the use of an approximate solution to the transient radial heat flow equation for short time. The value obtained is then used in another approximation to the equation for long times. This is equivalent to straightening the curve obtained by the first method somewhat earlier than would otherwise be the case, and theoretically makes it possible to use shorter experimental times.

The third method (Jaeger, [38]; Beck, et al., [7]) uses the exact solution of the transient radial heat flow equation and involves calculating families of theoretical curves using values of the appropriate constants which cover the range of values likely to be found in geophysical work. The experimental curve of temperature rise versus time is plotted on log-log paper and compared with the families of theoretical curves plotted on the same bases. From the best fit it is theoretically possible to find, from the displacement of the origin, both the thermal conductivity and the diffusivity of rocks. This method requires a shorter experimental time than any other method.

Beck [5] has pointed out that the practical problems associated with making measurements with a heated probe in a deep borehole are formidable. Optimum probe lengths should be 20 to 30 times the bore diameter so that a typical geothermal well, or oil well, would require a probe about 3 to 4 meters long. To obtain temperature rises of the order of several degrees per hour in such a large probe requires a substantial amount of electrical power transmitted downhole. The applied potential would have to be high to obtain the required power leading to insulation difficulties which are aggravated by the high temperatures in wells. Furthermore, since it is impossible to assure uniformly good contact between the probe and the borehole wall, additional heating times are required. It is difficult to systematically correct for these errors since natural convection of this fluid may be induced by heating the probe (Murphy, et al., [51]). Murphy and Lawton [51] extended the transient line source method described earlier to include effects caused by flowing fluid in the wellbore. By comparing the conductive heat flux from the rock to the convective heat transported by the wellbore fluid, Murphy and Lawton [51] showed that temperature measurements made between ~0.25 and 100 hours provide meaningful and sufficient data for independently estimating a mean conductivity λ and diffusivity α of the formation.

The above methods have been developed based on the assumptions that the geothermal gradient, $\partial T/\partial z$, and the

formation thermal conductivity do not vary within the interval being tested, which is often not the case. The assumption of constant thermal gradient may introduce an appreciable error in the results. Furthermore, the line source theory cannot be applied in the medium in which thermal conductivity varies.

2) Correlation Methods

Many empirical relations for predicting thermal conductivity have been derived based on other geophysical well log parameters. Dakhnov and Kjakonov [22] used data from the literature to provide the following correlation:

$$\lambda = D_B \left(\frac{3.1}{4680}\right) \tag{2.5}$$

where D_B = saturated bulk density, g/cm^3,

λ = thermal conductivity, cal/cm-s-°C.

Using the same approach, for classes of feldspathic rock, salt and other rock types, Karl [41] obtained

$$\lambda = A \times 10^{-8} V_p \tag{2.6}$$

where A = a constant depending on the rock's physical properties,

V = compressional velocity, cm/sec.

Tikhomirov [69] examined both dry and partially saturated samples of many rock types, and combined the results into one equation,

$$\lambda = 1.30 \exp (0.58 D_D + 0.40 S_W) \tag{2.7}$$

where D_D = bulk density of rock in the dry state,

S_W = fractional water saturation.

Using cores from a wide region of the Siberian lowlands, Moiseyinko and co-workers [50] proposed the relation

$$\lambda = [1.17 + 0.83\ (3.42 - 0.55\phi)]\times 10^{-3} \qquad (2.8)$$

where ϕ = the porosity in percent

λ = thermal conductivity in cal/cm-s-°C.

In an experiment with unconsolidated sands, Somerton, et al., [62] found that

$$\lambda = 0.735 - 0.013\phi + 0.363\lambda_s \sqrt{S_W} \qquad (2.9)$$

where λ_s is the thermal conductivity of the component solid grains. Anand, et al., [3] studied the thermal conductivity of sandstones and derived the following relation for dry samples,

$$\lambda_d = 0.340\rho_d - 0.032\phi + 0.53k^{0.10} + 0.013F - 0.031, \qquad (2.10)$$

and for saturated samples

$$\lambda = \lambda_d\left[1.0 + 0.30\left(\frac{\lambda_1}{\lambda_g} - 1.0\right)^{0.33} + 4.57\left(\frac{\phi}{100-\phi} \times \frac{\lambda_1}{\lambda_g}\right)^{0.48m} \times \left(\frac{\rho_b}{\rho_d}\right)^{-4.3}\right] \qquad (2.11)$$

where: k = permeability of the rock, millidarcy,

λ = thermal conductivity, Btu/ft hr °F,

F = formation resistivity factor,

ρ = density of the rock, g/cm^3,

ϕ = fractional porosity,

and subscripts d, 1, and g stand for dry rock, saturating liquid and gas, respectively; m is the cementation factor.

Goss and Combs [33], measuring core samples from Imperial Valley, proposed three predictive equations for

the thermal conductivity

$$\lambda = -1.42 + 2.18V_p \quad , R = 0.962 \tag{2.12}$$

$$\lambda = 2.01 - 0.095\phi + 1.66V_p \quad , R = 0.966 \tag{2.13}$$

$$\lambda = -0.534 - 0.082\phi + 0.0019\sigma + 2.11V_p, \ R = 0.971 \tag{2.14}$$

where: λ = thermal conductivity in mcal/cm-s-°C,

V_p = compressional velocity in km/sec,

ϕ = porosity in percent,

σ = electrical conductivity in mmho,

R = linear correlation factor.

Most of the relationships presented above are deficient since they are not based on sets of variables measured on the same samples (Goss and Combs, [33]). None of the above equations provided satisfactory results for a variety of rock types; they either gave lower or higher values compared with laboratory experimental results. It is also important to point out that, when measured in-situ, many variables in the empirical relations, such as S_w, ϕ, etc., for the thermal conductivity are not measured directly. They are derived empirically from other directly measured quantities.

3) Thermal Gradients in Wells

Another method for the determination of in-situ thermal conductivity involves the use of geothermal gradients. Many authors have worked on the problem of restoring the reservoir to the geothermal temperature after drilling, or injecting fluid. Bullard [14] estimated the time necessary for the temperature disturbance, caused by the process of

drilling, to die away by representing the operation of drilling by a line heat source Q. If drilling has gone on for time t_1, temperature T_o at distance r from the source will be approximately:

$$T_o = \left(\frac{Q}{4\pi\lambda}\right)[\ln(4\alpha t_1 / r^2) - 0.557] \quad , \qquad (2.15)$$

where λ = thermal conductivity of the formation,

α = thermal diffusivity of the formation.

The effect of ceasing to drill at time t_1 can be regarded as that of starting a negative source -Q at this time, so that the temperature at (r) at time (t) after the ceasation of drilling is given by:

$$T = (Q/4\pi\lambda)\ln(1+t_1/t) \qquad (2.16)$$

and the way in which the disturbances die away is given by

$$\frac{T}{To} = \frac{\ln(1+t_1/t)}{\ln(4\alpha t_1/r^2)-0.577} \qquad (2.17)$$

From this result Bullard concluded that, for the hole to return to within 1% of equilibrium, t must be of the order of $10 \times t_1$.

Jaeger [38] obtained a similar result after a more elaborate calculation. Lachenbruch and Brewer [44] showed that in the practical case, temperatures at $t = 3t_1$ are within 0.05°C of the equilibrium values. However, these results can be used only in the ideal case where the line source theory can be applied. Other investigators, such as Crosby [21], have derived empirical relations for the static temperature based on the same principle.

Edwardson, et al., [28], Schoppel and Gilarranz [59], and Dowdle and Cobb [26] have derived many techniques to evaluate static formation temperature based on the Horner method, similar to pressure build-up theory. Most of these techniques, however, have used an assumed formation temperature profile at the conclusion of circulation and provide no means to calculate this profile directly (Raymond, [55]). Moreover, this type of analysis can be only used under the condition that there is no variations in the geothermal temperature gradient and the formation thermal conductivity.

In the present study, the effect of variation in the formation thermal conductivity on the wellbore fluid temperature, during injection and shut-in periods, will be investigated. Once the relationship between the formation thermal conductivity and the fluid temperature behavior as well as geothermal temperature are known, it is possible to determine relative values of the formation thermal conductivity by the linear relationship:

$$q = -\lambda \frac{\partial T}{\partial z} \tag{2.18}$$

where: q = geothermal heat flux,

$\frac{\partial T}{\partial z}$ = geothermal temperature gradient.

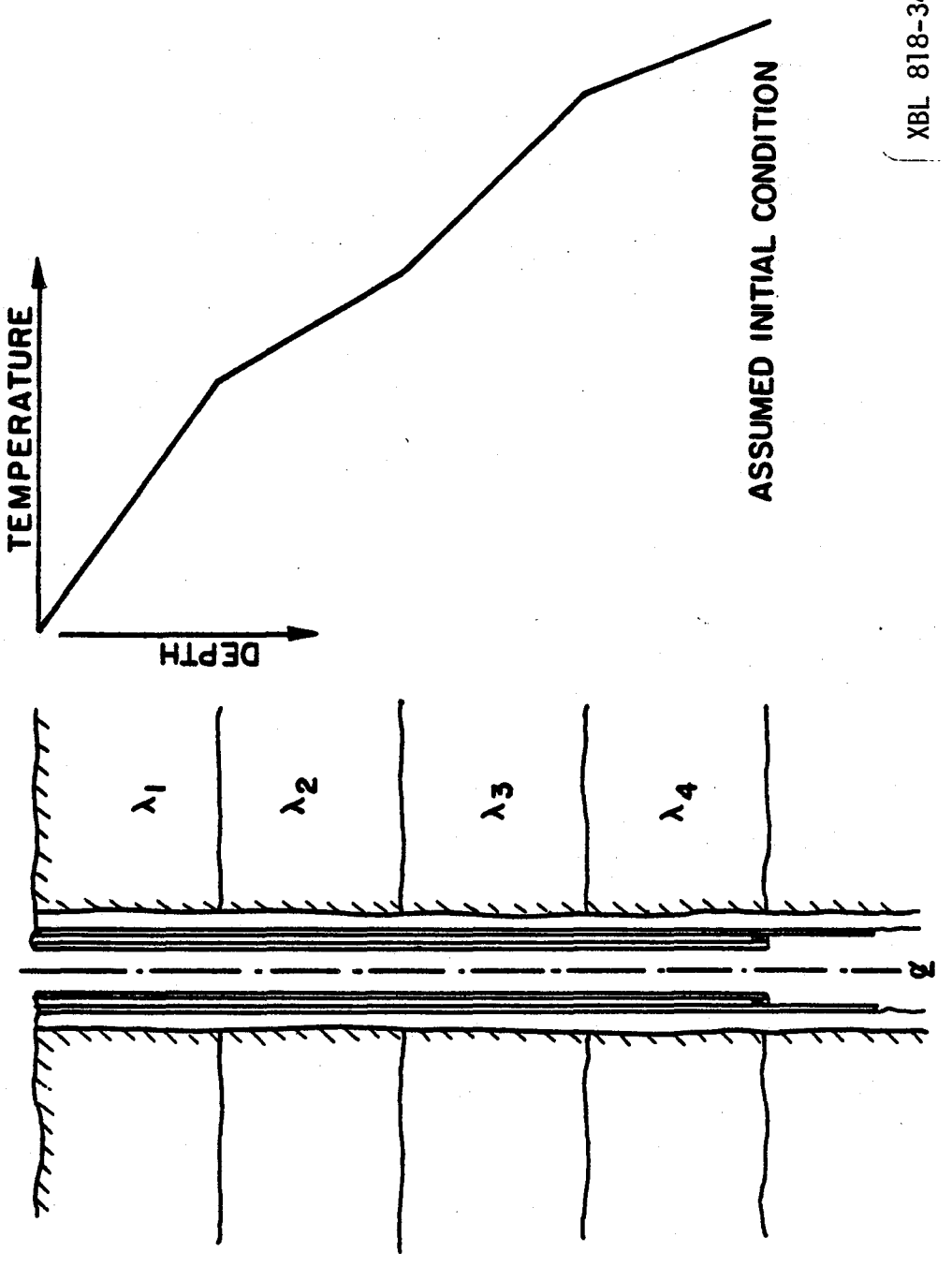

XBL 818-3487

FIG. 5 HYPOTHETICAL MODEL

CHAPTER III

DEVELOPMENT OF THE MODEL

3.1 General Considerations

Figure 5 shows the conceptual model used in this study. The model is composed of a wellbore and the surrounding formation. The injected or produced fluid enters the well and flows inside the tubing of outer radius, r_w. Any material external to the fluid column such as insulating material, mud, casing, or cement is regarded as the thermal resistance between the fluid and the surrounding formation. The formation which surrounds the wellbore consists of several horizontal layers infinite in lateral extent. Each layer is homogeneous and composed of material which has the thermal conductivity denoted by λ_i. In this model, the values of λ_i and the depth of formation layers can be varied as desired. Values of λ vary from 1.25 w/m°K for shale-clay to 5w/m°K for fully water saturated sandstone.

The injection process consists of the fluid entering the top of the well at a fixed temperature, flowing down the tubing and into the injection zone at the bottom of the well. As the fluid flows down the well, heat is exchanged by convection and by conduction between the fluid and the formations adjacent to the wellbore at a rate that is dependent on the relative temperatures and physical properties of the two media. When injection is stopped, the well is shut-in and the fluid becomes quiescent in the

wellbore. The wellbore fluid will lose, or gain, heat to the formation by conduction and possibly by natural convection inside the borehole during the shut-in period. The static fluid temperature in the wellbore approaches the geothermal temperature as the system comes to thermal equilibrium.

In this study, the formation temperature and that of the quiescent fluid in the wellbore initially are assumed to be the same as the geothermal temperature. This geothermal temperature varies with depth and is taken to be proportional to the magnitude of the formations' thermal conductivities. At time equal to zero, hot fluid is injected down the tubing and enters the injection zone at the bottom of the well. By analyzing the heat transfer process inside the tubing and in the surrounding formations, the temperature profiles of the fluid and the formation are obtained. Then, the injection is stopped and the well is shut-in. The temperature distributions inside the wellbore and in the surrounding formations at the end of the injection period are used as the initial conditions for the analysis of the system's temperature distribution during shut-in.

Analysis of the shut-in period will accomplish two goals. First, to study the progress of the return to equilibrium of the wellbore fluid temperatures; second, to study the effect of variable thermal conductivities of the formations on the fluid temperature distribution. In the great majority of the cases the amount of heat flowing along a

thermally stable borehole rarely changes by more than 15% from a mean value in the absence of disturbing factors such as heat sources and sinks, according to Beck and Judge [9]. On the other hand, the thermal conductivities of the formations through which boreholes pass may vary nearly by an order of magnitude. Since the thermal gradients for constant heat flux are inversely proportional to the thermal conductivities of the formation under equilibrium conditions, it follows that a temperature gradient log is generally a good approximation of a thermal resistivity log. Hence, the formation thermal conductivities can be determined relatively from a temperature gradient log. Because of the complexity of the problem, a numerical model is developed to provide the desired results.

3.2 Temperature Distribution During Injection

3.2.1 Mathematical Model

The system to be considered in this study is composed of two parts:

(1) the wellbore through which single phase fluid flows vertically downwards and where heat lost by the fluid transfers radially to the surroundings,

(2) the formation where heat transfers radially and vertically into the earth.

Except for extremely low flow rates, the flow of fluid in an oil well, or a geothermal well, is turbulent. The effective conductivity of the fluid would thus be many times

its molecular value, and since wellbore radii are small, the change in fluid temperature in the radial direction in the well would be negligible. For typical flow rates the Peclect number is extremely large (>100), so that axial conduction of heat in the fluid is negligible compared to axial convection (Kays, [42]). As a final simplification, the depth intervals at which fluid is actually leaving the well will not be rigorously analyzed - the convective heating of the formation by the fluid permeating this interval will not be accounted for in the heat conservation equations.

Under the above circumstances, the differential equation for axisymetric flow in a circular cylinder, satisfied by the fluid temperature T(t,z), is obtained by writing a heat balance on an element of fluid in the tubing between the depths z and z + dz

$$\dot{m}c\left(\frac{\partial T}{\partial z}\right) + \rho_w c_w \pi r_w^2 \left(\frac{\partial T}{\partial t}\right) = q, \qquad (3.1)$$

where: r_w = the well radius,

t = the time since the start of injection,

ρ_w = the fluid density,

c_w = the specific heat capacity of the fluid.

The quantity q is the rate per unit depth, z, at which heat is conducted to the formation from the fluid. $\dot{m}$ is the mass injection rate, and it is considered to be constant. In this case m can be expressed as

$$\dot{m} = \pi r_w^2 \rho_w u \ , \qquad (3.2)$$

where u = fluid velocity.

In this study, the density ρ_w of the fluid will vary along the wellbore depending on the fluid temperature,

$$\rho_w(T) = \frac{1.0}{A_1+B_1TP+C_1TP^2+D_1TP^3} \tag{3.3}$$

where $TP = (T + 273.0)\times 10^{-4}$, and A_1, B_1, C_1 and D_1 are constants for a particular fluid. For water $A_1 = -0.472\times10^{-3}$, $B_1 = 0.114213$, $C_1 = -2.996214$, $D_1 = 27.5958$, respectively.

Because turbulent flow is assumed, the velocity profile is relatively flat and the velocity u of the fluid is approximately constant independent of the coordinates. However, velocity will change in inverse proportion to the fluid density, i.e.,

$$\frac{u_1}{u_2} = \frac{\rho(T_2)}{\rho(T_1)} \quad . \tag{3.4}$$

Within the formation, from the cement-formation interface away from the wellbore, heat flows by conduction only. For this case, an unsteady-state, two-dimensional (radial and vertical) heat conduction equation is employed,

$$\frac{\partial\theta}{\partial t}-\alpha(z)\frac{1}{r}\frac{\partial}{\partial r}\left(r\frac{\partial\theta}{\partial r}\right)-\frac{\partial}{\partial z}\left(\alpha(z)\frac{\partial\theta}{\partial z}\right) = 0 \ , \tag{3.5}$$

where θ is the formation temperature. The variable $\alpha(z) = \lambda(z)/\rho c$ is the thermal diffusivity of the formation, and $\lambda(z)$ is its thermal conductivity which varies with depth. These equations were developed under the assumption that physical and thermal properties of the formation and the injected fluid, except the fluid density, do

not vary in the range of temperatures considered. However, the extension of the model to temperature dependent properties can be made.

The heat transfer must be the same on both sides of the well/formation interface. The boundary conditions that couple Equations (3.1) and (3.5) are

$$\text{at } r = r_w, \qquad q = 2\pi r_w \lambda(z) \frac{\partial \theta}{\partial r} \tag{3.6}$$

$$\text{and} \qquad \lambda(z)\frac{\partial \theta}{\partial r} = U_T(\theta - T) \quad . \tag{3.7}$$

The overall heat transfer coefficient U_T refers to the outside tubing surface area and represents the net resistance to heat flow offered by the flowing fluid, tubing, insulation, annulus, casing, and the cement sheath. On the basis of several assumptions, discussed by Willhite [68], U_T can be simplified as follows:

$$U_T = \frac{1}{r_i}\left[\frac{\ln\frac{r_{ins}}{r_i}}{k_{ins}} + \frac{1}{r_{ins}(h_c+h_r)} + \frac{\ln\frac{r_h}{r_{co}}}{k_{cem}}\right] \tag{3.8}$$

where: r_i = outside radius of tubing,

r_{ins} = radius of the outside insulation surface,

r_h = radius of drill hole,

r_{co} = outside radius of casing,

h_c = heat transfer coefficient for natural convection based on the outside insulation surface and the temperature difference between the outside insulation and inside casing surface,

h_r = radiation heat transfer coefficient based on the outside tubing surface and the temperature difference between the outside tubing and inside casing surface,

k_{ins} = thermal conductivity of insulation,

k_{cem} = thermal conductivity of cement.

Initially the formation and the quiescent fluid are assumed to be at the same temperature, i.e. equilibrium temperature. Thus,

$$\text{at } t = 0, \quad T(0,z) = \theta(0,r,z) = T_i(z) = T_a + \sum_i^m \frac{q}{\lambda_i(z)} \Delta z_i, \tag{3.9}$$

where T_a is the ambient temperature. Far from the wellbore the temperature is undisturbed.

Thus, at $r \to \infty$, $\theta(t,r,z) = T_i(z)$. (3.10)

The temperature of the entering fluid is considered constant and z is measured from the point where the fluid enters the system and in the direction of flow:

$$\text{at } z = 0, \quad T(t,0) = T_{inj} \quad , \tag{3.11}$$

and the fluid is allowed to flow into the wellbore and for a finite length L. At the surface and at the bottom of the well the boundary conditions for the formation are

$$\text{at } z = 0, \quad \theta(t,r,0) = T_a \tag{3.12}$$

$$\text{at } z = L, \quad \theta(t,r,L) = T_a + \sum_i^m \frac{q}{\lambda_i(z)} \Delta z_i \tag{3.13}$$

where L is the depth of the well.

3.2.2 Numerical Formulation

Temperatures of the flowing fluid inside the wellbore and the surrounding formation are obtained by solving Equations (3.1) through (3.13). An exact analytical solution to the system of Equations (3.1) and (3.5), which satisfies the appropriate boundary and initial conditions, is very difficult, if not impossible. This is due to the fact that analytical methods can be applied most effectively to homogeneous problems of simple geometry. However, these types of problems can be solved efficiently by numerical methods.

A numerical solution to an initial value problem such as Equation (3.1) can be obtained by the finite difference method. Terms that would impose very restrictive time steps such as $\Delta t \leq \Delta z/u$, where Δz is the vertical increment and u is the fluid velocity, are evaluated implicitly for computational efficiency. An implicit backward difference scheme with m equally spaced grid nodes is used to solve for the fluid temperature inside the wellbore. Adopting the notation of subscripts i, j, to denote the position (z, r), and superscript n to denote time step (t), Equation (3.1) is expressed in the finite difference form as:

$$T_i^{n+1} - T_i^n = - (u_i \Delta t/\Delta z) (T_{i-1}^{n+1} - T_i^{n+1}) +$$

$$(2U_T \Delta t/\rho_w c_w r_w) \cdot (\theta_{1,i}^n - T_i^{n+1}) \quad , \qquad (3.14)$$

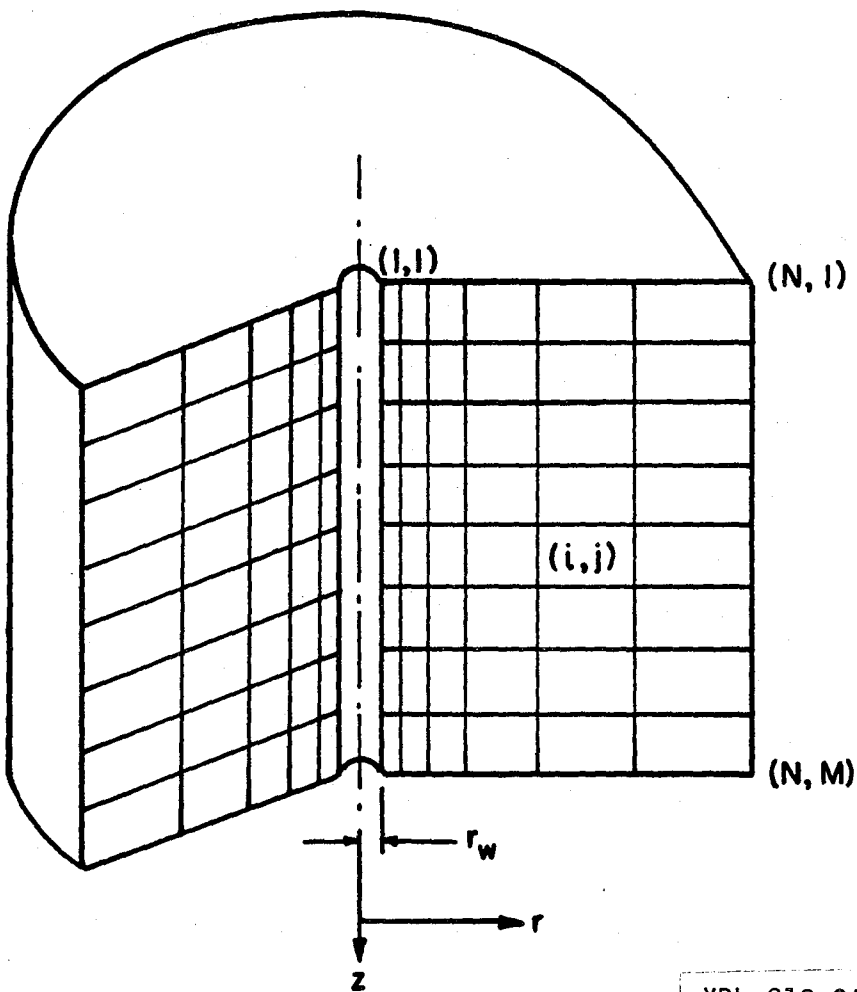

XBL 818-3488

FIG. 6 GRID SYSTEM USED IN NUMERICAL FORMULATION

where i = 1 is at the top of the well and $\theta^n_{1,i}$ is the formation temperature at the node adjacent to the wellbore.

The wellbore model is connected to a reservoir model so that the heat lost from the wellbore is the same as the heat flow into the formation. In the formation surrounding the well, a two dimensional grid system is set up. Because of the low value of the formation thermal conductivity, most of the temperature change will occur close to the wellbore (Edwardson, et al., [28]). To be able to examine this effect, a variable radial grid system is used (Figure 6). Near the bore wall, a grid spacing small enough to resolve a drastic change in the temperature gradients is needed, whereas a much larger grid spacing can be used farther from the well where the formation temperature gradient is much smaller. The radial grid spacing is calculated by using a logarithmic transformation (Miller, [48]),

$$r_j = a \left[\frac{k^{Nj/\Delta N_o} - 1.0}{k^{1/\Delta N_o} - 1.0} \right] + r_w \quad , \tag{3.15}$$

where: $N_j = (j - 1)\,\Delta N$

$1/\Delta N$ = total number of radial grid points,

k, a, ΔN_o are constants that can be varied to give the desired grid spacing.

Uniform grid spacing is used in the vertical direction. To obtain the formation temperature distribution, an alternating direction implicit (ADI) technique is employed. By using this technique, temperature is expressed impli-

citly in one of the coordinate directions leaving the other explicit and considering that time is advanced over half a time step. Then the roles of the implicit and explicit parts are interchanged to complete the time step. This technique, along with the finite difference representation of the governing equations, are discussed further in Appendix A. Equation (3.5) is expressed in the finite difference form as follows:

$$\frac{\theta_{i,j}^{n+1/2} - \theta_{i,j}^{n}}{1/2\Delta t} - \frac{2\alpha_i}{r_{j+1} - r_{j-i}} \left\{ r_{j+1/2} \frac{\theta_{i,j+1}^{n+1/2} - \theta_{i,j}^{n+1/2}}{r_{j+1} - r_j} - r_{j-1/2} \frac{\theta_{i,j}^{n+1/2} - \theta_{i,j-1}^{n+1/2}}{r_j - r_{j-1}} \right\} - \frac{\alpha_{i+1}\theta_{i+1,j}^{n} - 2\alpha_i\theta_{i,j}^{n} + \alpha_{i-1}\theta_{i-1,j}^{n}}{\Delta z^2} = 0 \quad , \tag{3.16}$$

and

$$\frac{\theta_{i,j}^{n+1} - \theta_{i,j}^{n+1/2}}{1/2\Delta t} - \frac{2\alpha_i}{r_{j+1} - r_{j-1}} \left\{ r_{j+1/2} \frac{\theta_{i,j+1}^{n+1/2} - \theta_{i,j}^{n+1/2}}{r_{j+1} - r_j} - r_{j-1/2} \frac{\theta_{i,j+1}^{n+1/2} - \theta_{i,j-1}^{n+1/2}}{r_j - r_{j-1}} \right\} -$$

$$\frac{\alpha_{i+1}\theta_{i+1,j}^{n+1} - 2\alpha_i\theta_{i,j}^{n+1} + \alpha_{i-1}\theta_{i-1,j}^{n+1}}{\Delta z^2} = 0 \quad , \tag{3.17}$$

where: i-1, i, i+1 = step in z direction,

j-1, j, j+1 = step in r direction,

and $r_{j+1/2}, r_{j-1/2}$ are computed by:

$$r_{j+1/2} = \frac{r_{j+1} + r_j}{2}$$

and

$$r_{j-1/2} = \frac{r_j + r_{j-1}}{2} \quad .$$

Equations (3.16) and (3.17) can be written as AP = x, where A is a tridiagonnal matrix. The solution is straightforward if the boundary and initial conditions are specified. At the formation/wellbore boundary, the heat transfer is matched. When the energy equation in the fluid is solved, the heat transfer at the wall is

$$q = 2\pi r_w \Delta z U_T (\theta^n_{1,i} - T^n_i) \quad . \tag{3.18}$$

When the temperature in the formation is calculated, the boundary condition at the formation/well interface is

$$\lambda(z_i) \frac{\partial \theta(1,i)}{\partial r} = U_T (\theta^{n+1}_{1,i} - T_i^{n+1}) \quad . \tag{3.19}$$

The heat transfer is matched throughout the calculation except for the first time step for the energy in the fluid, that is, the heat transfer into the reservoir for the calculation of the reservoir temperature at time n+1 is just the heat that will leave the fluid during the calculation for n+2. The only heat transfer not matched is for the first calculation of the fluid energy, but usually $\theta_{(1,i)} = T_i$ at first time step for this case, so q will be negligible.

The solution procedure is to decouple Equations (3.1) and (3.5) by solving these two equations alternatively. The new fluid temperature in the wellbore is solved first using the old value of the formation temperature. Then the new temperature in the formation is calculated by determining the heat flowing from the well into the formation over that time. First, the fluid density is calculated based on the fluid temperature distribution at time t. The velocity of the injected fluid, as a function of the fluid density, is calculated for all grid nodes. Then the new temperature of the fluid, at time $t+\Delta t$, inside the wellbore is computed. Once the new temperature in the well is determined, the change in the formation temperature is calculated as a function of r and z at all nodal points.

3.2.3 Numerical Results and Discussion

A series of calculations was made to study the behavior of the fluid temperature in a wellbore and the surrounding formations during the injection period. In every case, the physical properties and average thermal properties of the fluid, and the physical dimensions of the well corresponded closely to the values reported by Boberg [13] and Ramey [54]. The overall heat transfer coefficient U_T, thermal conductivities of the formations, and the injection rate are allowed to vary.

The calculated temperature distributions of the fluid in the wellbore during the injection period are shown in Figures

7 to 11. Figure 7 shows the temperature profiles at various times from the start of injection. As the fluid flows down the well its temperature decreases due to heat loss to the adjacent formations and to the convection process. A rapid change in the injection temperature occurs at early times, followed by an approach to constant temperature at long times. At early times, due to the large temperature differences in the fluid and the adjacent formations, larger amounts of heat are lost to the formation than at later times when the temperature difference is less. This has the effect of heating up the part of the formation adjacent to the wellbore and heat conducts away from the wellbore slowly because of the low values of formation thermal conductivities. (This is shown in Figure 12.) When the formation adjacent to the wellbore is heated up, the heat loss from the wellbore decreases and approaches a constant value. Furthermore, the order of magnitude analysis by Murphy, et al., [51] shows that as the injection time increases, the magnitude of the transient term becomes negligible compared with the other terms so that a steady state solution can be applied for the wellbore at long injection times.

The order of magnitude analysis of Equation (3.1) and the results shown in Figure 11 indicate that during injection the fluid temperature is controlled mainly by two factors: 1) the injection rate and, 2) the rate of heat loss from the fluid to the surrounding formations. Variable

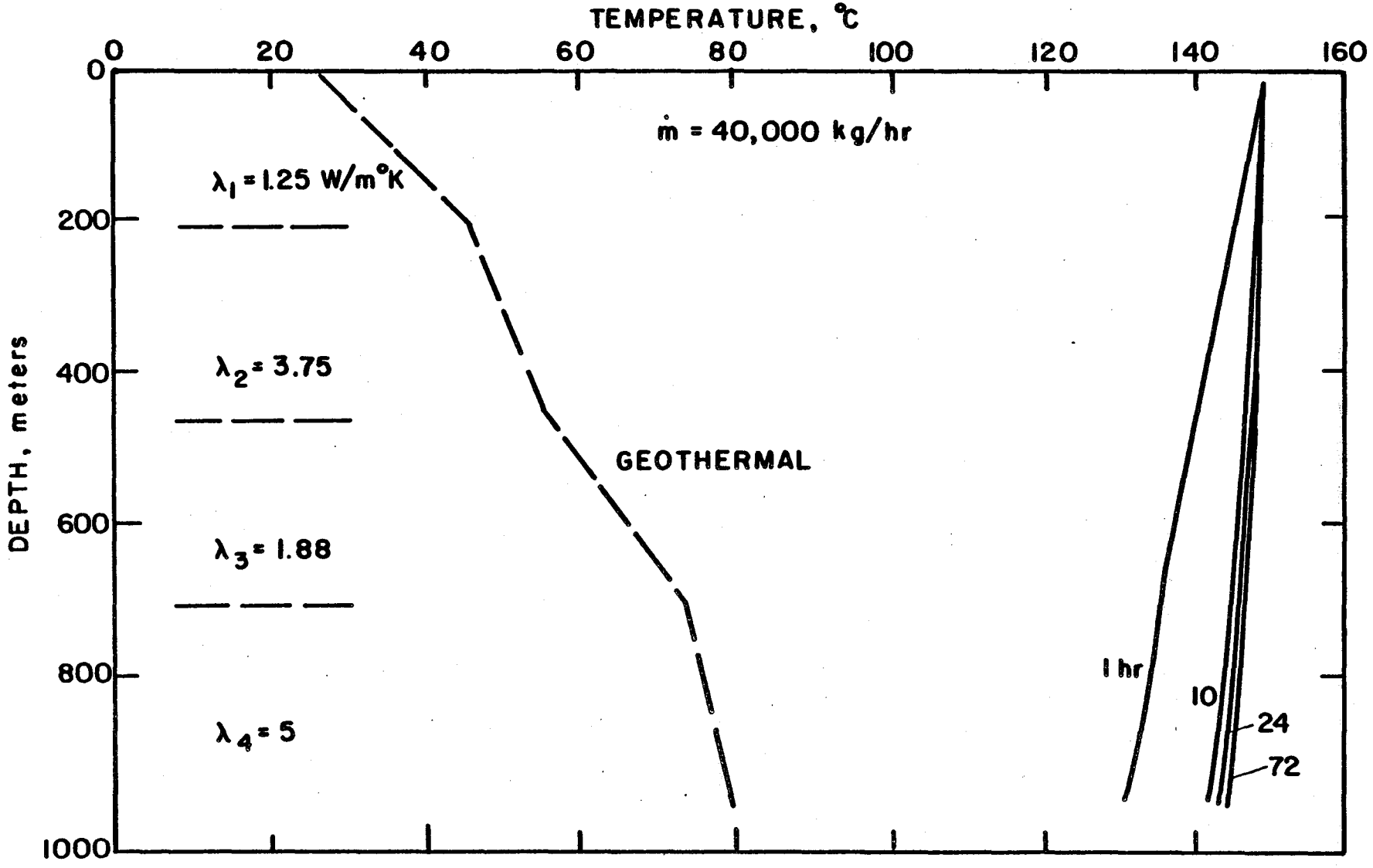

FIG. 7 WELLBORE FLUID TEMPERATURE DISTRIBUTION DURING INJECTION

XBL 819-7407

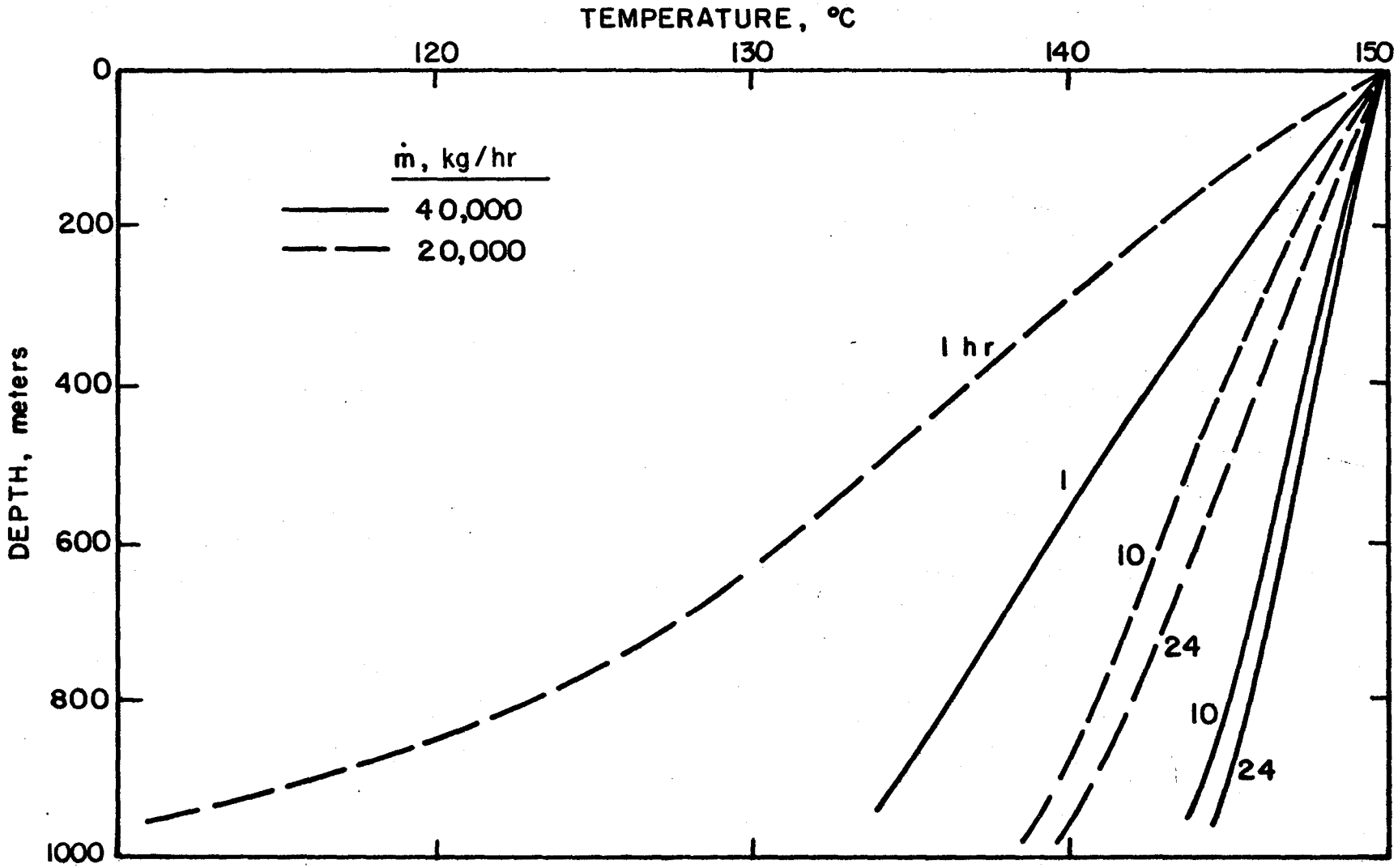

FIG. 8 EFFECT OF INJECTION RATE ON WELLBORE FLUID TEMPERATURE DISTRIBUTION

XBL 8010-12123

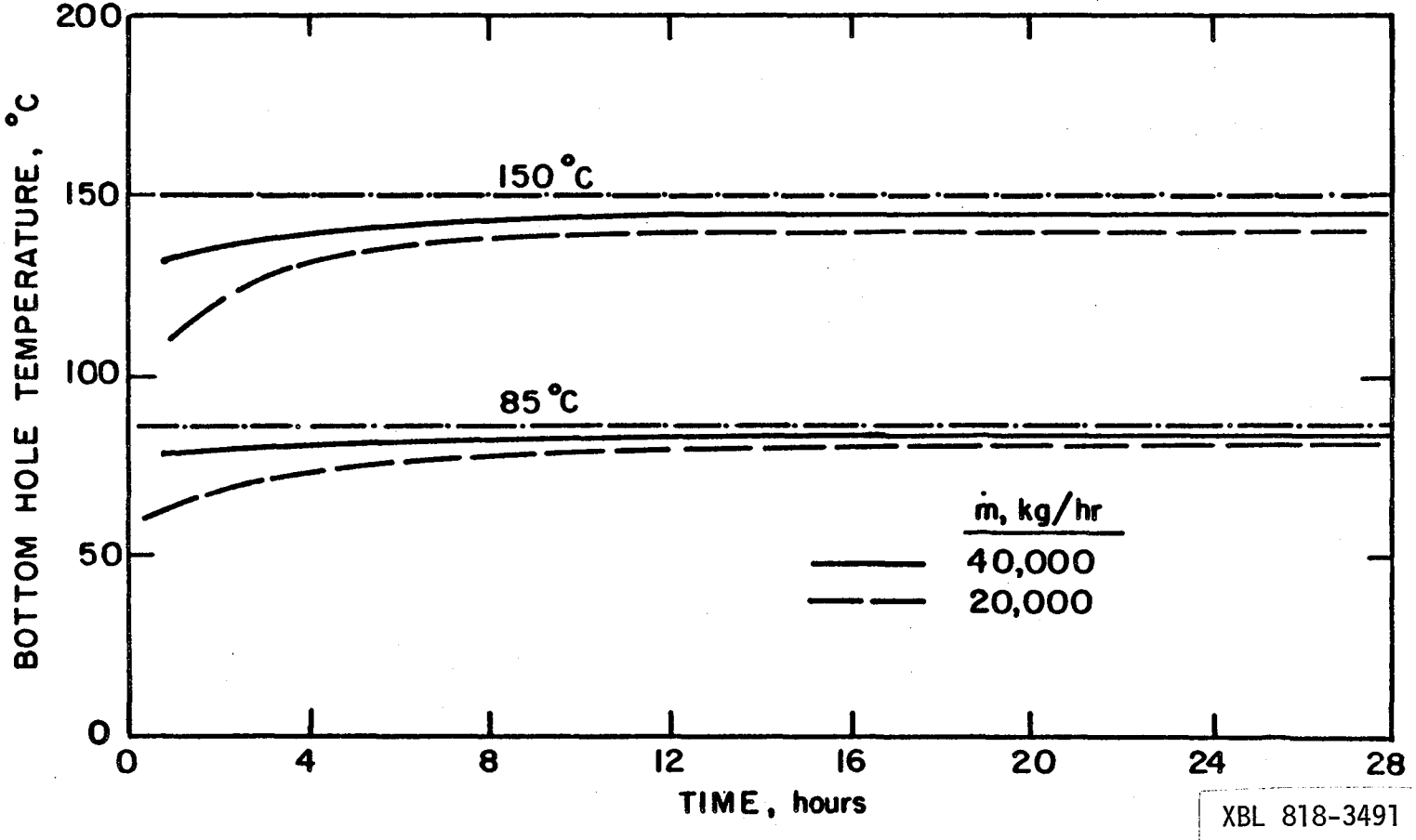

FIG. 9 EFFECT OF INJECTION RATE ON BOTTOM HOLE TEMPERATURE

thermal conductivities of the formations do not have much effect on the fluid temperature profile except at early times.

(1) Effect of Injection Rate

In this study, the hot fluid at 150°C is injected down the well and two injection rates are selected (20,000kg/hr and 40,000 kg/hr) to study the effect of the injection rate on the fluid temperature behavior. For the very high injection rate cases, the injected fluid would have very little time to exchange heat with the surrounding formations. Thus the resultant temperature profile would be nearly a straight line as shown in Figure 8. In these cases most of the heat is transported axially down the well by convection. For the lower injection rate, however, the effect of axial convection is smaller and the radial heat loss from the wellbore is relatively large. As the fluid flows down the well it loses heat to the surroundings and its temperature decreases with depth. In both cases, the steady state condition is reached after 24 hours of injection. Figure 9 shows the effect of injection rate on the fluid temperature as the bottom of the well for fluids having surface temperatures of 150°C and 85°C. In both cases, the initial bottom hole temperature was 80°C. This figure also indicates the rate with which the bottom-hole temperature approaches the surface injection temperature. The results indicate that at the higher injection rate, more heat is transported down the well by the convection and mixing processes so that the fluid temperature rises more rapidly, and a steady state

condition is reached more quickly.

(2) Effect of Overall Heat Transfer Coefficient

Various techniques have been employed in attempts to reduce heat loss during hot fluid injection, such as painting and insulation of the outer surface of the tubing. The effect of these completion techniques is to reduce the value of the the overall heat transfer coefficient. Figure 10 shows the effect of insulation on the injection temperature profile. Three values of the overall heat transfer coefficient, U_T, are used for comparison. These values are taken from Wilhite [71]. The lowest value of U_T (5.67 $w/m^2°K$) represents the case of well-insulated tubing. The intermediate value of U_T ($56.7 w/m^2°K$) represents the case when a standard completion technique is used. The highest value of U_T($5670 w/m^2°K$) corresponds to the case where no tubing is used and there is only a small temperature difference between the flowing hot fluid and the surface of the adjacent formation. The rate of heat loss from the well to the formation is proportional to the magnitude of the overall heat transfer coefficient and the difference between the fluid temperature and the temperature of the adjacent formation, i.e., $U_T(T-\theta) = -\lambda\frac{\partial\theta}{\partial r}\Big|_{r_w}$.
At early times,temperature difference between the adjacent formation and the fluid is large, resulting in a high rate of heat loss and the magnitude of the overall heat transfer coefficient is the dominant factor. As a result, after a few hours of injection, the temperature of the upper part of the formation adjacent to the wellbore increases very quickly and the rate of

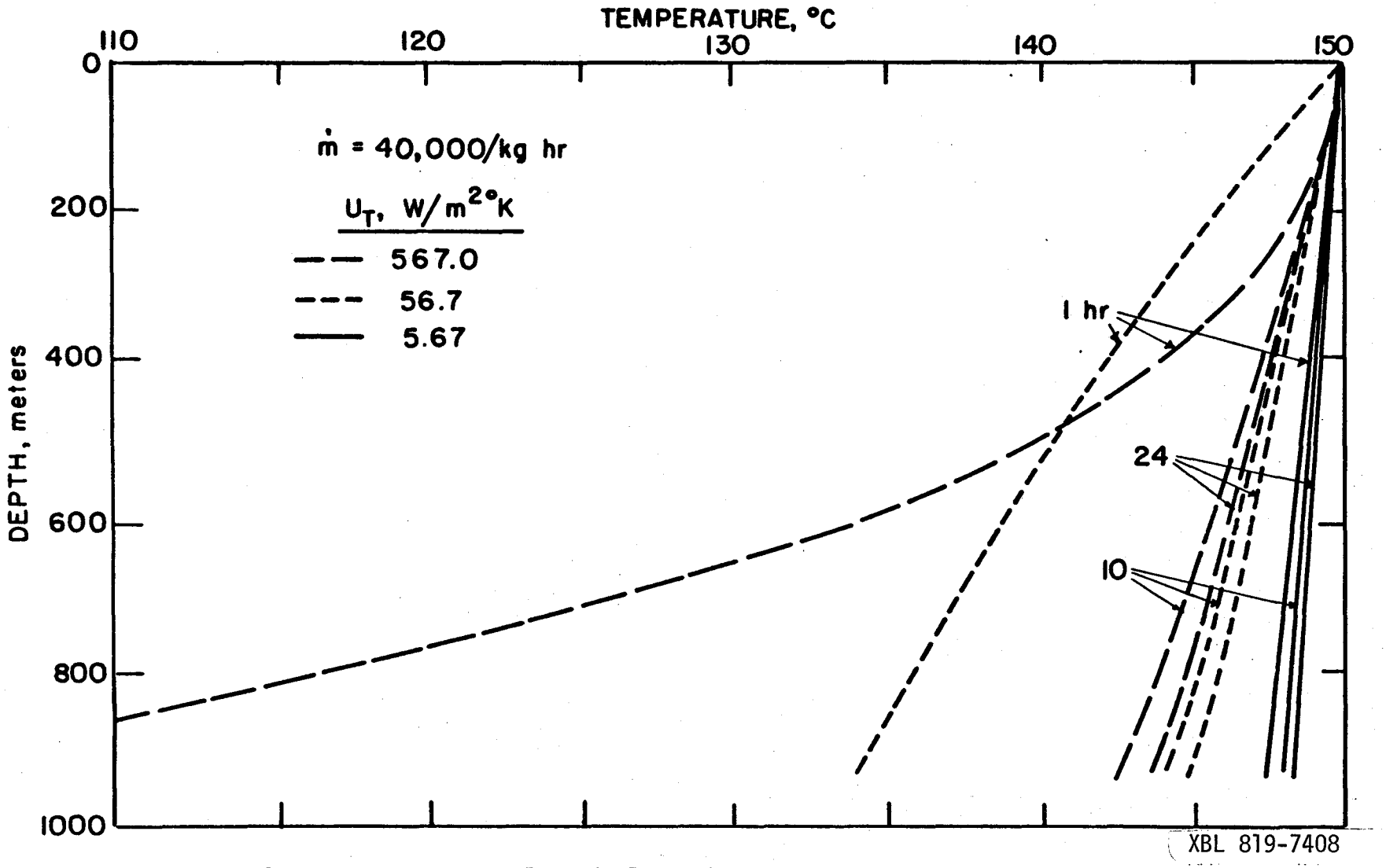

FIG. 10 EFFECT OF INSULATION ON WELLBORE FLUID TEMPERATURE DISTRIBUTION DURING INJECTION

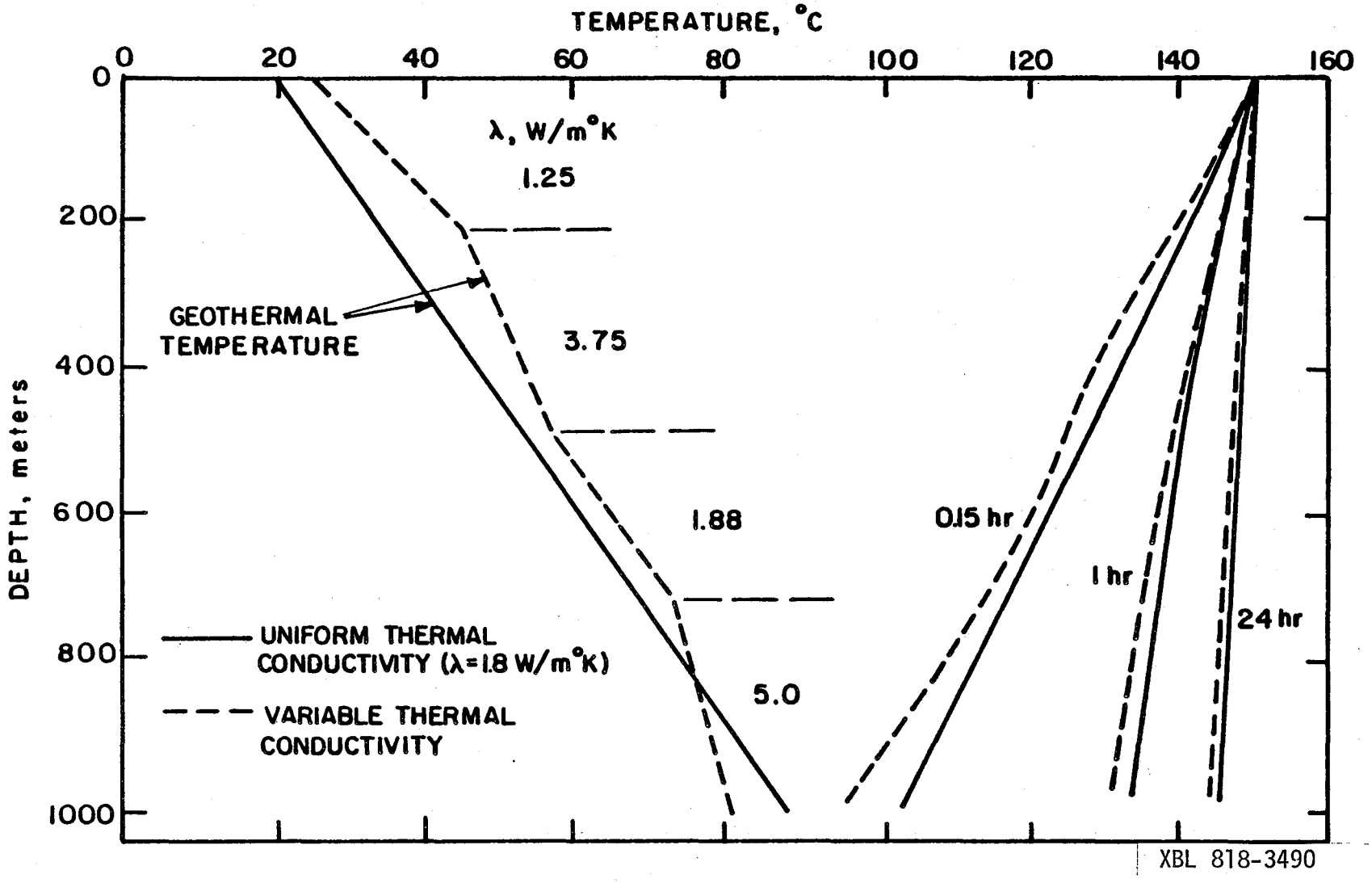

FIG. 11 EFFECT OF VARIABLE THERMAL CONDUCTIVITY ON WELLBORE FLUID TEMPERATURE DISTRIBUTION DURING INJECTION

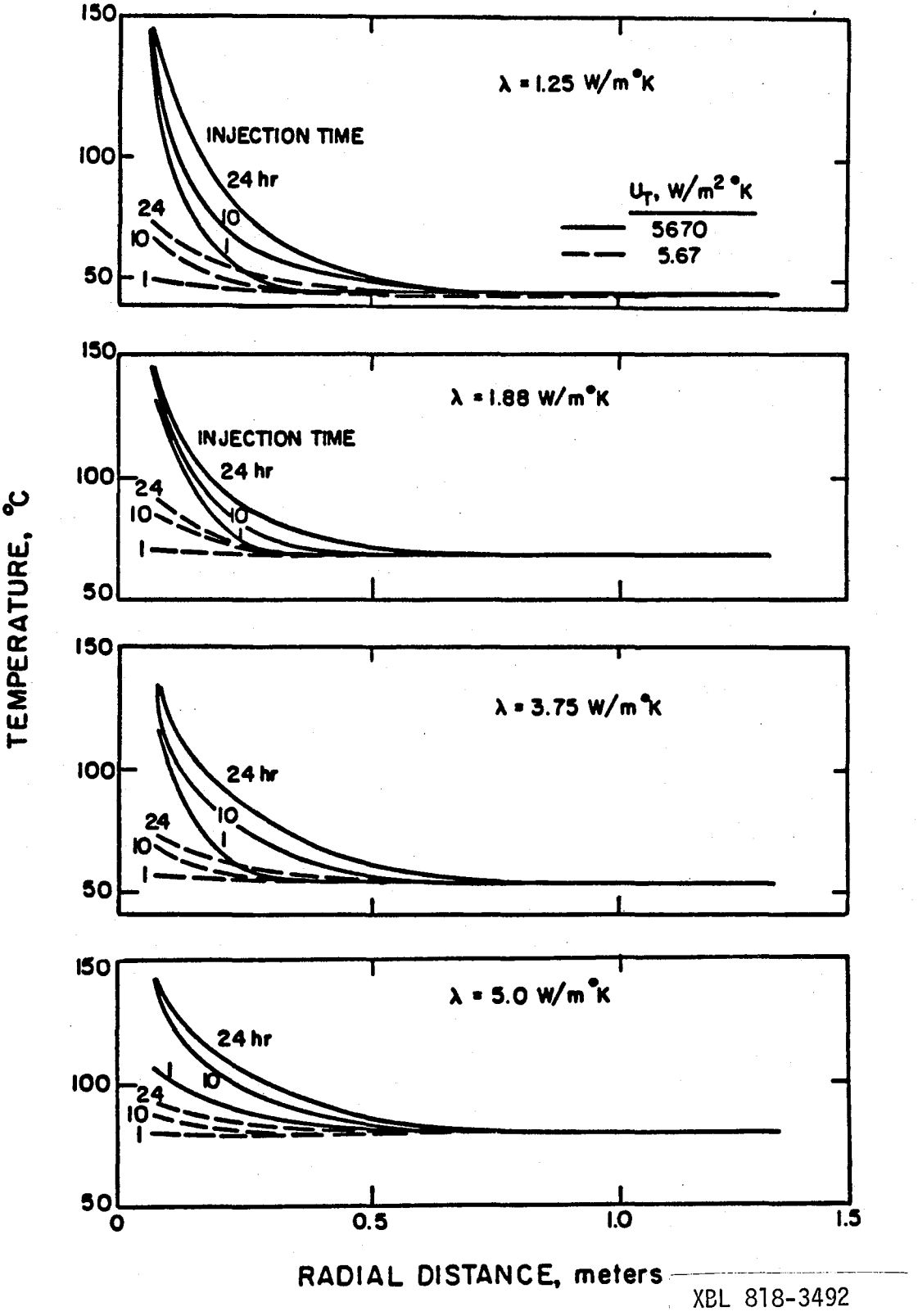

FIG. 12 RADIAL TEMPERATURE DISTRIBUTION IN FORMATION DURING INJECTION

heat loss is reduced. In the lower part of the formation the temperature is still low, relative to the fluid temperature, and the rate of heat loss remains large. As the injection time increases, the rate of heat loss will become relatively constant, proportional to the value of the overall heat transfer coefficient when the adjacent formation has reached a temperature close to that of the fluid opposite it. The temperatures of the fluid and formation then increase very slowly with time. For the case of well-insulated tubing (very low value of the overall heat transfer coefficient) there is is only a small amount of heat lost from the fluid to the surrounding formation. This results in a nearly vertical line for the temperature profile.

(3) Effect of Injection Time

Results of the analysis shown in Figures 7 and 9 indicated that as the injection time becomes large (over 24 hours) the injected fluid temperature approaches a constant value, except at the bottom of the well where the fluid temperature continually changes slowly with time. Injection time, however, is a variable primarily influencing the formation temperature profile. Figure 12 shows the relationship between radial distance and temperature in the formation with time at four different depths corresponding to four different conductivity layers of the formation. It is observed that the temperature at the formation-cement interface rises very rapidly but the the heat is slowly propagated away into the earth because of the low values of the formation thermal diffusivity. Heat

transferred from the hot fluid is found to diffuse more rapidly in the vicinity of the wellbore, and in the formation layers having higher values of thermal conductivity.

(4) Effect of Variable Thermal Conductivity

In Figure 11 the injected fluid temperatures were calculated for the case of uniform thermal conductivity of the formations and compared with the case when it varied. As indicated earlier, because of the high injection rate the fluid temperature profile is mainly controlled by convective heat transfer and at long flow durations, variable thermal conductivity has little effect on the fluid temperature profile. Figure 11 shows that for the injection rate of 40,000kg/hr, the fluid temperature profile was slightly affected by the variable thermal conductivity of the formations at a very early injection time, t = 0.15 hr. As injection continues the effect of variable thermal conductivity on the fluid temperature profile is diminished. However, the results presented in Figures 11 and 12 indicate that the temperature change of the fluid which contacts the higher thermal conductivity formation layers is more rapid because of greater amounts of heat conducted away from the wellbore. The important point to note with respect to the variable thermal conductivity of the formations is that layers which have the higher values of thermal conductivity conduct heat away from the wellbore more rapidly and the change in fluid temperature depends upon the magnitude of the formation thermal conductivity.

3.2.4 Comparison with Published Field Data

The validity of the present mathematical model for fluid injection is demonstrated through a comparison of the calculated results with the few wellbore measurements, which have been published. The first comparison is made with the long time temperature profile of water injection at a low flow rate. The field data are taken from Nowak [52]. The second comparison is made with the temperature profile for cold water injection published in Ramey's paper [54].

Figure 13 presents a comparison of temperatures measured in a water injection well in Nowak's paper [52] with computed temperatures. Water at the surface temperature of 28.4°C is injected at the rate of 5960kg/hr through an 18cm diameter casing for three years. Values of heat capacities and thermal conductivities of the formation are not given in the reference. Based on the given geothermal temperature profile, a conductivity of 2.25w/m°K is used for the first 200 meters of the formation, and a value of 2.42w/m°K is used for the remaining depth of the formation. The value of 2.39×10^{-6}J/m°C is assigned for the formation volumetric heat capacity. In the upper portion of the wellbore, the measured temperature curve is higher than the geothermal temperature for the first few hundred meters. Consequently, the curve crosses over the geothermal temperature curve at about the 190 meters depth. The temperature profile straightens out at about 600 meters and reaches a constant

gradient thereafter. As shown in Figure 13 the calculated temperatures are within 1°C of the measured temperatures for the lower part of the curve. For the depths between 300 and 900 meters the discrepancy is relatively large, about 3°C. However, the measured temperatures between 300 and 900 meters depths are a little lower than one might expect from the geothermal temperature. After crossing over the geothermal temperature curve, the water temperature profile should have a positive gradient since it is in contact with the hotter formation. The only explanation for the negative temperature gradient effect is water lost through a hole found in the casing at a depth of 900 meters. The lower temperature water lost to the formation would have the effect of cooling down the surrounding formation after long injection time, so that the water temperature decreases below the injection temperature.

Another set of field data available for comparison is taken from Ramey [54]. The water injection rate at the time of the survey was 31,700kg/hr; the well had been on injection for a period of approximately 75 days. Water at surface temperature of about 15°C is injected through a 18 cm diameter tubing, 2015 meters long. The geothermal gradient temperature of 0.0165°C/m and thermal conductivity of 2.42 w/m°C are used in the calculations. As shown in Figure 14, because of the high flow rate, the water temperature profile is nearly a straight line and increases with depth. The calculated temperatures exceed the measured

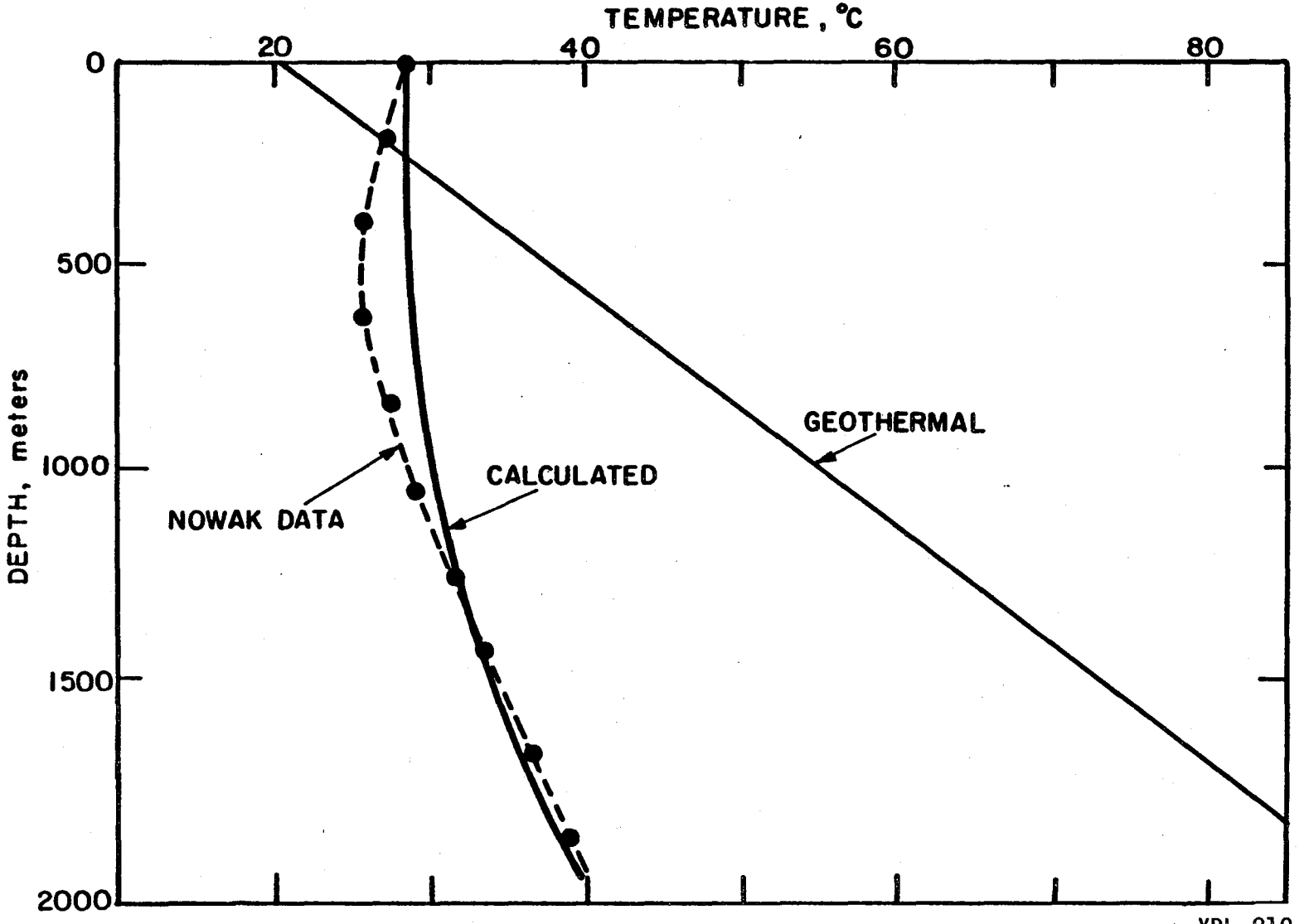

FIG. 13 COMPARISON OF MEASURED AND CALCULATED TEMPERATURES

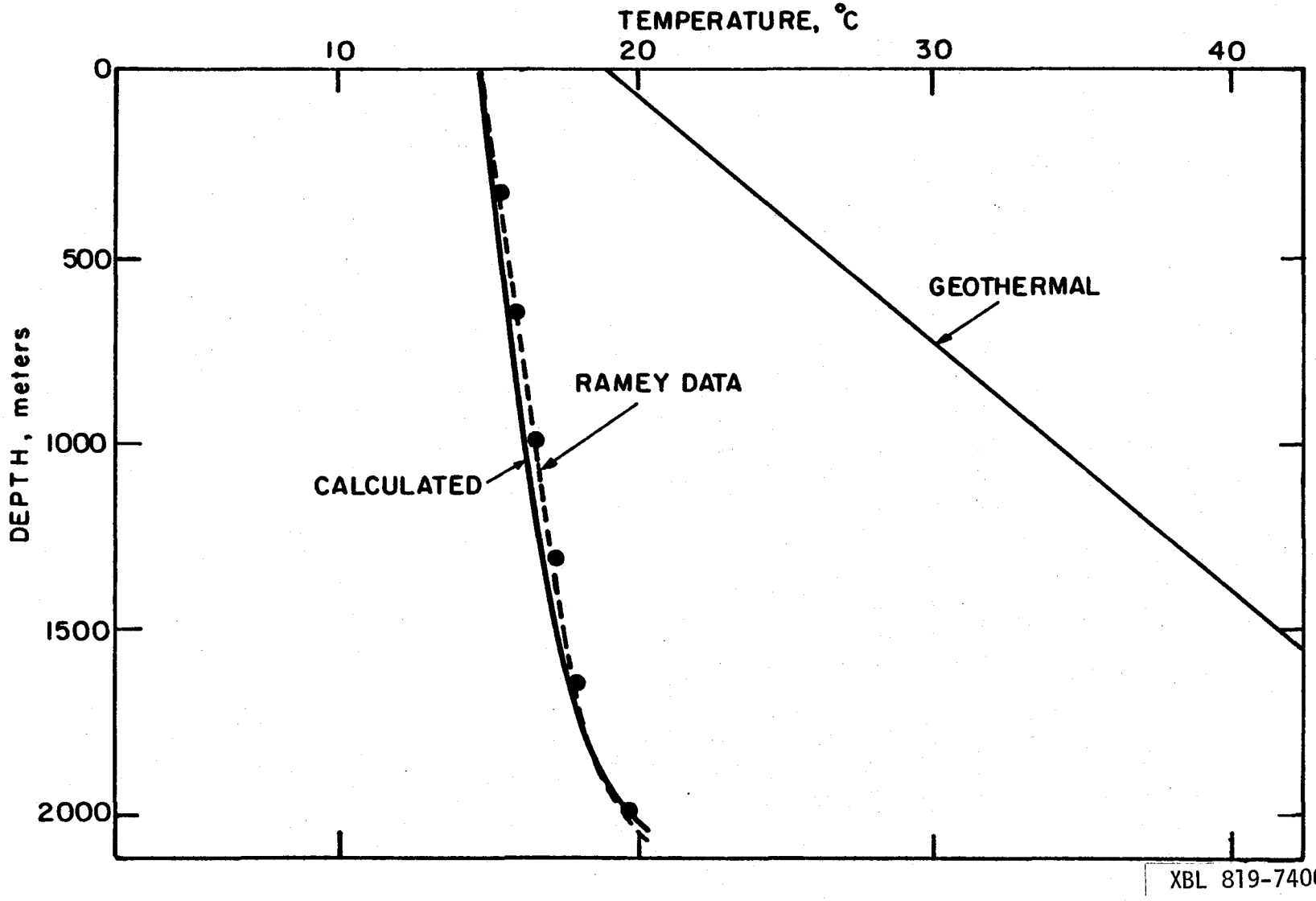

FIG. 14 COMPARISON OF MEASURED AND CALCULATED TEMPERATURES

temperatures except at the bottom of the well. The calculated temperatures, however, are within 0.5°C of the measured temperatures showing excellent agreement.

3.3 Temperature Distribution During Shut-in

3.3.1. Mathematical Model

In this section, study is directed towards simulating the temperature conditions that the fluid inside the wellbore experiences during shut-in. At the end of an injection period, the flow of fluid is stopped and the fluid becomes quiescent in the borehole. Just at shut-in, the fluid inside the borehole and the surrounding formation have the temperature distribution $T(z,r)$ and $\theta(z,r)$, respectively, as given by Equations (3.1) and (3.5).

The problem involved is that of determining the temperature as a function of time and position within a system which initially has some spatial distribution of temperature established within it. Inside the borehole, since there is no forced convection during shut-in, the major mode of heat transfer is either conduction or natural convection in the fluid. In order to develop a mathematical model, it is necessary to make several assumptions. These assumptions are:

(1) The kinematic viscosity, the thermal diffusivity, and the coefficient of volumetric expansion do not vary in the range of temperatures considered.

(2) Using the Boussinesq approximation, the law of variation of density with temperature is

$$\rho^{-1} = \rho_o^{-1}\{1 + \beta(T - T_o)\}, \qquad (3.20)$$

where ρ = density of the fluid at temperature T,

ρ_o = density of the fluid at temperature T_o,

β = coefficient of volumetric expansion of the fluid at temperature T_o.

(3) The boundary layer approximation applies, i.e. the radial rate of diffusion of momentum and heat is much more rapid than the axial rate. This may be justified by the large aspect ratio h, length/radius ratio. However, axial heat conduction in the wellbore and in the formation is taken into account in order to study the effect of variable thermal conductivities.

(4) The flow is symmetrical about the axis.

At the end of the injection period, the higher temperature fluid is at the top and the lower temperature fluid is as the bottom of the wellbore. Thus there is no fluid motion along the borehole axis at the beginning of the shut-in period. However, there may be movement of the fluid in the radial direction caused by the temperature difference between the center of the fluid column and the wall of the wellbore. This radial temperature gradient is induced by the heat conduction inside the fluid. This may result in a weak, steady circulation in the wellbore. The warmer fluid near the center of the wellbore rises up and flows towards the wall, the cooler fluid near the wall is drawn downwards and replaces the warmer fluid. To determine the fluid temperature distribution in the wellbore, the Navier-Stokes

equations of mass, momentum, and energy, which apply to the liquid for axis-symmetrical flow, and with the boundary layer approximation, are employed:

$$\frac{\partial u}{\partial z} + \frac{\partial v}{\partial r} + \frac{v}{r} = 0 \quad , \tag{3.21}$$

$$\frac{\partial v}{\partial t} + u\frac{\partial u}{\partial z} + v\frac{\partial u}{\partial r} = -g\,\frac{1}{\rho}\frac{\partial P}{\partial z} + \nu\left(\frac{\partial^2 u}{\partial r^2} + \frac{1}{r}\frac{\partial u}{\partial r}\right) \quad , \tag{3.22}$$

$$\frac{\partial P}{\partial r} = 0 \quad , \tag{3.23}$$

$$\frac{\partial T}{\partial t} + u\frac{\partial T}{\partial z} + v\frac{\partial T}{\partial r} = \frac{\alpha_w}{r}\frac{\partial}{\partial r}\left(r\frac{\partial T}{\partial r}\right) + \alpha_w\frac{\partial^2 T}{\partial z^2} \tag{3.24}$$

where: u = fluid velocity in axial direction,

v = fluid velocity in radial direction,

g = acceleration due to gravity,

p = pressure,

ν = kinematic viscosity of the fluid,

α_w = thermal diffusivity of the fluid.

The effect of natural convection is specified by the Rayleigh number, given by:

$$Ra = \beta g \Delta T r_w^3 / \alpha_w \nu \quad ,$$

where: β = volumetric expansion coefficient of the fluid,

$\Delta T = T_{\ell} - T_w$

T_{ℓ} = fluid center line temperature,

T_w = wall temperature,

and the aspect ratio $h = L/r_w$, where L is the length of the wellbore and r_w is the wellbore radius.

To determine whether the effect of natural convection can be ignored in this study, a model of purely heat conduction will be analyzed first. The maximum radial temperature gradient will be calculated from the conduction model, since convection would have the effect of reducing the temperature gradient. This maximum temperature gradient will be used to evaluate the Raleigh number later in the study.

(1) Conduction Model

Similar to the previous analysis, the model is divided into two parts; the fluid in the wellbore and the surrounding formation. Inside the wellbore, heat is conducted radially from the hot fluid through the tubing and insulating materials, if present, into the lower temperature formation. Because of the axial temperature gradient established during the injection period, heat is also conducted along the length of the wellbore. Under these circumstances, application of an energy balance to a cylindrical elemental volume of the fluid of thickness dz yields the equation:

$$\rho_w c_w \frac{\partial T}{\partial t} = \lambda_w \frac{\partial^2 T}{\partial z^2} + \lambda_w \left(\frac{\partial^2 T}{\partial r^2} + \frac{1}{r} \frac{\partial T}{\partial r} \right), \qquad (3.25)$$

where: λ_w = thermal conductivity of the fluid,

ρ_w = density of the fluid,

c_w = specific heat capacity of the fluid.

Because of symmetry there is no heat flow at the center of the wellbore or,

at $r = 0$,
$$\frac{\partial T}{\partial r} = 0 \quad . \tag{3.26}$$

At the wellbore wall the boundary condition for Equation (3.25) requires that the heat flux out of the wellbore be the same as the heat flux into the formation, i.e.,

at $r = r_w$,
$$\lambda_w \frac{\partial T}{\partial z} = \lambda \frac{\partial \theta}{\partial r} \quad , \tag{3.27}$$

At the top of the borehole, heat is lost from the fluid to the ambient and is given by:

at $z = 0$,
$$\lambda_w \frac{\partial T}{\partial z} = H\,(T-T_a) \tag{3.28}$$

where H is the heat transfer coefficient for surface heat loss, T_a is the ambient temperature. During the shut-in period, the fluid temperature at the bottom of the well changes continuously with time to reach the geothermal temperature. Therefore, it is very difficult to specify the boundary condition for the fluid at the bottom of the well. However, analysis of the injection zone indicated that in this zone the major part of the heat is transferred away from the wellbore in the radial direction by convection (Spillette, [65]; Smith, [62]). Heat conducted in the vertical direction into the overburden and underburden

formations are assumed to be relatively small. Moreover, because heat conduction is much larger in the radial direction than in the vertical direction in the fluid column, the axial boundary condition at the bottom of the well does not have much effect on the results of the upper parts. Under these circumstances, the fluid temperature at the bottom of the well is very close to the temperature of the fluid in the injection zone below it. Based on the solution obtained by Lauwerier [45], the boundary condition for the fluid at the bottom of the well can be specified as:

$$\text{at } z = L, \quad T(t,r,L) = \theta(t,r_w,L) + [T_{inj} - \theta(t,r_w,L)]\left(1.0 - \text{erfc}\ \frac{1}{\sqrt{\alpha_w t}}\right), \tag{3.29}$$

where: T_{inj} = injection temperature,

$\theta(t,r_w,L)$ = formation temperature at the bottom of the well,

α_w = fluid thermal diffusivity,

erfc = complimentary error function,

t = the time since the start of shut-in.

After shut-in, heat is continuously flowed from the hot fluid inside the wellbore into the adjacent formations to attain the thermal equilibrium condition. The heat is then diffused farther into the earth away from the wellbore/formation interface. As the shut-in time increases, temperatures of both the fluid in the wellbore and the formation approach the geothermal temperature.

Within the formation, heat flows by the conduction process. To describe the temperature of the formation surrounding the wellbore, the diffusion equation (3.5) and its boundary conditions are applicable:

$$\frac{\partial\theta}{\partial t} - \alpha(z)\frac{1}{r}\frac{\partial}{\partial r}\left(r\frac{\partial\theta}{\partial r}\right) - \frac{\partial}{\partial z}\left(\alpha(z)\frac{\partial\theta}{\partial z}\right) = 0 \qquad (3.5)$$

$$\text{at } r = r_w, \quad \lambda(z)\frac{\partial\theta}{\partial r} = U_T(\theta - T), \qquad (3.7)$$

$$\text{at } r \to \infty, \quad \theta = T_i(z), \qquad (3.10)$$

$$\text{at } z = 0, \quad \theta = T_a, \qquad (3.12)$$

$$\text{at } z = L, \quad \theta = T_a + \sum_i^m \frac{\Delta T}{\lambda_i(z)}\Delta z_i \qquad (3.13)$$

Just at shut-in, the formation has the temperature at the conclusion of injection:

$$\text{at } t = 0, \quad \theta = \theta_1$$

where θ_1 is the formation temperature evaluated at the end of injection from the injection model calculations.

(2) Modified Model with Natural Convection

In this section, a mathematical model which takes into account the effect of natural convection is developed based on the conduction model. The Rayleigh number, based on the radius of the wellbore and the maximum temperature difference of the fluid in the wellbore from the results of the conduction model calculations, is between 10^3 and 10^4. Elder [29] indicated that for Rayleigh numbers less

than 10^5, or less than 1770h, where h is the aspect ratio, conduction is the dominant mode of heat transfer in vertical enclosures. In this case, for Ra $<10^5$, relatively large temperature gradients develop near the wall, and in the inner region the temperature field closely satisfies LaPlace's equation. The higher temperature fluid near the center of the borehole flows toward the wall and displaces the lower temperature fluid. The convection occurs in the form of weak, local convection cells. The magnitude of the radial convection velocity v is of the order $(\lambda/\rho c r_w)_w$, as derived from the balance of conduction and convection (Gebhart, [32]). Using the approximation of the density variation given by Equation (3.20) the convection velocity can be approximated as:

$$v_{max} = [g\beta r_w (T_w - T_b)]^{1/2} \quad , \qquad (3.20)$$

where: g = acceleration due to gravity,

β = coefficient of volumetric expansion of the fluid,

r_w = wellbore radius,

$(T_w - T_b)$ = maximum radial temperature gradient.

This is an estimate of the maximum value since it was made neglecting viscous forces. For water and fluids with moderate and high Prandtl numbers, the maximum velocity will be much less than this value. In this wellbore model the magnitude of the maximum velocity is

$$v_{max} = 0.7 \times 10^{-4} \quad m/sec.$$

It is important to note here that the magnitude of the Rayleigh number and the maximum velocity are dependent upon radius of the wellbore and the radial temperature gradient. Natural convection would have the effect of flattening the temperature profile and reducing heat transfer in this direction. Thus the Rayleigh number and the maximum velocity reduce as the shut-in time increases.

For a detailed theoretical description of the natural convection heat transfer process, three equations are necessary: continuity, momentum, and energy. However, under these circumstances, as discussed above, the effect of natural convection is small compared with conduction, the fluid velocity induced by natural convection is relatively small and the convection cells are weak and local. A modified model is developed in order to take these effects into account. Instead of solving a set of three equations, additional terms will be added to the energy equation of the conduction model. These terms have the same form as the diffusion term in the energy equation, but produce the effect of reducing the heat transfer in the radial direction and flattening the radial temperature profile. One term simulates the process of warmer fluid flowing radially outwards toward the wellbore wall and another term simulates the process of cooler fluid flowing downward and displacing the warmer fluid. The modified energy equation, which takes the effect of weak and local natural convection into account, is expressed as follows:

$$\frac{\partial T}{\partial t} = \alpha_w \frac{\partial^2 T}{\partial z^2} + \alpha_z \frac{\partial^2 T}{\partial z^2} + \frac{\alpha_w}{r}\left(\frac{1}{r}\frac{\partial T}{\partial r} + \frac{\partial^2 T}{\partial r^2}\right)$$

$$- \frac{\alpha_r}{r}\left(\frac{1}{r}\frac{\partial T}{\partial r} + \frac{\partial^2 T}{\partial r^2}\right) \qquad (3.21)$$

where: α_w = thermal diffusivity of the fluid,

$\alpha_z = a\alpha_w$,

$\alpha_r = b\alpha_w$.

Coefficients a and b can be varied so that the maximum Rayleigh number is less than 10^3. For Ra $<10^3$ the effect of natural convection is negligible. The initial and boundary conditions for the conduction model are applicable in this case.

To solve for the temperature of the formation surrounding the wellbore, the diffusion equation (3.5) and its initial and boundary conditions are employed.

3.3.2 Numerical Formulation

Similar to the previous section, temperature distributions of the fluid inside the wellbore and the surrounding formation are obtained numerically. An implicit (ADI) finite difference technique is employed to solve for both the fluid and formation temperatures. The resulting finite difference equations for the temperature of the fluid inside the wellbore are given as:

$$T_{i,j}^{n+1/2} - T_{i,j}^{n} = \frac{\alpha_w \Delta t}{r_{j+1} - r_{j-1}} \left\{ r_{j+1/2} \frac{T_{i,j+1}^{n+1/2} - T_{i,j}^{n+1/2}}{r_{j+1} - r_j} - r_{j-1/2} \frac{T_{i,j}^{n+1/2} - T_{i,j-1}^{n+1/2}}{r_j - r_{j-1}} \right\}$$

$$+ \frac{\alpha_w \Delta t}{2} \frac{T_{i+1,j}^{n} - 2T_{i,j}^{n} + T_{i-1,j}^{n}}{\Delta z^2} \qquad (3.22)$$

and

$$T_{i,j}^{n+1} - T_{i,j}^{n+1/2} \frac{\alpha_w \Delta t}{r_{j+1} - r_{j-1}} \left\{ r_{j+1/2} \frac{T_{i,j+1}^{n+1/2} - T_{i,j}^{n+1/2}}{r_{j+1} - r_j} - r_{j-1/2} \frac{T_{i,j}^{n+1/2} - T_{i,j-1}^{n+1/2}}{r_j - r_{j-1}} \right\}$$

$$+ \frac{\alpha_w \Delta t}{2} \frac{T_{i+1,j}^{n+1} - 2T_{i,j}^{n+1} + T_{i-1,j}^{n+1}}{\Delta z^2} \quad . \qquad (3.23)$$

To solve these equations and to resolve the boundary layer regime where the fluid temperature changes rapidly, again, a variable radial grid system is used.

A reservoir model is connected to the wellbore model so that the heat transfer is consistent with the temperature field of the system. The heat flow rate out of the wellbore and into the formation must be equal. A set of finite difference equations, similar to Equations (3.16) and (3.17), are applicable to solve for the formation temperature in this case.

$$\frac{\theta_{i,j}^{n+1/2} - \theta_{i,j}^{n}}{\Delta t/2} - \frac{2\alpha_i}{r_{j+1} - r_{j-1}} \left\{ r_{j+1/2} \frac{\theta_{i,j+1}^{n+1/2} - \theta_{i,j}^{n+1/2}}{r_{j+1} - r_j} - r_{j-1/2} \frac{\theta_{i,j}^{n+1/2} - \theta_{i,j-1}^{n+1/2}}{r_j - r_{j-1}} \right\}$$

$$- \frac{\alpha_{i+1}\theta_{i+1,j}^{n} - 2\alpha_i \theta_{i,j}^{n} + \alpha_{i-1}\theta_{i-1,j}^{n}}{\Delta z^2} = 0 \qquad (3.24)$$

$$\frac{\theta_{i,j}^{n+1} - \theta_{i,j}^{n+1/2}}{\Delta t/2} - \frac{2\alpha_i}{r_{j+1} - r_{j-1}} \left\{ r_{j+1/2} \frac{\theta_{i,j+1}^{n+1/2} - \theta_{i,j}^{n+1/2}}{r_{j+1} - r_j} - r_{j-1/2} \frac{\theta_{i,j}^{n+1/2} - \theta_{i,j-1}^{n+1/2}}{r_j - r_{j-1}} \right\}$$

$$- \frac{\alpha_{i+1}\theta_{i+1,j}^{n+1} - 2\alpha_i \theta_{i,j}^{n+1} + \alpha_{i-1}\theta_{i-1,j}^{n+1}}{\Delta z^2} = 0 \ . \tag{3.25}$$

The new fluid temperature in the wellbore is solved first using the old value of the formation temperature. Then the new temperature in the formation is calculated by determining the heat that flowed from the wellbore into the formation over that time interval. When the energy equation of the fluid inside the wellbore is solved, the heat transfer at the wall is:

$$\lambda_w \frac{\partial T}{\partial r} = U_T(\theta^n - T^n) \ . \tag{3.26}$$

Because this boundary condition for the heat flow is solved partially explicitly, there is a stability limit. The stability condition in terms of the radial spacing is (Miller [49]):

$$\left| \frac{(\Delta r_m + \Delta r_{m-1}) r_{m-1} \Delta r_m + 2\alpha\Delta t \left[\frac{\Delta r_m}{\Delta r_{m-1}} r_{\frac{m-1}{2}} \pm \left(r_{\frac{m}{2}} + \frac{\Delta r_m}{\Delta r_{m-1}} r_{\frac{m-1}{2}} \right) \right]}{(\Delta r_m + \Delta r_{m-1}) r_{m-1} \Delta r_m - 2\alpha\Delta t r_{\frac{m}{2}}} \right| \geq 1.0 \tag{3.27}$$

where: $\Delta r_m = r_m - r_{m-1}$, $\Delta r_{m-1} = r_{m-1} - r_{m-2}$

and $r_{\frac{m}{2}} = (r_m + r_{m-1})/2$, $r_{\frac{m-1}{2}} = (r_{m-1} + r_{m-2})/2$.

Once the fluid temperature in the wellbore at new time level is known, the new value of the formation temperature can be calculated using this new value of the wellbore fluid temperature. When the temperature of the formation is calculated, the boundary condition at the formation/wellbore interface is:

$$\lambda\frac{\partial\theta}{\partial r} = U_T(\theta^{n+1} - T^{n+1}) \quad . \qquad (3.28)$$

No stability problems are encountered because the temperature of the formation is solved implicitly, even at the boundary.

The model is now solved for the fluid temperature in the wellbore, including heat loss to the surrounding formations.

3.3.3 Numerical Results and Discussion

At shut-in, the flow of fluid in the wellbore is stopped and the effect of ceasing injection can be regarded as that of stopping a heat source inside the wellbore. The temperature of the fluid will gradually return to its initial state by transfer of heat into the surrounding formations. Several calculations are made to illustrate the development of the fluid temperature profile inside the wellbore during shut-in. The intent is to determine the effects of the formation thermal conductivities and the wellbore characteristics on the fluid temperature behavior.

Just after shut-in, radial conduction becomes important. Heat is conducted from the hot fluid at the center of the borehole towards the borehole wall through the wellbore tubing, insulating material, casing, and cement, and into the formation. Initially, at the end of injection, there is assumed to be no radial temperature gradient in the fluid because of the mixing process in the turbulent flow during injection but, as the radial conduction becomes larger, the radial temperature gradient develops and reaches the maximum value at about one hour after shut-in. The growth of the fluid temperature gradient near the borehole wall causes the heat transferred from the wellbore fluid to the adjacent formations to increase. However, due to the relatively low value of the formation thermal conductivity, most of the heat lost from the wellbore will stay in the portion of formation adjacent to the well and conduct slowly farther into the earth away from the wellbore. This will slow down the rate of heat transfer from the wellbore fluid to the formation. After the fluid radial temperature gradient reaches the maximum value,it decreases as the shut-in time increases. These effects are shown in dimensionless form in Figure 15. The development of the radial heat conduction in the fluid, inside the wellbore, after shut-in can be seen by comparing the radial temperature gradient to its maximum value.

Another calculation using a modified form of the model was carried out to illustrate the effect of natural

convection in the wellbore. The resulting fluid temperature behavior is also shown in Figure 15, where the results of the two models are compared. As indicated in the analysis, natural convection has the effect of flattening the radial temperature gradient of the fluid in the inner region of the wellbore. However, since the higher temperature fluid moves toward the borehole wall and exchanges heat with the adjacent formation, the temperature profile is steeper near the borehole wall during early shut-in times. After four hours of shut-in the temperature profiles of the two models are similar and after twelve hours of shut-in they nearly coincide. This result indicates that the effect of natural convection on the fluid temperature profile in the wellbore is only important in the early shut-in times, and becomes negligible in comparison with heat conduction after long shut-in times, say twelve hours. This also shows that natural convection does not have much effect on the rate of return of the wellbore fluid temperature to equilibrium at long shut-in times.

(1) Effect of Changing Wellbore Radius

Figure 16 shows the effect of changing the wellbore radius on the fluid temperature distribution in the wellbore during shut-in. It is observed that, for the same initial condition and other variables kept constant, as the wellbore radius decreases the radial temperature gradient decreases since Rayleigh number and convection velocity vary in proportion to the wellbore radius.

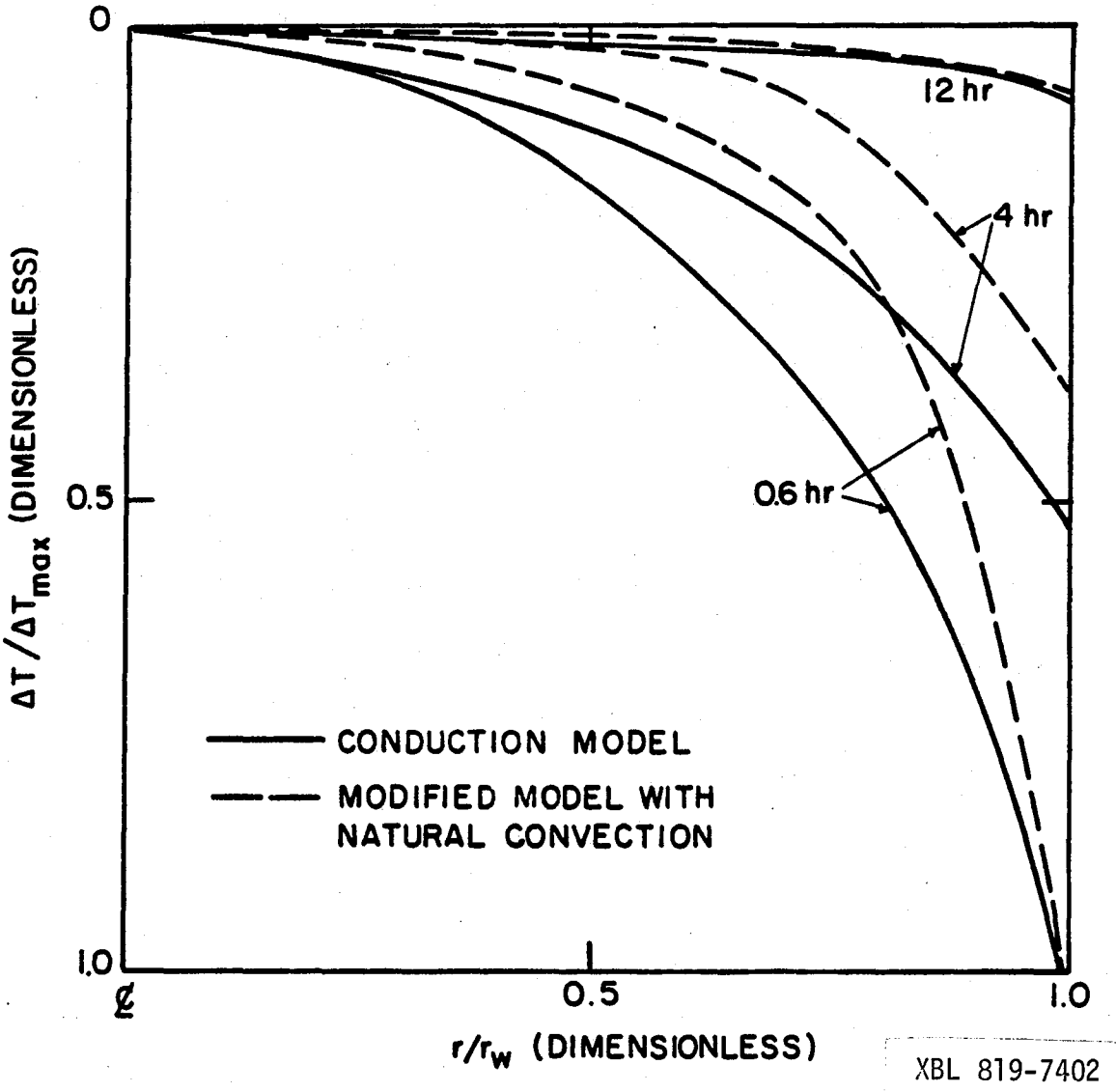

FIG. 15 RADIAL TEMPERATURE DISTRIBUTION INSIDE WELLBORE DURING SHUT-IN

However, the rate of return of the fluid temperature to equilibrium increases as the wellbore radius decreases. The area available for heat transfer at the wall, $2\pi L r_w$ varies linearly with the radius r_w, while the volume of the fluid inside the wellbore, $\pi L r_w^2$, varies with r_w^2 and so does the amount of heat contained in the fluid column needed to be transferred away to return to equilibrium. As the radius is reduced by one-half, the amount of heat needed to be transferred into the formation is reduced by a factor of four so that the fluid temperature inside the wellbore will reach the geothermal temperature faster. Figure 16 indicates that after 96 hours of shut-in, for r_w = 0.08m the fluid temperature inside the wellbore is within 4% of the geothermal temperature, while for r_w = 0.04m the fluid temperature is within 2.5% of the geothermal temperature at the same time.

(2) Effect of Overall Heat Transfer Coefficient

In this section the effect of insulation on the fluid temperature is investigated. Effects of a ten-fold change in the overall heat transfer coefficient on the temperature profile can be seen on Figure 17. The effect is very apparent near the borehole wall, where heat is transferred from the fluid to the formation through the wellbore. The higher value of overall heat transfer coefficient results in a steeper temperature gradient in the fluid near the borehole wall at early shut-in times. Similarly, for the higher value of overall heat transfer coefficient, the fluid

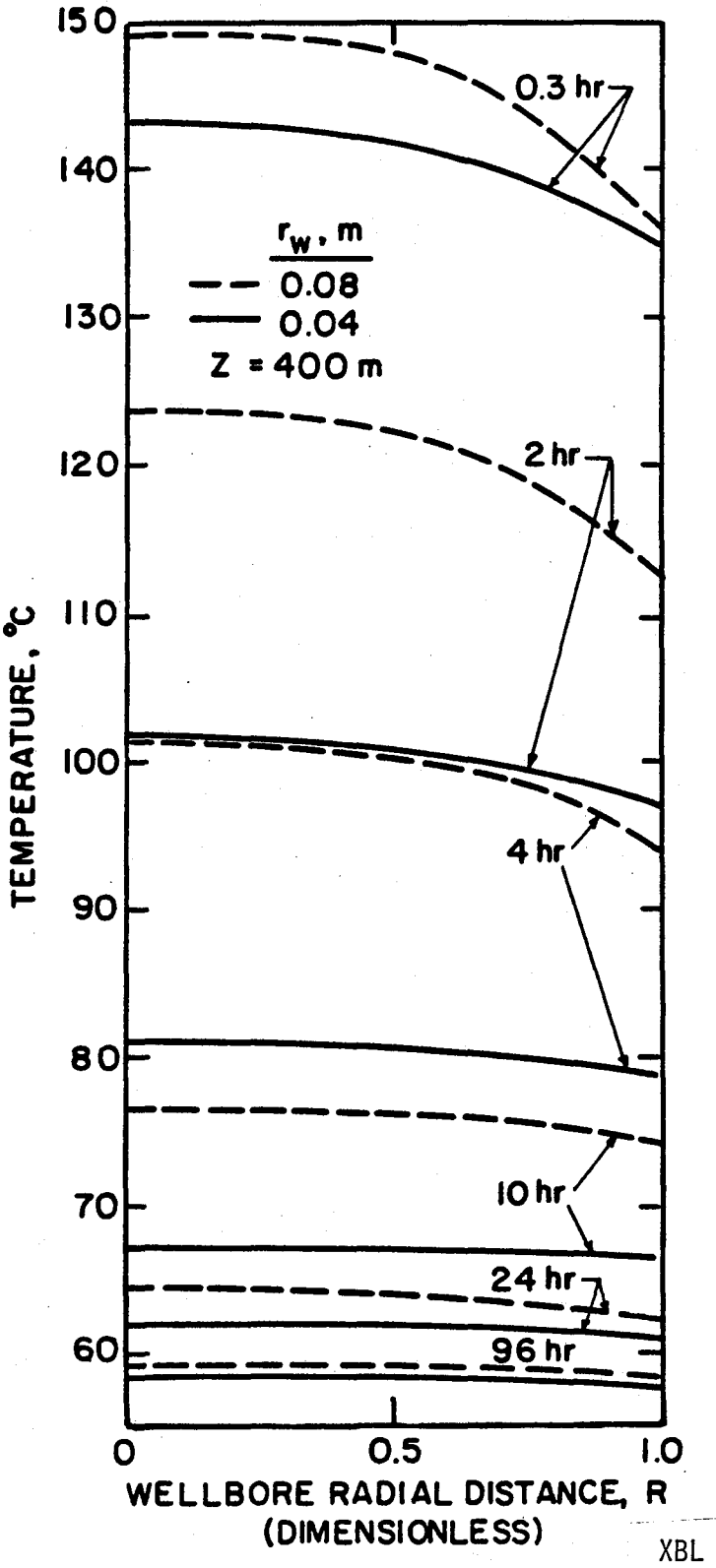

XBL 819-7405

FIG. 16 WELLBORE FLUID TEMPERATURE DISTRIBUTION DURING SHUT-IN EFFECT OF WELLBORE RADIUS

temperature inside the wellbore will return to its initial value faster at early shut-in times since more heat is transferred to the adjacent formations. However, as the fluid temperature decreases the difference between the fluid temperature and the adjacent formation temperature is reduced and becomes negligible when the shut-in time is very long as seen in Figure 18. This will reduce the rate of heat transfer from the fluid to the formation at long times. For the case of the lower overall heat transfer coefficient, U_T, there is a large temperature difference between the fluid and adjacent formation during early shut-in times. This temperature difference still exists even at long times, but with smaller magnitude, so that heat is continuously transferred from the fluid to the formation at larger rates than the case of higher overall heat transfer coefficient when the shut-in time is very long. Moreover, during injection, conduction heats the formation more in the case of the high U_T than in the case of low U_T. As a result, the fluid temperature approaches the geothermal temperature faster at long shut-in times for the case of low U_T. It is important to note here that the overall heat transfer coefficient has an effect only on the rate of temperature return but not on the temperature profile at long shut-in times. After 24 hours of shut-in time, the fluid temperature profiles for different values of the overall heat transfer coefficient are similar, as shown in Figures 17 and 22.

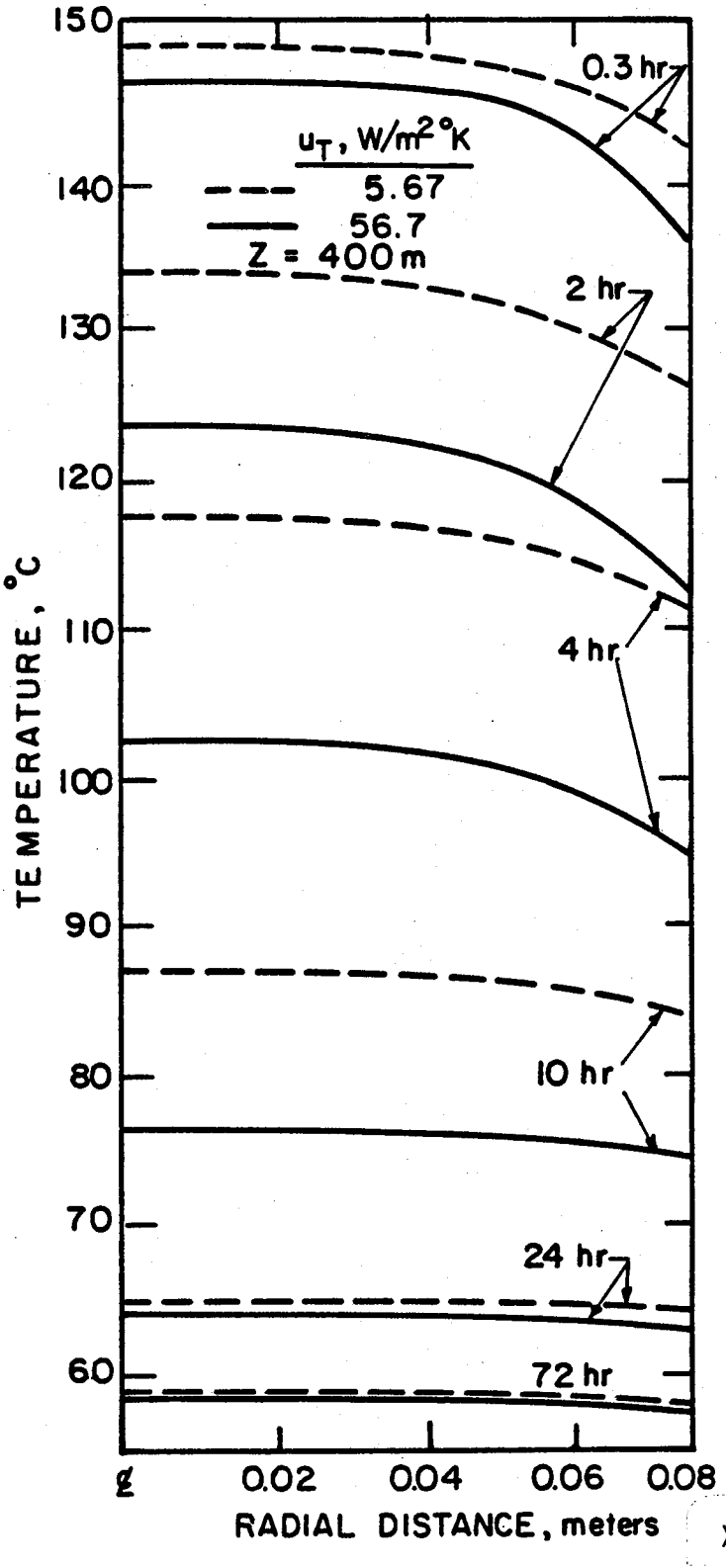

FIG. 17 WELLBORE FLUID TEMPERATURE DISTRIBUTION DURING SHUT-IN EFFECT OF THE OVERALL HEAT TRANSFER COEFFICIENT

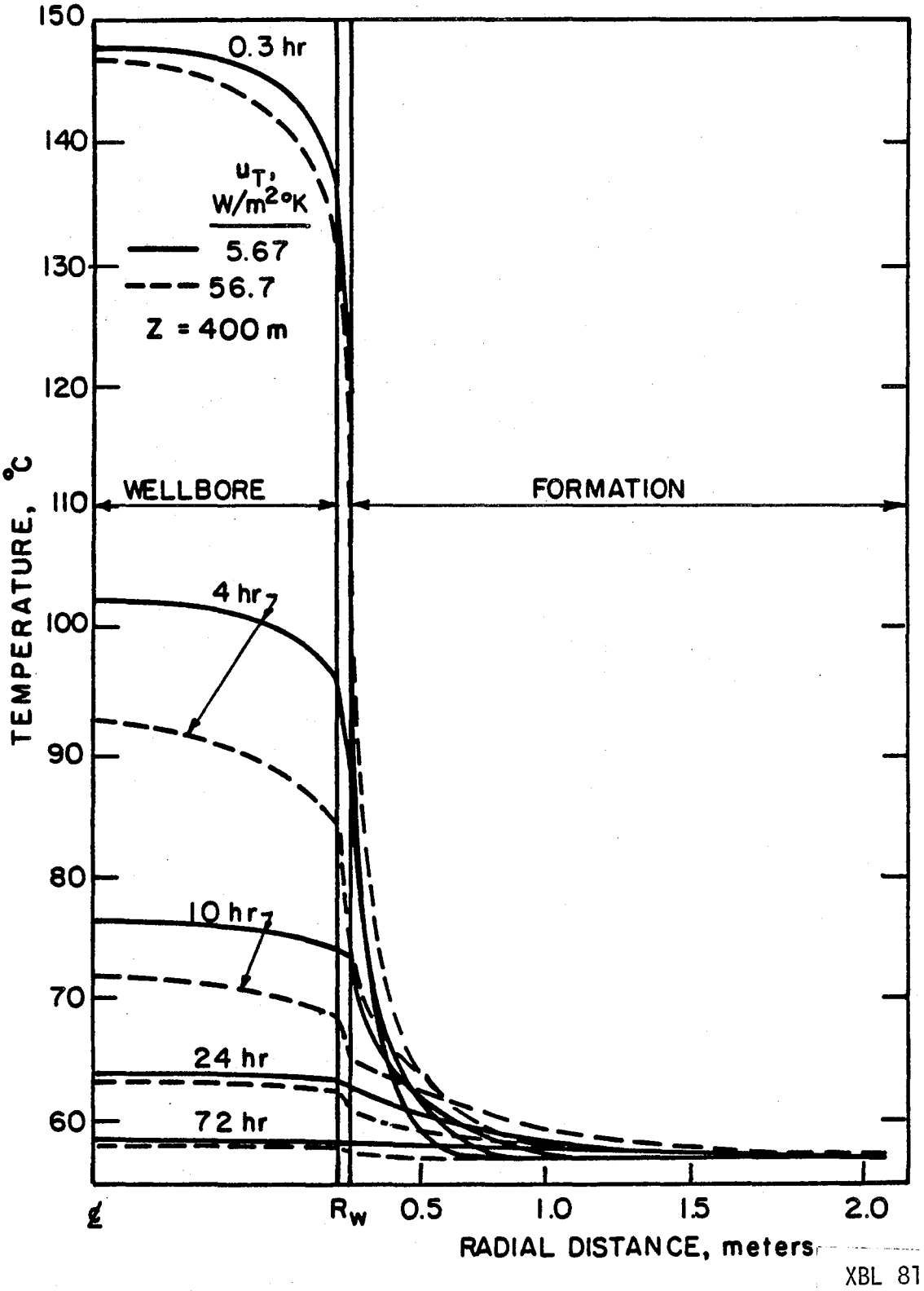

FIG. 18 TEMPERATURE TRACE DURING SHUT-IN

(3) Effect of Injection Time

As indicated earlier, even though the fluid temperature profile during injection is not very sensitive to injection time, at long times, more heat is accumulated in the formation adjacent to the wellbore and the temperature of a larger volume of formation surrounding the wellbore is increased as the injection time increases. As a result, there is less heat return at early shut-in times and as one would expect, longer times are needed for the fluid temperature to return to its initial value. Wellbore fluid temperature curves after 24 hours of shut-in are presented for cumulative injection times of 24 hours and 72 hours at a constant injection rate of 40,000kg/hr and variable thermal conductivities of the formations in Figure 19. The higher cumulative injection time causes the 24 hour shut-in curve to be displaced farther from the geothermal temperature.

(4) Effect of Variable Thermal Conductivities

During the shut-in period, the fluid temperature profile inside the wellbore is strongly affected by differences in formation thermal conductivities. Since conduction is the dominant heat transfer process during shut-in, the formation which has the higher value of thermal conductivity will conduct heat away from the wellbore faster than the lower thermal conductivity region. As a result, the fluid inside the wellbore which is in contact with the high thermal conductivity formation will have the temperature

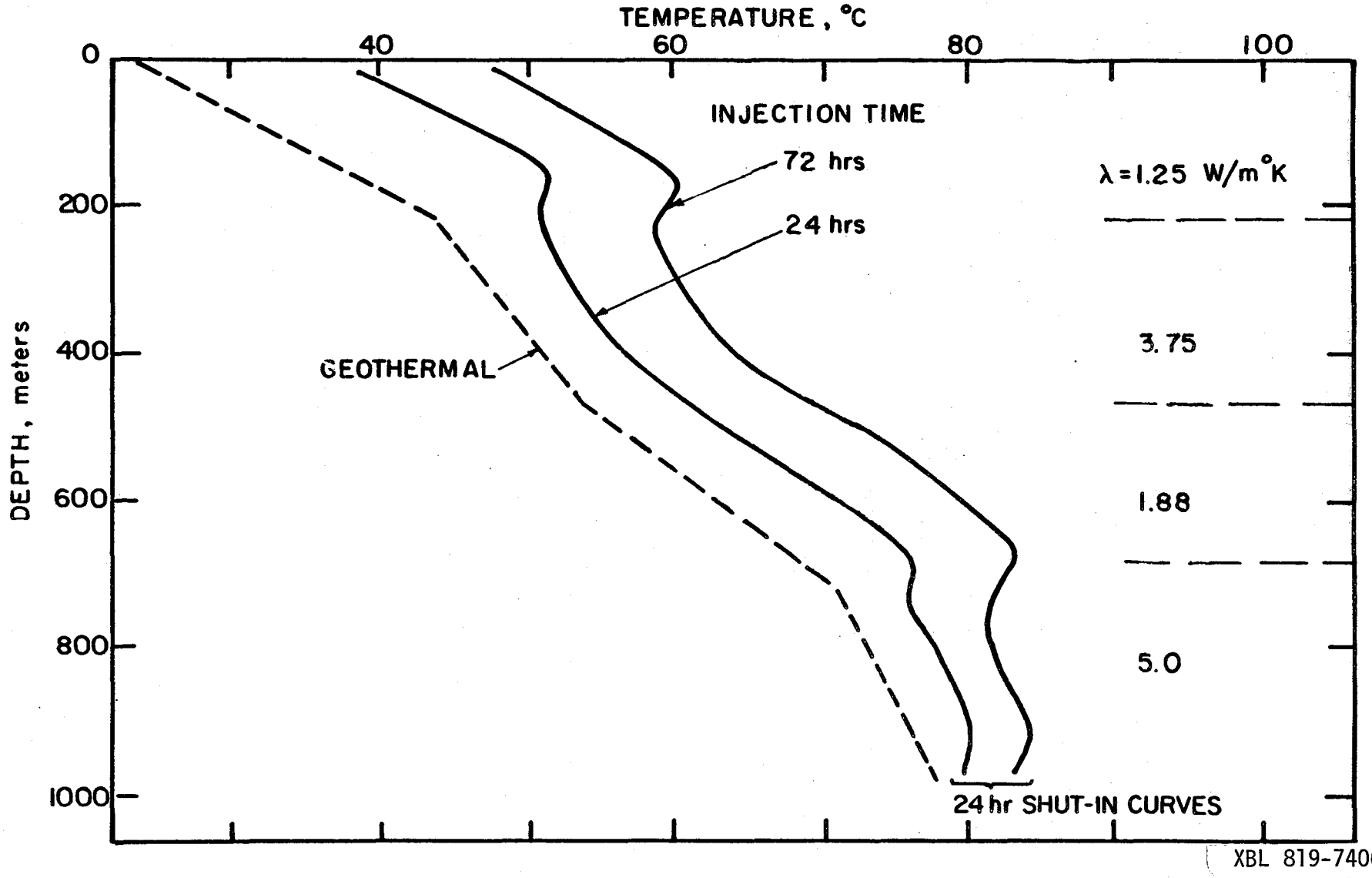

FIG. 19 WELLBORE FLUID TEMPERATURE DISTRIBUTION DURING SHUT-IN (CUMULATIVE INJECTION EFFECT)

return to its initial value rapidly. Figure 19 shows that, because of the variable thermal conductivity of the formations, the fluid temperature gradients are not constant but vary along the length of the wellbore at the locations where thermal conductivity of the formations change abruptly. It also shows that the fluid temperature profiles have the shape similar to the geothermal temperature profile. Figure 20 shows the approach to equilibrium with time of the fluid temperature inside the wellbore which is surrounded by variable thermal conductivity formations. The ratio of temperature differences $(T_s - T)/(T_s - T_i)$, where T_s is the fluid temperature just at shut-in and T_i is its initial value, i.e. geothermal temperature, is plotted versus time. After 12 hours of shut-in, the fluid temperature is within 17% of the original geothermal value for the λ= 5.0w/m°C formation layer, 23% for the λ = 3.75w/m°C formation layer, and 34% for the λ = 1.25w/m°C formation layer. After 72 hours of shut-in the fluid temperature is witin 2.5% of the original geothermal value for the λ = 5.0w/m°C formation layer, 4% for the λ= 3.75w/m°C formation layer, and 7.5% for the λ = 1.25w/m°C formation layer. The rate of return to equilibrium of the fluid temperature (during shut-in) increases very rapidly in the first 12 hours of shut-in and begins to approach a slow, logarithmic rate after 48 hours of shut-in.

Figure 21 shows the fluid temperature profile along the wellbore axis during shut-in. Effect of variable

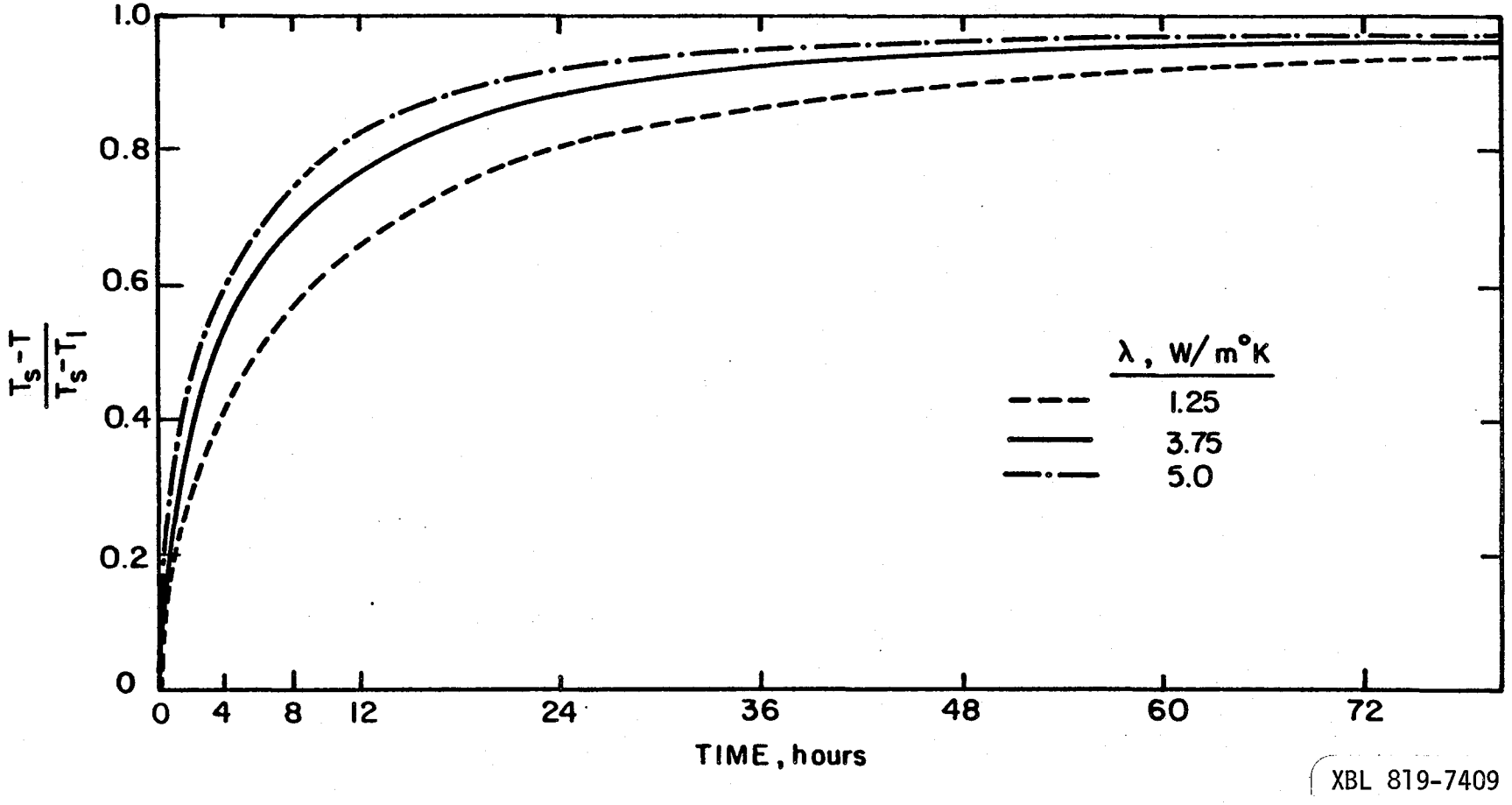

FIG. 20 EFFECT OF VARIABLE THERMAL CONDUCTIVITY ON THE PROGRESS OF RETURN TO EQUILIBRIUM OF THE FLUID TEMPERATURE DURING SHUT-IN

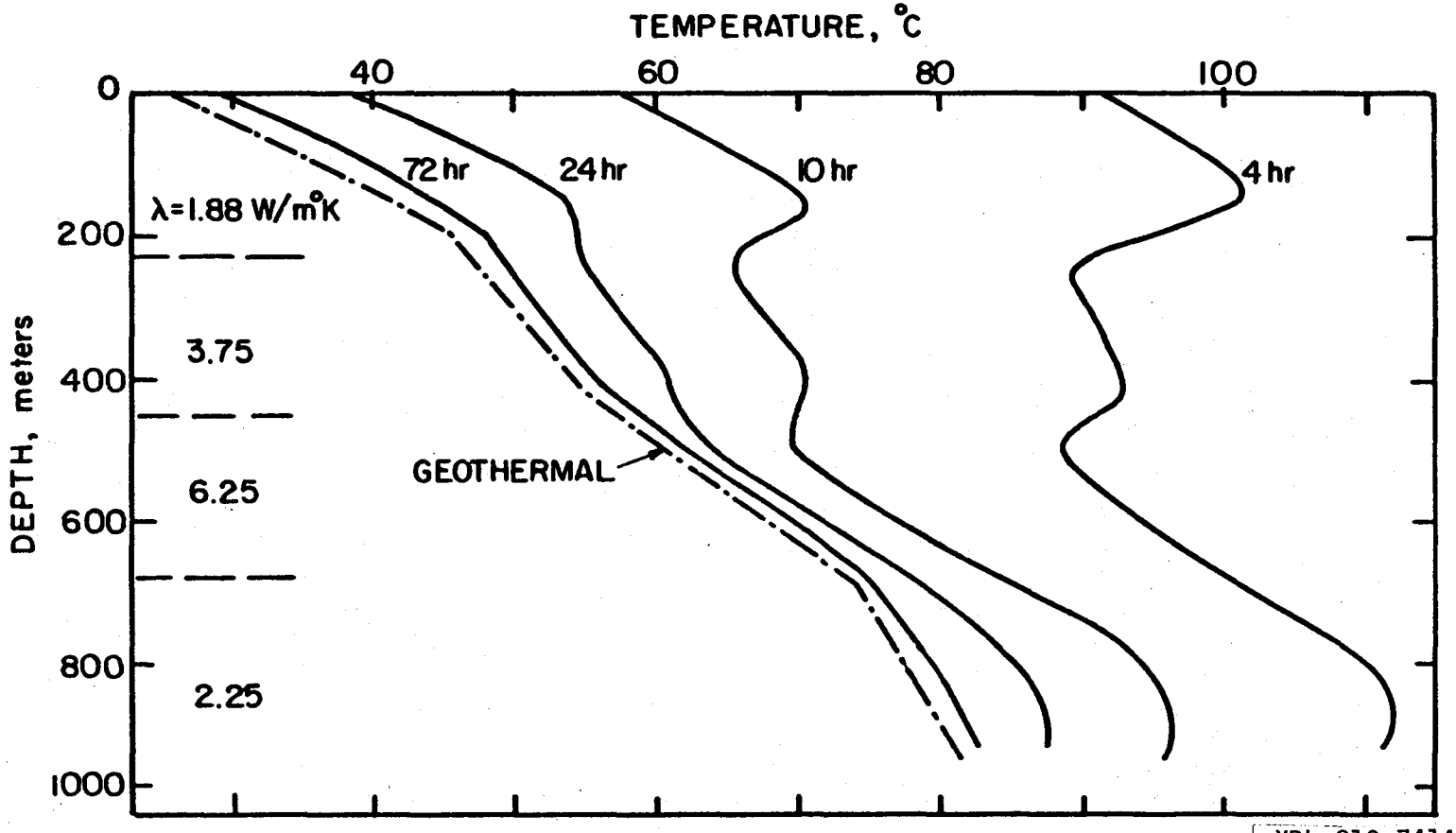

FIG. 21 WELLBORE FLUID TEMPERATURE DISTRIBUTION DURING SHUT-IN VARIABLE THERMAL CONDUCTIVITY

thermal conductivities of the formation is very apparent after four hours of shut-in. The fluid temperature in the wellbore, which is in contact with the higher thermal conductivity formation layers, approaches the geothermal temperature very rapidly during the first 12 hours of shut-in whereas the fluid temperature in the lower thermal conductivity layers approaches the geothermal temperature more slowly. After 24 hours of shut-in the fluid temperature profile has the shape similar to that of the geothermal. After 72 hours of shut-in the fluid temperature inside the wellbore is very close to the geothermal temperature, and this temperature profile varies along the depth of the wellbore proportional to the value of the formation thermal conductivities.

Figures 21 and 22 show that during early shut-in times, there exist negative gradients in the wellbore fluid temperature profile where the formation thermal conductivity changes abruptly from a smaller value to a greater value. A three-fold change in thermal conductivity is not uncommon in subsurface formations. It can be explained that in the low thermal conductivity formation region, heat is conducted slowly away from the wellbore whereas in the high thermal conductivity formation region heat is conducted much faster so that the fluid temperature returns to the original geothermal value more quickly. Differences in the formation thermal conductivities lead to uneven rates of return of temperature to equilibrium and will result in the negative gradients in some

sections of the fluid profile. These negative temperature gradients are relatively large at early shut-in times and become smaller as the time increases. The decrease in the temperature differences between the fluid and the formation with time and the approach to a constant value of the rate of heat transfer from the fluid to the formation will cause these negative temperature gradients to diminish. Figure 22 indicates that for different values of the overall heat transfer coefficient the fluid temperature profiles inside the wellbore are similar after 24 hours of shut-in. However, in the case of low overall heat transfer coefficient, the negative gradient persists for a longer shut-in time. This result implies that after long shut-in times, say 24 hours, the fluid temperature profile inside the wellbore is primarily controlled by the formation thermal conductivities.

Figure 22 shows the fluid temperature distribution during shut-in with a different set of formation thermal conductivities than Figure 21. It indicates that the fluid temperature profile during shut-in is very sensitive to the formation thermal conductivity variation. This contrast can be seen by comparing the fluid temperature distributions in Figures 22 and 23. Figure 23 shows the wellbore fluid temperature distributions during shut-in for a well which is surrounded by a uniform thermal conductivity formation. In both cases, the wellbore fluid temperature exhibits the same behavior as the formation thermal conductivity variation

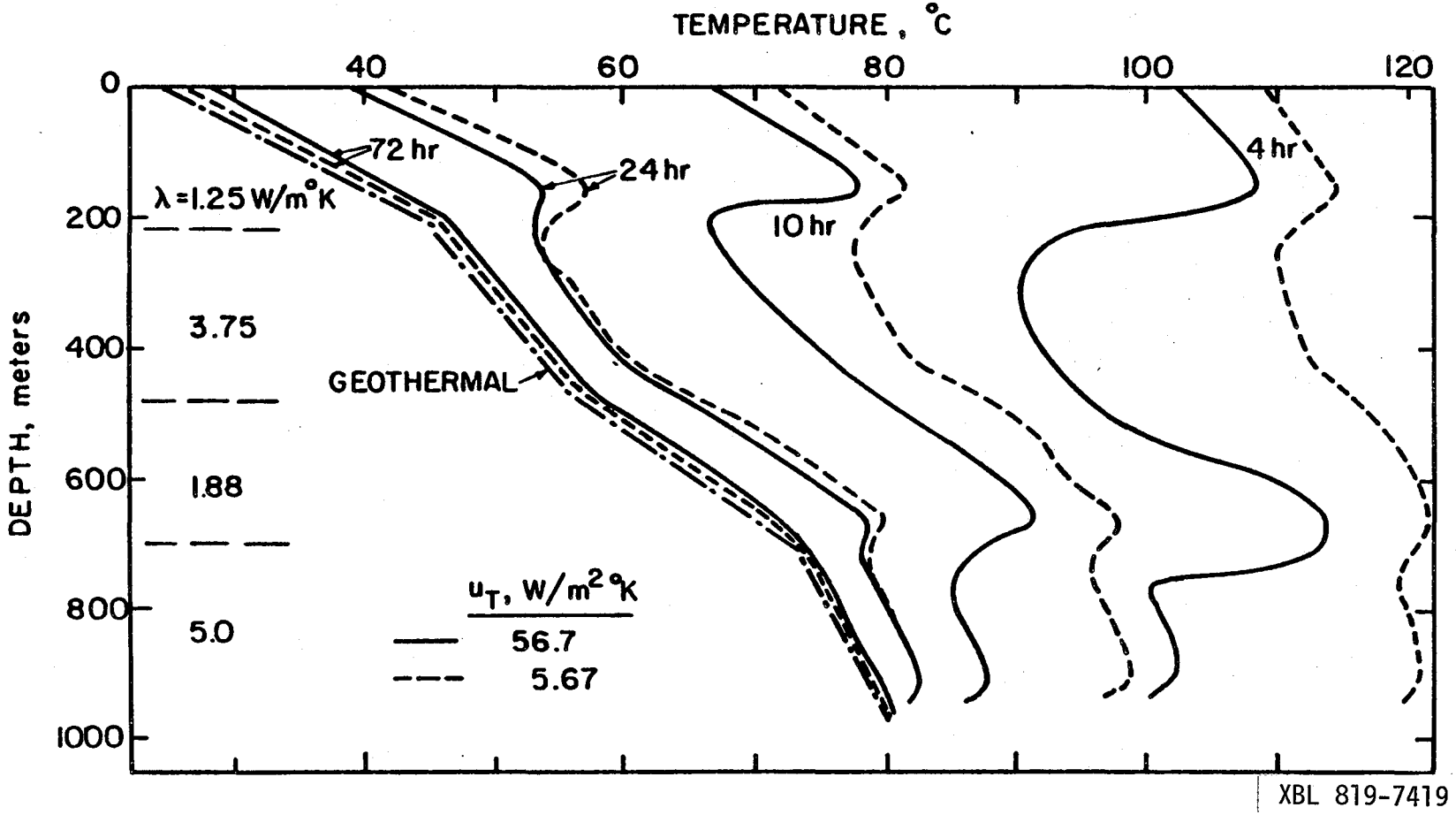

FIG. 22 WELLBORE FLUID TEMPERATURE DISTRIBUTION DURING SHUT-IN VARIABLE THERMAL CONDUCTIVITY AND OVERALL HEAT TRANSFER COEFFICIENT

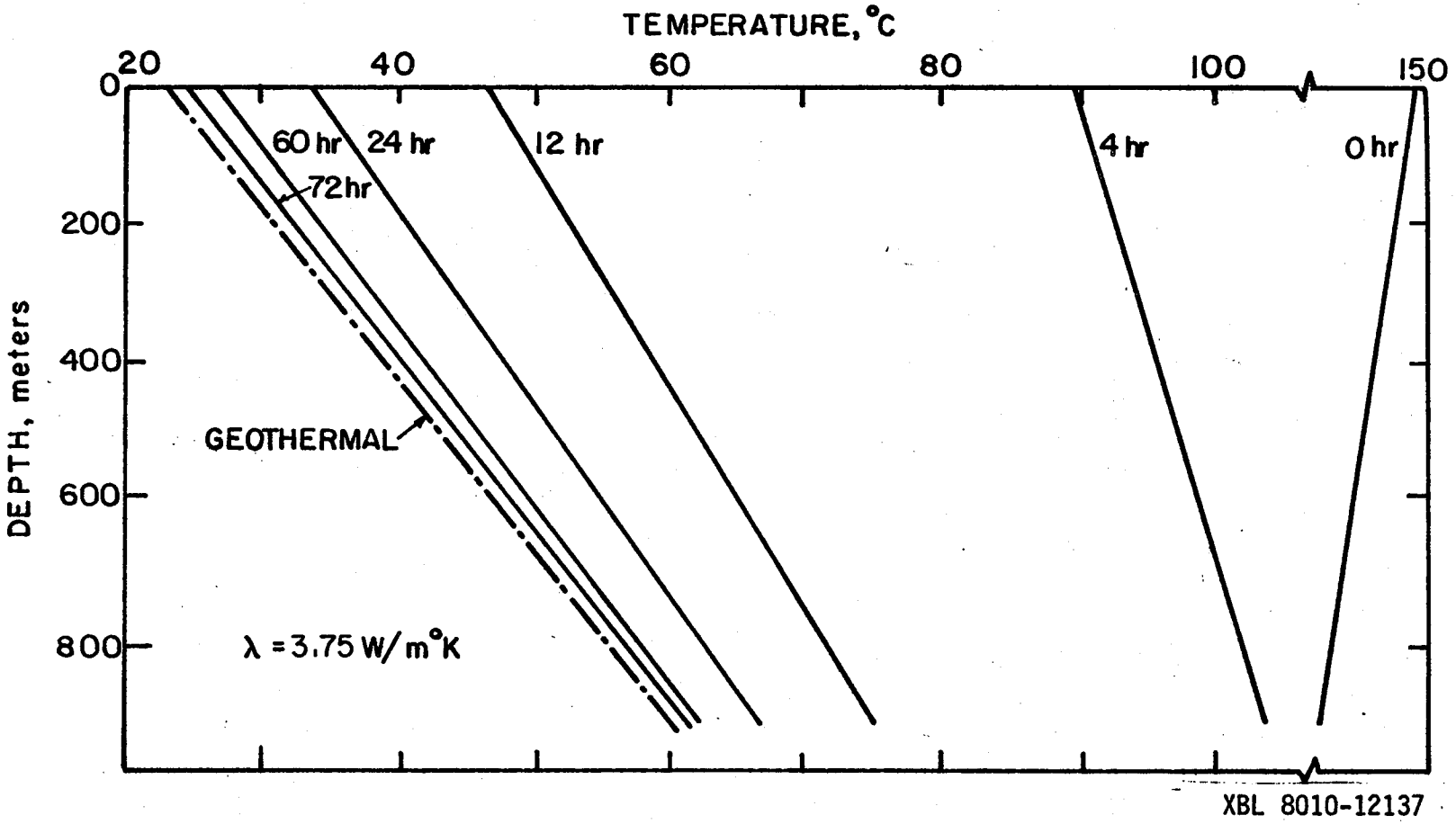

FIG. 23 WELLBORE FLUID TEMPERATURE DISTRIBUTION DURING SHUT-IN
UNIFORM THERMAL CONDUCTIVITY

after 72 hours of shut-in, i.e., the gradients vary along the length of the wellbore in proportion to the magnitude of the thermal conductivity of the formations.

3.3.4. Comparison with Published Field Data

The temperature behavior of the shut-in wellbore from calculations based on the mathematical model can be compared with published field results. The comparison is made with the temperature profile of a water injection well during the shut-in period. These well measurements are reported by Nowak [52]. Figure 24 presents a comparison of temperatures measured in a water injection well after three days of shut-in,with calculated temperatures. Water at a surface temperature of 28.4°C is injected down the well at a rate of 5960kg/hr for a period of three years. A temperature survey is made after three days of shut-in. In the upper portion of the wellbore measured temperature profile, the fluid temperature is higher than the formation temperature and at shut-in it is cooled off towards the geothermal temperature. In the lower portion of the temperature profile, the fluid temperature is lower than the formation temperature and it is heated up approaching geothermal. The temperature profile becomes linear at about 1500m depth and has the same slope as the geothermal temperature curve. The calculated temperatures, shown by the solid line in Figure 24, exceed the measured temperatures for the depths between 190m and 1500m, and become lower than the measured temperatures for the remaining portion of the well. Except for

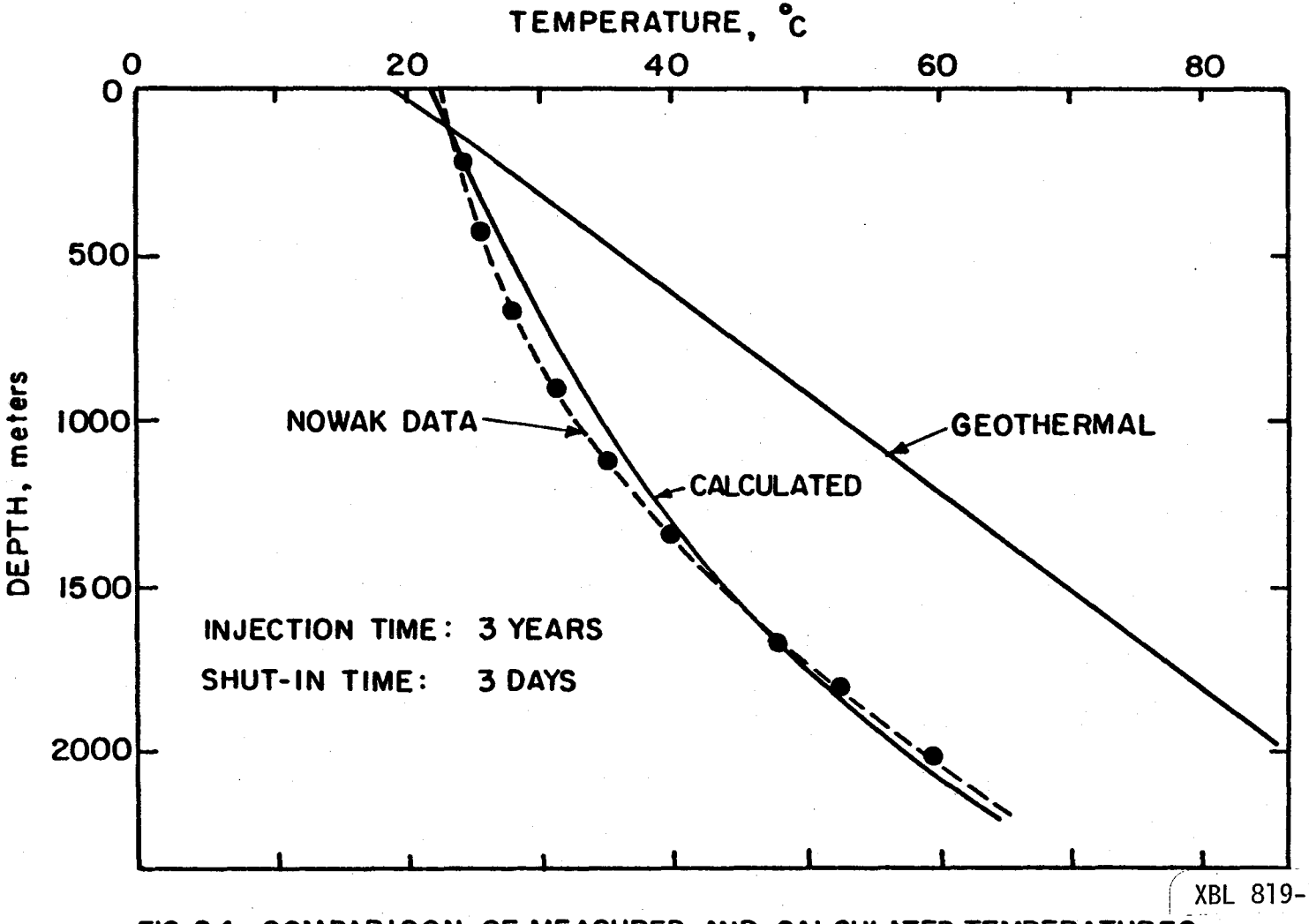

FIG. 24 COMPARISON OF MEASURED AND CALCULATED TEMPERATURES DURING SHUT-IN

the depths between 400m and 1000m where water loss from the casing was found and the discrepancy is relatively large, the calculated temperatures are within 1°C of the measured temperatures. This indicates satisfactory agreement between the two results.

3.4 Temperature Distribution in the Shut-in after Production Case

3.4.1. Analysis

In this section, the temperature conditions that the fluid inside the wellbore experiences during shut-in after producing the well, will be investigated. In the production well, hot fluid from the producing zone of the formation enters at the bottom of the well and flows up the wellbore. As the fluid flows up the wellbore, its temperature is determined by the rate of heat convection up the borehole and the rate of heat exchange between the formations adjacent to the wellbore and the fluid inside the well.

The mathematical model of the injection shut-in case is applicable for this case, except that the origin is taken at the bottom of the well and the flow is positive upwards. During production, the temperature of the fluid entering the wellbore is the same as the temperature in the producing interval. Under these circumstances, the system of equations which describes the temperature of the fluid and the surrounding formation during the production period is:

$$u\frac{\partial T}{\partial z} + \frac{\partial T}{\partial t} = \frac{\lambda_w}{r_w(\rho c)_w} \left.\frac{\partial \theta}{\partial r}\right|_{r_w}, \qquad (3.29)$$

$$\frac{\partial\theta}{\partial t} - \alpha(z)\frac{1}{r}\frac{\partial}{\partial r}\left(r\frac{\partial\theta}{\partial r}\right) - \frac{\partial}{\partial z}\left(\alpha(z)\frac{\partial\theta}{\partial z}\right) = 0 \quad , \tag{3.39}$$

where $(\rho c)_w$ = product of the heat capacity and the density of the in-flowing fluid,

$\alpha(z)$ = thermal diffusivity of the formation, varies with depth.

The appropriate initial and boundary conditions are:

$$\text{at } t = 0,\ T(t,z) = \theta(t,r,z) = T_i(z) = T_o - \sum_i^m \frac{\Delta T}{\lambda_i(z)} \Delta z_i \quad , \tag{3.31}$$

$$\text{at } z = 0,\ T(t,z) = \theta(t,r,z) = T_o \quad , \tag{3.32}$$

$$\text{at } z = L,\ \theta(t,r,z) = T_a \tag{3.33}$$

$$\text{at } r = r_w,\ \lambda_{(z)}\frac{\partial\theta}{\partial r} = U_T(\theta - T) \quad , \tag{3.34}$$

$$\text{at } r \to \infty,\ \theta(t,r,z) = T_i(z) \quad , \tag{3.35}$$

where L is the depth of the well, T_a is the ambient temperature, and T_o is the producing formation temperature.

For the shut-in period after production, the analysis is the same as for the injection shut-in case. A modified form of the conduction model is employed to solve for the temperature profiles of the fluid in the wellbore and the adjacent formation. For the fluid tem-

perature inside the wellbore, the governing equation and its boundary conditions are:

$$\frac{\partial T}{\partial t} = (\alpha_w + \alpha_z)\frac{\partial^2 T}{\partial z^2} + (\alpha_w - \alpha_r)\left(\frac{1}{r}\frac{\partial T}{\partial r} + \frac{\partial^2 T}{\partial r^2}\right), \tag{3.36}$$

$$\text{at } r = 0, \quad \frac{\partial T}{\partial r} = 0 \quad , \tag{3.37}$$

$$\text{at } r = r_w, \quad \lambda_w \frac{\partial T}{\partial r} = \lambda \frac{\partial \theta}{\partial r} \quad , \tag{3.38}$$

$$\text{at } z = 0, \quad T(t,r,z) = T_o \, , \tag{3.39}$$

$$\text{at } z = L, \quad \lambda_w \frac{\partial T}{\partial z} = H(T - T_a) \quad . \tag{3.40}$$

The following equations and boundary conditions are used to describe the formation temperature during shut-in :

$$\frac{\partial \theta}{\partial t} - \alpha(z)\left(\frac{1}{r}\frac{\partial \theta}{\partial r} + \frac{\partial^2 \theta}{\partial r^2}\right) - \frac{\partial}{\partial z}\left(\alpha(z)\frac{\partial \theta}{\partial z}\right) = 0, \tag{3.41}$$

$$\text{at } r = r_w, \quad \lambda(z)\frac{\partial \theta}{\partial r} = U_T(\theta - T) \quad , \tag{3.42}$$

$$\text{at } r \to \infty, \quad \theta(t,r,z) = T_i(z) \quad , \tag{3.43}$$

$$\text{at } z = 0 \, , \quad \theta(t,rz) = T_o \tag{3.44}$$

$$\text{at } z = L, \quad \theta(t,r,z) = T_a \quad . \tag{3.45}$$

The temperatures of the fluid and the formation at the end of the production period will be used as the initial conditions for the shut-in period.

Equations (3.29), (3.30), (3.36), and (3.41) are solved numerically and two computer programs, TEMP1 and TEMP2 used in the injection shut-in case, will be modified and utilized in this case.

3.4.2 Numerical Results and Discussion - Production/Shut-in Case

(1) Production Period

During the production period, hot fluid flows out of the production zone, enters the wellbore and flows up the well. As the fluid flows up the wellbore it contacts the lower temperature formations, its temperature decreasing due to heat loss to the adjacent formations. The rate of heat loss is proportional to the temperature difference between the flowing fluid and the formation. The wellbore fluid temperature increases with time as the formations surrounding the wellbore become heated. A rapid increase in the wellbore fluid temperature occurs at early times, followed by an approach to a steady condition at long times. Figure 25 shows that after ten hours of production, the fluid temperature in the wellbore changes very slowly and approaches a constant value after 24 hours.

Similar to the injection case, as the production rate increases, the produced fluid is transported up the well very fast and due to the convection and mixing process,

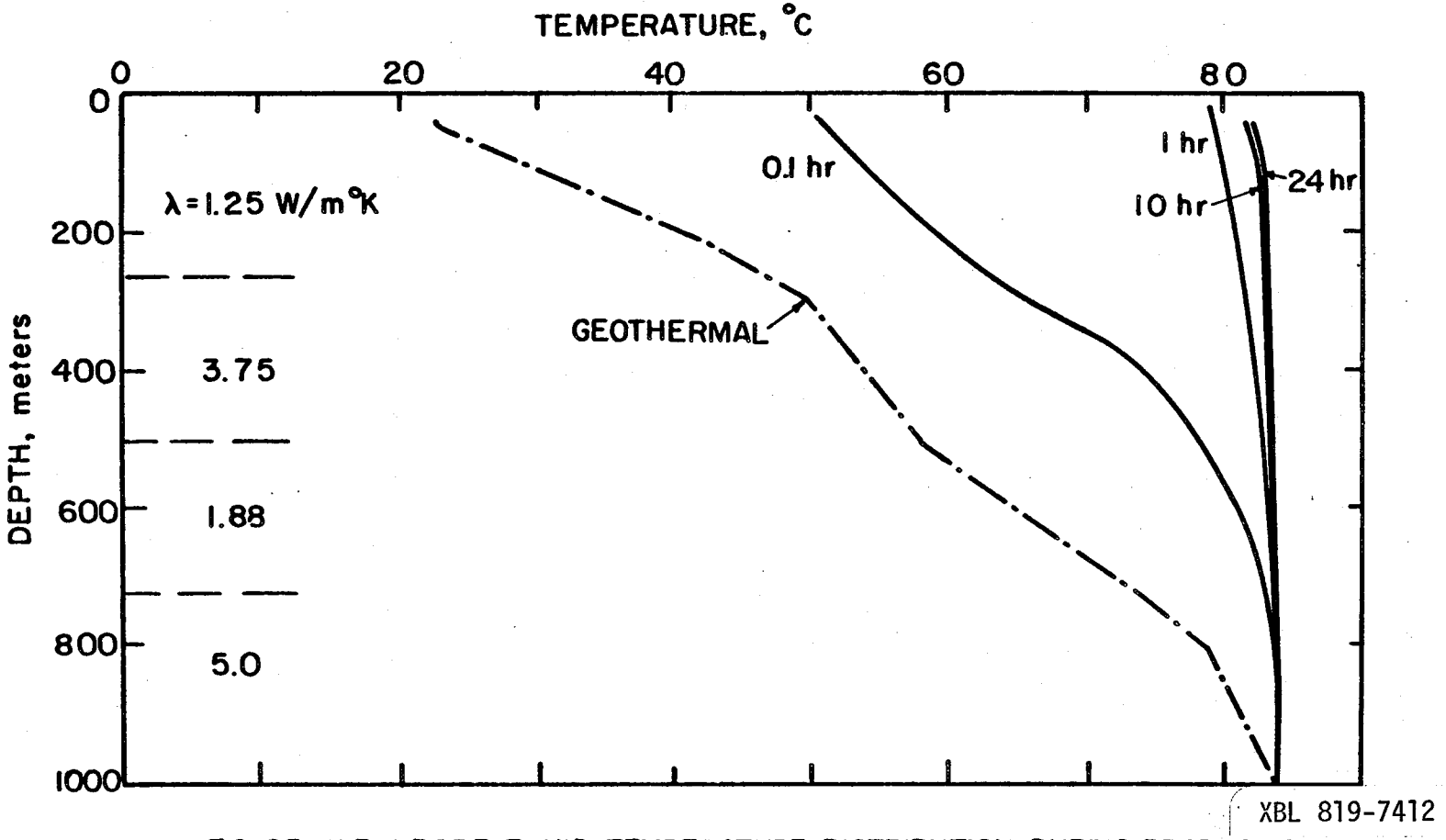

FIG. 25 WELLBORE FLUID TEMPERATURE DISTRIBUTION DURING PRODUCTION

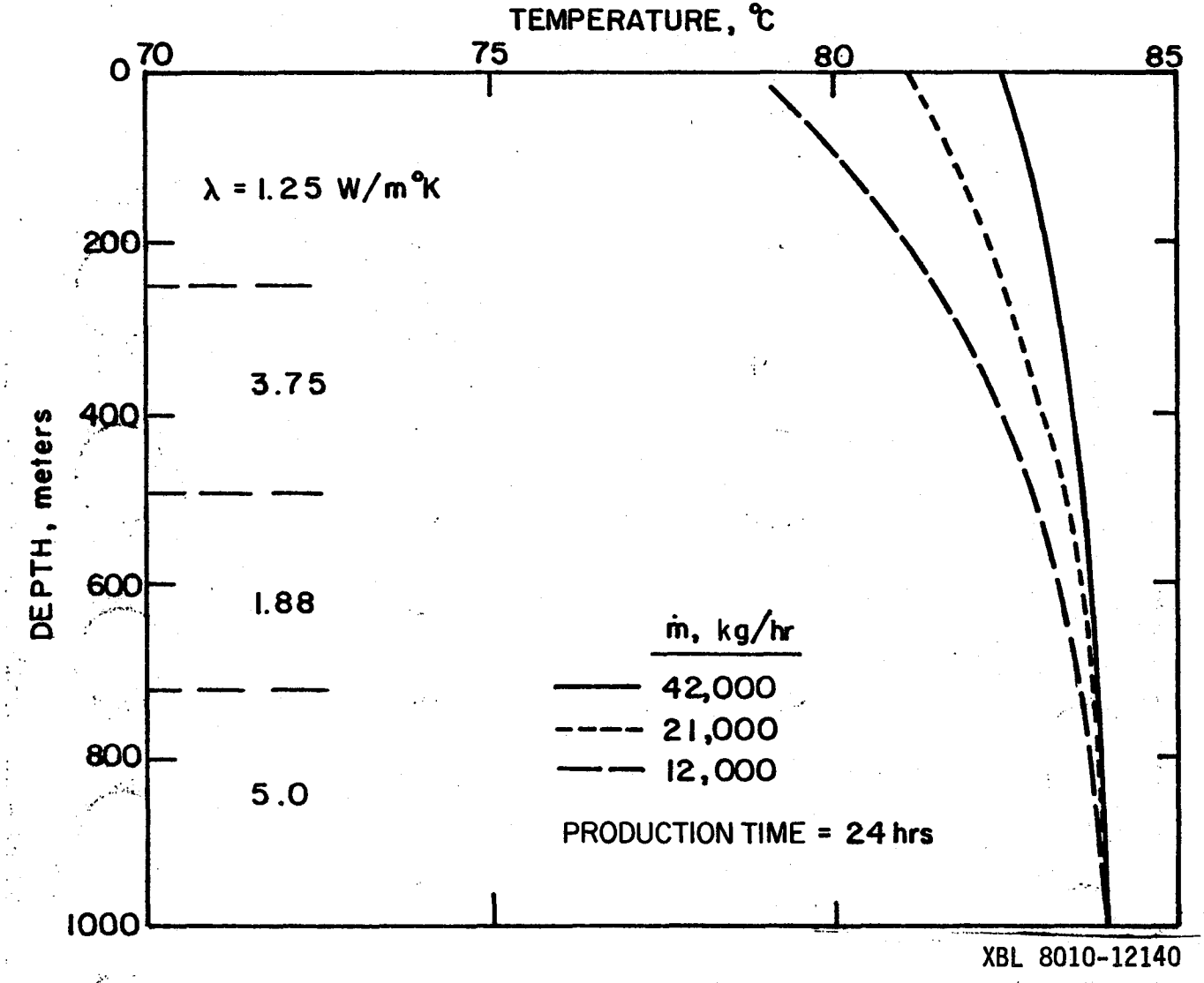

FIG. 26 WELLBORE FLUID TEMPERATURE DISTRIBUTION DURING PRODUCTION
EFFECT OF PRODUCTION RATE

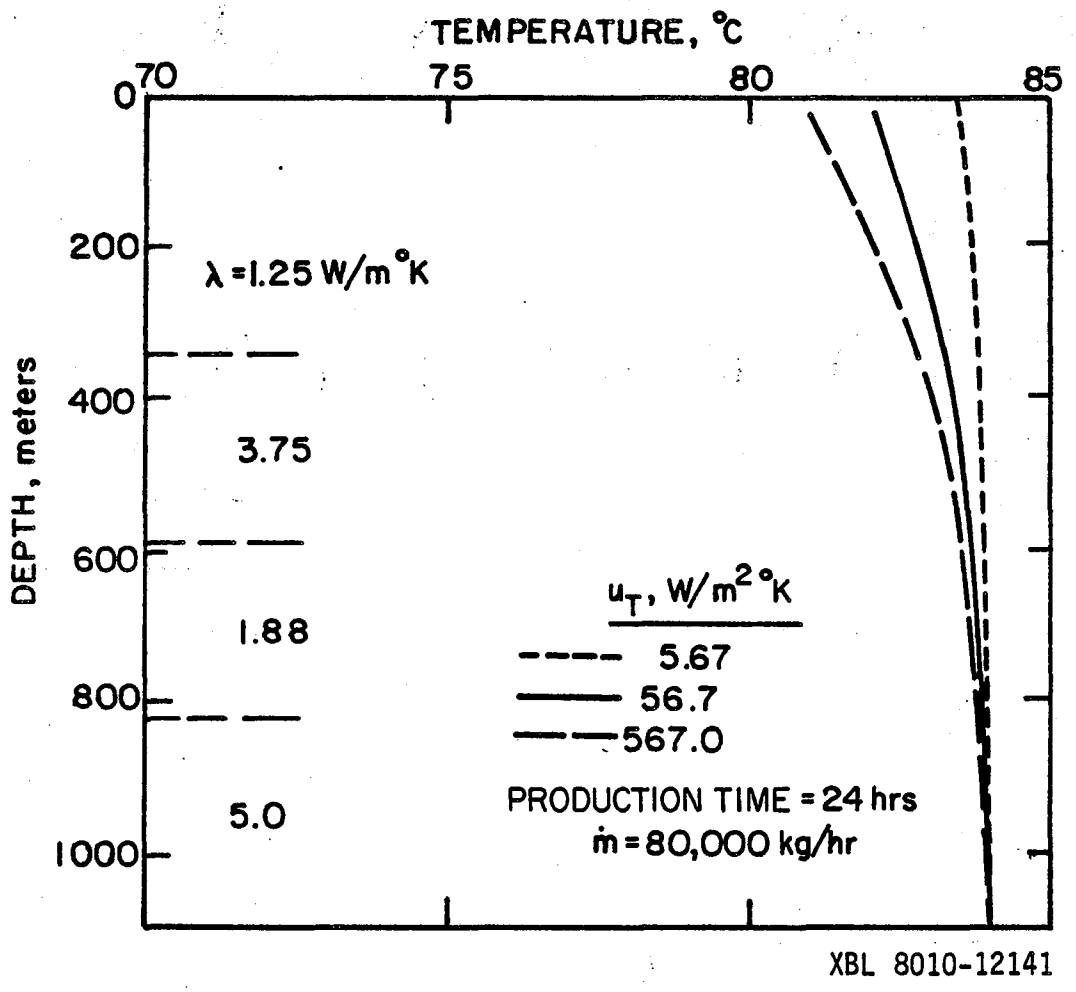

FIG. 27 EFFECT OF OVERALL HEAT TRANSFER COEFFICIENT ON THE FLUID TEMPERATURE DISTRIBUTION DURING SHUT-IN

the fluid temperature rises rapidly with time. This will result in a nearly vertical line for the temperature profile at earlier times and a steady state condition is reached more rapidly than at lower production rates. Figure 26 shows that fluid produced at 84°C at a depth of 1000m, is reduced in temperature to only 82.5°C at the top of the well in 24 hours for the flow rate of 42,000kg/hr. For the flow rates of 21,000kg/hr and 12,000kg/hr the fluid surface temperature is shown to be reduced to 81°C and 79°C, respectively, after 24 hours of production.

Figure 27 shows the effect of the overall heat transfer coefficient on the fluid temperature distribution during production. For the same production rate, the higher value of overall heat transfer coefficient, U_T, leads to lower fluid surface temperature because of greater heat loss. The hot fluid produced at 1000m depth at 84°C is reduced to 82°C for $U_T = 56.7 w/m^{2}{}^{0}K$ and is reduced to only 83.5°C for $U_T = 5.67 w/m^{2}{}^{0}K$ at the top of the well after 24 hours of production as shown in Figure 27.

During production, except for extremely low flow rates, the flow of the produced fluid is turbulent and well mixed in the wellbore so that variable thermal conductivity of the formation has very little effect on the fluid temperature profile.

(2) Shut-in After Production

When the production is stopped, the fluid becomes quiescent inside the borehole. Heat from the hot fluid

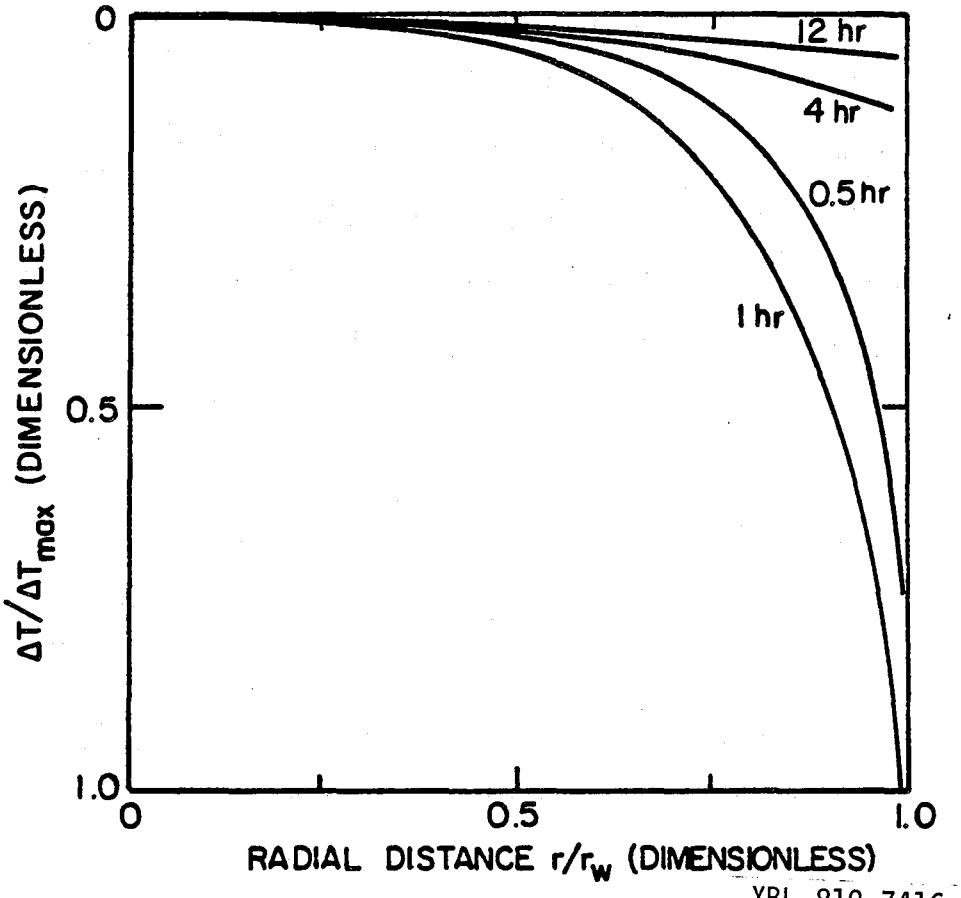

FIG. 28 RADIAL TEMPERATURE DISTRIBUTION INSIDE THE WELLBORE DURING SHUT-IN

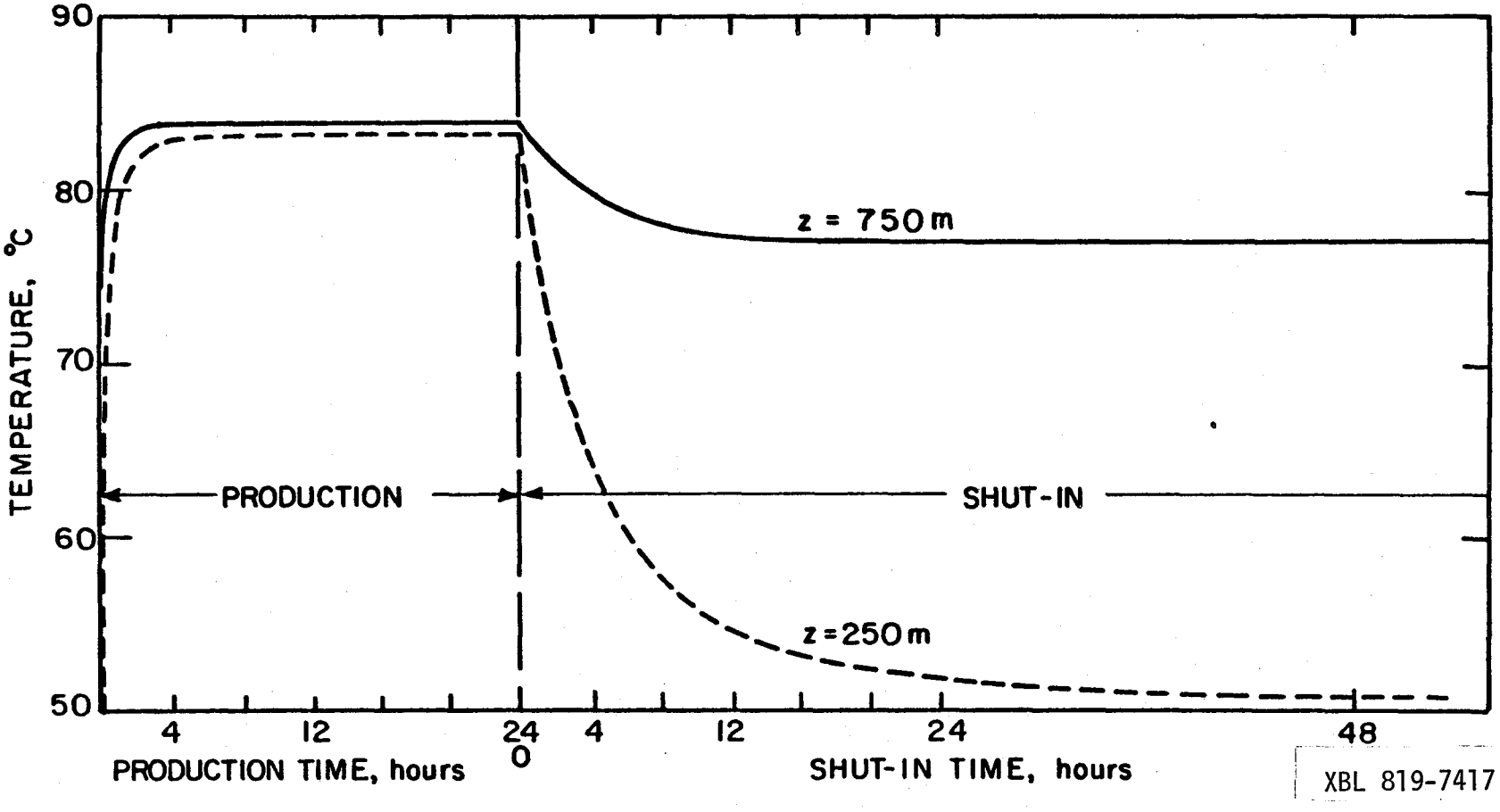

FIG. 29 TEMPERATURE DISTRIBUTION IN THE WELLBORE DURING PRODUCTION AND AFTER SHUT-IN

column conducts into the surrounding formation and dissipates away from the wellbore. Gradually, the fluid temperature inside the wellbore will come to equilibrium with the formation. After shut-in, due to heat conducted to the formation, the radial temperature gradient develops rapidly near the borehole wall. This temperature gradient reaches a maximum value at about one hour after shut-in as shown in Figure 28. As the heat stored in the fluid is transferred away from the wellbore, the radial temperature gradient in the wellbore decreases and becomes very small after 24 hours of shut-in as shown in Figure 28. Figure 29 shows the wellbore fluid temperature versus time, for two different depths, 250m and 750m. The fluid temperature in the wellbore is heated up during the production period and then cooled off during shut-in. During shut-in the fluid temperature changes rapidly during the first twelve hours of shut-in and begins to approach a slow, logarithmic decline after that.

When the well is produced for longer periods of time, more heat is accumulated in the formation adjacent to the wellbore so that longer times are needed for the heat to diffuse away. Thus more time is needed for the fluid temperature to return to its initial value.

Figure 31 shows the fluid temperature distribution along the wellbore axis during shut-in. As indicated in the previous section of this study, the fluid inside the wellbore which is in contact with the higher thermal

conductivity formations approaches the geothermal temperature faster than formations with lower thermal conductivity. This effect is very apparent during the first few hours of shut-in. Negative temperature gradients occur at boundaries where thermal conductivity of the formations change from a smaller value to a larger value. As the shut-in time increases, the fluid temperature inside the wellbore approaches closer to the geothermal and the temperature distribution curve has the shape of the geothermal temperature profile after 72 hours of shut-in. This result indicates that under thermal equilibrium conditions, the fluid temperature is inversely proportional to the magnitude of the formation thermal conductivities.

Effects of the overall heat transfer coefficient on the fluid temperature profile are the same as in the injection shut-in case. The hot fluid is cooled off faster in the wellbore having the higher value of overall heat transfer because of the higher rate of heat transfer to the formation during early shut-in times as shown in Figure 30. After 24 hours of shut-in, however, the fluid temperature profiles for different values of overall heat transfer coefficients are very close to each other. Both temperature profiles approach the geothermal temperature profile after 72 hours of shut-in. Figure 30 shows that the fluid temperature profiles vary in proportion to the formation thermal conductivities at long shut-in times for both values of the overall heat transfer coefficient.

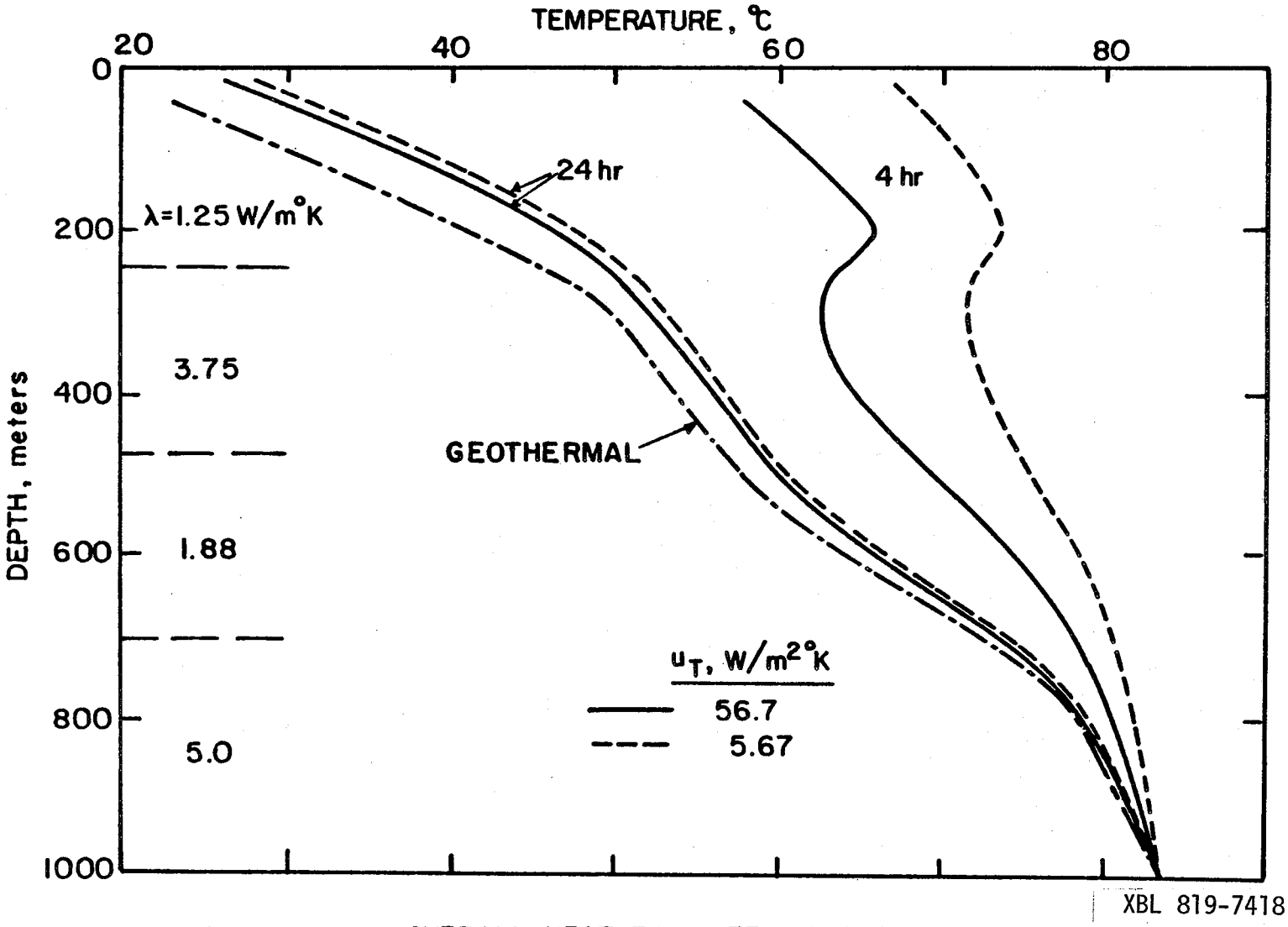

FIG. 30 EFFECT OF OVERALL HEAT TRANSFER COEFFICIENT ON WELLBORE FLUID TEMPERATURE DISTRIBUTION DURING SHUT-IN

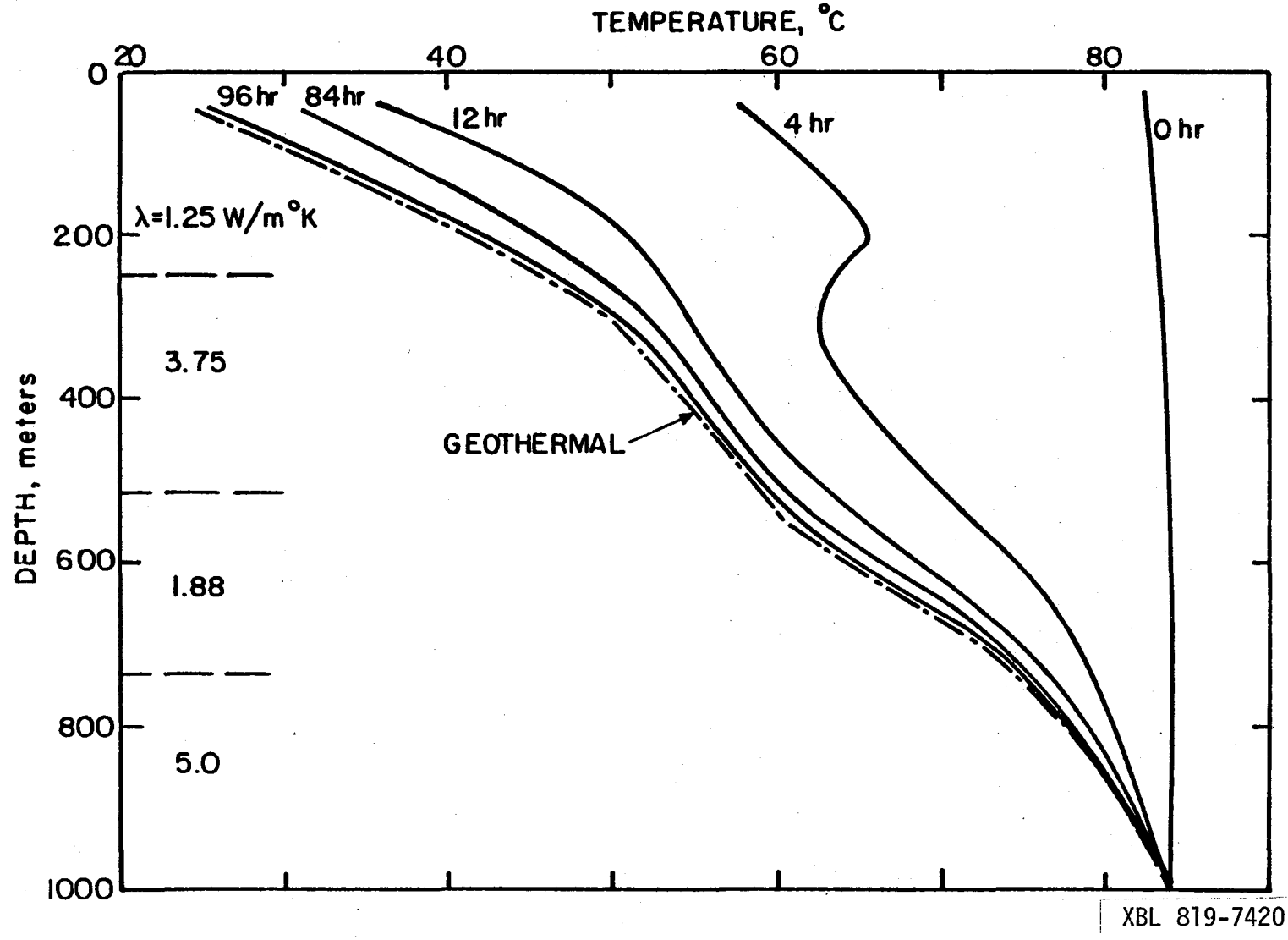

FIG. 31 WELLBORE FLUID TEMPERATURE DISTRIBUTION DURING SHUT-IN

CHAPTER IV

ESTIMATION OF IN-SITU THERMAL CONDUCTIVITIES FROM MEASURED TEMPERATURE GRADIENTS IN WELLS

4. 1. Transient Method

4.1.1. Transient Heating or Cooling

From the results of the analysis in the previous chapters of this study, it can be concluded that during injection or production and during the shut-in period, fluid temperature behavior in the wellbore depends on many factors such as the rate of heat conduction and convection in the fluid, and the rate of heat transfer from the fluid into the formation, the latter being a strong function of the formation thermal conductivities. It is difficult to present a direct quantitative evaluation of the effects of the formation thermal conductivity variation on the fluid temperature during the injection or production process and on the restoration of thermal equilibrium during shut-in. It should be possible, however, to draw certain semi-quantitative conclusions from consideration of the numerical results of this study.

After heating by a heat source, the cooling of the fluid at a point interior to a homogeneous stratum of finite thickness will, for sufficiently small values of time, behave as if the medium were infinite and homogeneous, possessing the thermal properties of that stratum. During injection or production, if the fluid with heat capacity c is pumped either

up or down the well at a mass flow rate $\dot{m}$, then the heating rate of $q = \dot{m}c\,\partial T/\partial z$ will be induced per unit of well depth. The results presented in Chapter III of this study indicate that except at early stages of injection or production, the fluid temperature gradient $\partial T/\partial z$ can be considered constant. Therefore, the heating rate q induced by the in-flowing fluid is approximately uniform. During injection or production and at early shut-in times, vertical temperature gradients in the formation are small compared to radial temperature gradients induced by injection or production, i.e. $\partial\theta/\theta z << \partial\theta/\partial r$. Radial conduction is the dominant mode of heat transfer in the formation. The well bore fluid temperature during injection or production and early shut-in times can be approximated from the heat source concept with the following considerations:

(1) the heating rate q is uniform during injection or production;

(2) the form of the heating or cooling curve at any depth during injection or production will not depend upon the thermal properties of the adjacent strata;

(3) radial heat flow is far more important than vertical heat flow in the formation.

Under the above conditions the temperature at any depth of the system of the wellbore and formation, can be approximated as follows:

$$q + \pi r_w^2 (\rho c)_w \frac{\partial T_D}{\partial t} = 2\pi r_w \lambda \frac{\partial \theta}{\partial r}\Big|_{r_w} \qquad (4.1)$$

$$\text{i.e.,} \quad q' + \frac{M}{2} \frac{\partial T_D}{\partial t} = \lambda \frac{\partial \theta_D}{\partial r}\Big|_{r_w} \quad , \qquad (4.1a)$$

$$\frac{\partial^2 \theta_D}{\partial r^2} + \frac{1}{r} \frac{\partial \theta_D}{\partial r} = \frac{1}{\alpha(z)} \frac{\partial \theta_D}{\partial t} \quad , \qquad (4.2)$$

where $T_D = (T - T_i)$,

$\theta_D = (\theta - T_i)$,

q = heat supplied/unitlength/unit time ,

$= \dot{m} c \, \partial T/\partial z$,

$q' = q/2\pi r_w$,

$M = (\rho c)_w r_w$.

These are subjected to the initial and boundary conditions:

at $t = 0$, $T_D = \theta_D = 0$, (4.3)

at $r = r_w$, $\lambda \frac{\partial \theta_D}{\partial r} = U_T (\theta_D - T_D)$, (4.4)

and θ_D is bounded as $r \to \infty$. (4.5)

The solution of this system of equations can be obtained by using a LaPlace transformation technique (Blackwell, [11]). Procedure for solving these equations is outlined in Appendix B. The result is:

$$T_D \simeq \frac{r_w q'}{2\lambda} \left[\ln 4\tau - \gamma + \frac{2\lambda}{r_w U_T} + \frac{1}{2\tau} \left\{ \ln 4\tau - \gamma + 1.0 - \frac{(\rho c)_w}{2\rho c} \left(\ln 4\tau - \gamma + \frac{2\lambda}{r_w U_T} \right) \right\} \right], \qquad (4.6)$$

where γ=Euler's constant = 5722,

$$\tau = \alpha t / r_w^2 \quad .$$

This result indicates that the change of fluid temperature at any depth is a function of time, formation thermal conductivity and diffusivity, heating rate, overall heat transfer coefficient, and ratio of heat capacity of the fluid in the wellbore and the formation.

The application of this result to the determination of thermal conductivity and thermal diffusivity is as follows:

Rewrite Equation (4.6) in the form,

$$T_D(t) \simeq A \ln(t) + B + \frac{1}{t}\{C \ln(t) + D\} \qquad (4.7)$$

where $$A = \frac{r_w q'}{2\lambda} ,$$

$$B = \frac{r_w q'}{2\lambda}\left[\ln\alpha - 2\ln r_w + \ln 4 - \gamma + \frac{2\lambda}{r_w U_T}\right] .$$

Similarly C, D may be expressed in terms of the above constants. If the injection time is long enough, after a few hours of injection the contribution of the term of the order (1/t) can be neglected.

It can be seen that, if the heating rate can be estimated and the wellbore parameters are known, a fit of suitable experimental data to this expression will yield a value of λ at the desired depth directly from the constant A. Once λ and U_T are known, a value of α can be estimated from the constant B.

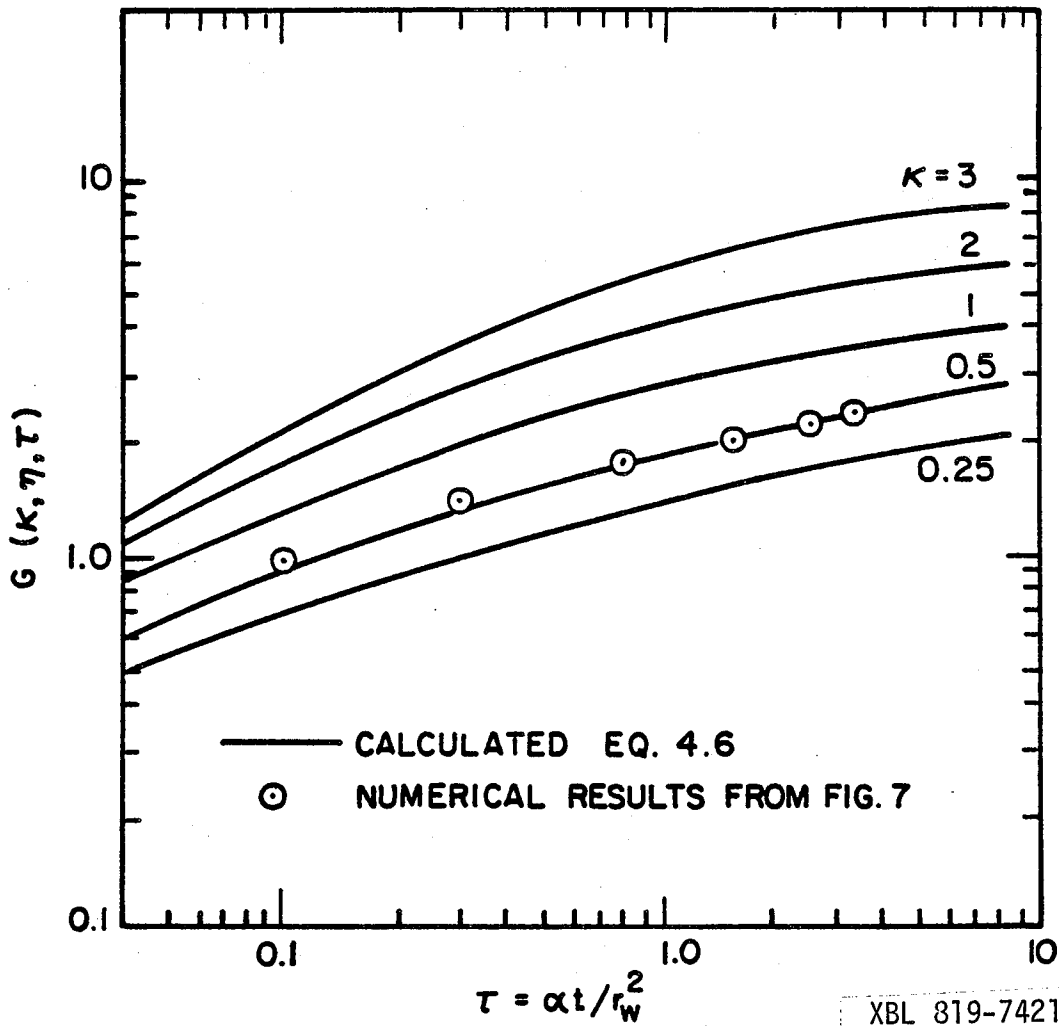

FIG. 32 TYPE CURVES FOR THEORETICAL TRANSIENT HEATING

To improve the accuracy of determination of λ and α the method of curve-fitting can be employed, as shown by Beck, et al., [7]. The temperature rise T of the fluid at time t can be written as:

$$T = (q/\lambda)\ G\ (\kappa, \eta, \tau) \qquad (4.8)$$

where G is a complex function of κ, η, τ given by Equation (4.6) where κ, η, τ are dimensionless parameters:

$$\kappa = \frac{\lambda}{r_w U_T} \quad ,$$

$$\eta = \frac{2\,(\rho c)}{(\rho c)_w} \quad ,$$

$$\tau = \frac{\alpha t}{r_w^2} \quad .$$

If the flowing fluid is water, η is 1.35 (Murphy, et al., [51]). It follows from (4.8) that

$$\ln T = \ln (q/\lambda) + \ln G\ (\kappa, \eta, \tau) \quad . \qquad (4.10)$$

Values of $G(\kappa, \eta, \tau)$ can be evaluated and plotted against τ for a specific value of η and various values of κ on log-log paper. The experimental values of temperature are plotted against time on transparent log-log graph paper and slid over a family of theoretical curves, G versus τ, keeping the axes parallel, until the best fit is obtained. The displacement of the axes then gives log (q/λ) and log (α/r_w^2).

A plot of $G(\kappa, \eta, \tau)$ against τ for $\eta = 1.35$ and various values of κ is shown in log-log form in Figure 32. A number of numerical data points taken from Figure 7 of this study are shown by circles in the same figure fitted to a curve of the family. A good match is obtained for the curve $\kappa = 0.5$ and the value of λ was found to be 3.4 w/m°K.

4.1.2. Transient Shut-in

During early shut-in times, the fluid temperature is a complex function of the formation thermal conductivities, the overall heat transfer coefficient, and the surrounding formation temperatures, as shown in Figures 21 and 22 and as given by Equation (3.21). Results of the mathematical analysis shown in Figures 21 and 22 indicate a strong effect of variable thermal conductivity of the formation on the fluid temperature profile. These figures also show that the fluid temperature gradients inside the wellbore change very rapidly, proportionly to the magnitude of the formation thermal conductivities during the first four hours of shut-in and they slowly approach the geothermal gradients with time after ten hours of shut-in. From the fluid temperature measurements during early shut-in it should be possible to find a relationship between the fluid temperature and the thermal conductivity of the formations. Unfortunately, there is no simple relationship between those two parameters. However, the temperature measurements at any depth give a temperature-time curve at that depth which can be used to estimate the thermal conduc-

tivity of the formation at that depth. During early shut-in, the temperature distribution in the formation shown in Figure 18 and the analysis in Section 3.2 indicate that within the formation surrounding the wellbore, radial conduction is much more important than axial conduction. After four hours of shut-in the effect of natural convection in the wellbore is small and can be neglected in comparison to radial conduction (Figure 15). Under the above conditions, the previous analysis can be modified to solve for the thermal conductivity of the formations. After shut-in, the heating induced by the fluid is stopped. If the well has been injected into or produced from time zero to t_1, the fluid temperature after t_1 may be calculated by adding to Equation (4.6) that for a negative source of strength q starting at t_1. If the shut-in time is small compared to injection or production time, the result is:

$$T_D \simeq \frac{q'}{\lambda}\left(\frac{r_w}{2}\right)\left\{\ln\frac{t}{t_2} + \frac{1}{2\tau}\left[\ln 4\tau - \gamma + 1 - \frac{(\rho c)_w}{\rho c}\left(\ln 4\tau - \gamma + \frac{2\lambda}{r_w U_T}\right)\right] + \frac{1}{2\tau_2}\left[\ln 4\tau_2 - \gamma + 1 - \frac{(\rho c)_w}{\rho c}\left(\ln 4\tau_2 - \gamma + \frac{2\lambda}{r_w U_T}\right) - \frac{1}{2}\frac{\alpha}{\alpha_w}\right] + 0\left(\frac{1}{t^2}\right)\right\} , \tag{4.11}$$

where $t_2 = t - t_1$.

The temperature T of the fluid after shut-in can be written as: $T = \left(\frac{q}{\lambda}\right) F(\kappa, \eta, \tau_2)$, (4.12)

or

$$\ln T = \ln (q/\lambda) + \ln F(\kappa, \eta, \tau_2) , \tag{4.13}$$

where $\tau_2 = \frac{\alpha}{r_w^2}(t-t_1)$ and κ, η are defined as before. Similar to the previous method, values of $F(\kappa, \eta, \tau)$ are evaluated for a specific value of η and plotted against τ_2 on log-log paper. To reduce the experimental results, observed values of the fluid temperature are plotted against time and slid across a family of theoretical curves, $F(\kappa, \eta, \tau_2)$ versus τ_2, keeping the axis parallel until a match with the theoretical curve is achieved. The thermal conductivity and the thermal diffusivity can be calculated from the shifts of the axes since they give $\ln(q/\lambda)$ and $\ln(\alpha/r_w^2)$.

A plot of $F(\kappa, \eta, \tau_2)$ against τ_2 for $\eta = 1.35$ and various values of κ is shown in Figure 33. Numerical data points from this study are shown fitted to the curves for $\kappa = 1.0$ and 1.5. It may be seen that the curve for which = 1.0 gives a slightly better fit, but the two curves give the same value $\lambda = 3.5$ w/m°K. The result by the previous method was 3.4w/m°K.

In concept then, the thermal conductivity of the formations surrounding the wellbore at any depth can be estimated by shutting the well for a time sufficient to allow equilibrium conditions to prevail, positioning a temperature measuring device in the well at the desired depth, establishing a constant rate of flow, and finally plotting the subsequent heating or cooling versus time curve to determine the conductivity.

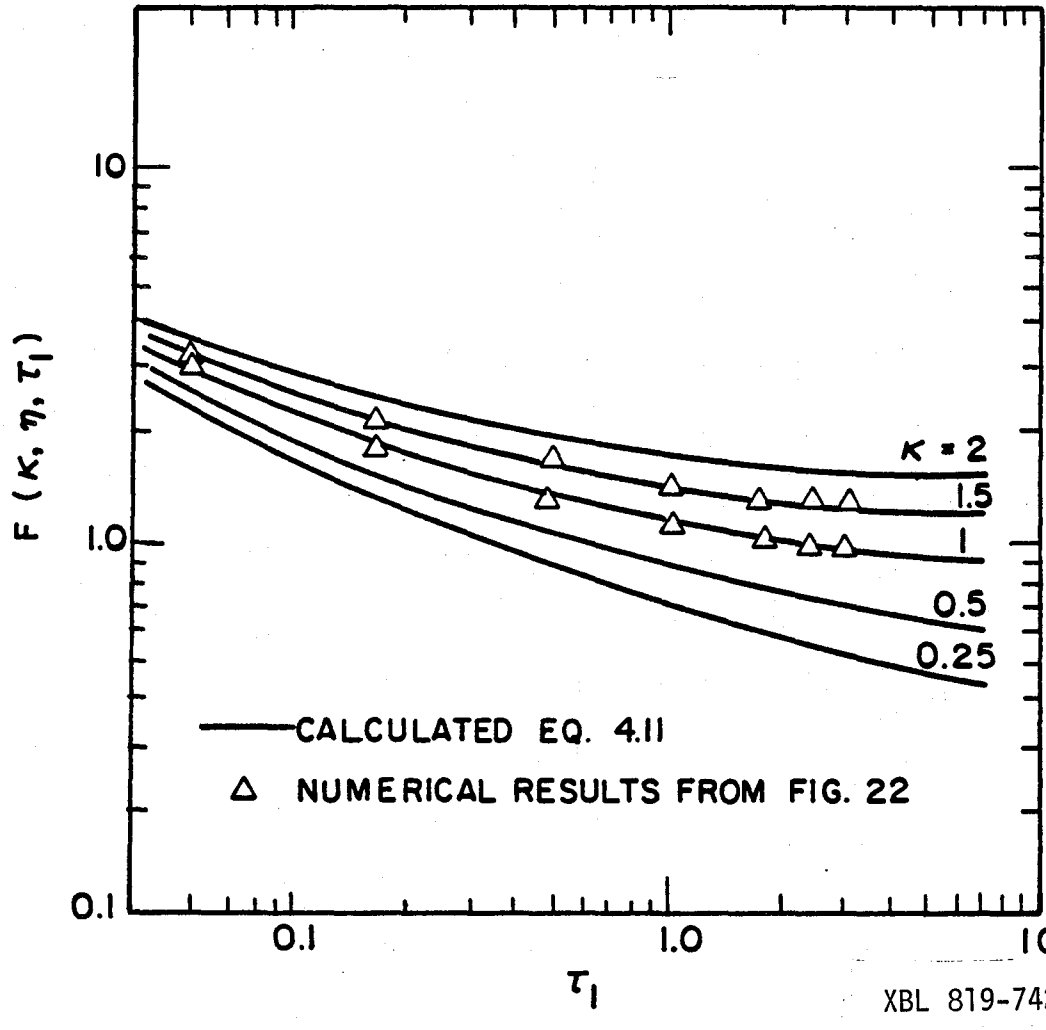

FIG. 33 TYPE CURVES FOR THEORETICAL SHUT-IN

The above analysis is restricted to the condition that the heating rate induced by the in-flow fluid during injection and production can be considered constant and axial heat conduction is negligible in comparison to radial conduction in the formations.

4.2. Steady State Method

As the shut-in time increases, effects of the overall heat transfer coefficient and the surrounding formation temperatures on the fluid temperature behavior diminish. On the other hand, the percentage contribution of heat initially liberated in the adjacent strata during injection or production to the temperature disturbance at the observed point will increase. Thus the form of cooling curve at any depth will depend upon the thermal properties of all strata in which the initially liberated heat contributes appreciably to the temperature disturbance at that depth. For large shut-in times the effect of the terms $\partial T/\partial t$ and $\partial\theta/\partial T$ in Equations (3.25) and (3.5), of the order of $(1/t)$, will diminish and the effect of natural convection inside the wellbore is negligible. The factors which influence the fluid temperature in the well are the heat transfer from the fluid to the surrounding formation, $\lambda_w(\partial T/\partial r)=\lambda(\partial\theta/\partial r)$, and the rate of heat conducted away from the wellbore which are directly proportional to the formation thermal conductivities. Even though during this period of shut-in the main factors which control the fluid temperature behavior are the formation thermal conductivities, it is

very difficult to obtain a direct relationship between the temperature and the formation thermal conductivities. This is because the analytical solution for the heat flow equations in a variable thermal conductivity medium is difficult. However, as the fluid temperature approaches the geothermal, its gradients are about the same as the geothermal gradients, as shown in Figures 22 and 31. In this study, after 72 hours of shut-in, the fluid temperature gradients are within four percent of the geothermal gradients. The magnitudes of the fluid temperature gradients are controlled by the geothermal heat flux and the formation thermal conductivities. If it is assumed that the heat flow is constant along the length of the borehole, then any changes in temperature gradient, even over small sections of the borehole, must be assumed to be due to changes in thermal conductivity of the surrounding formations. These temperature gradients are inversely proportional to the change of the formation thermal conductivity with depth. The temperature gradients are directly proportional to the changes of thermal resistivity, reciprocal of thermal conductivity, with depth.

Under thermal equilibrium conditions, and in the absence of obvious disturbing influences from heat sources or sinks in the vicinity of the borehole, a log of temperature gradient versus depth is essentially the same as a log of thermal resistivity with depth. For the case of short injection or production times, sufficiently accurate

values of thermal conductivity can be obtained by using a continuous temperature gradient log and calibrating the complete log by meaurements of thermal conductivity at three or four selected locations of high, low, and intermediate temperature gradient log values. The conductivity measurements can be carried out using standard divided bar techniques on borehole cores (Somerton, [63]; Beck, [5]), on recovered drilling chips (Sass, et al., [58]) or by in-situ techniques (Beck, et. al.,[10]).

Figure 34 shows the comparison between estimated thermal conductivities calculated from a temperature gradient log and measured thermal conductivities. These thermal conductivity values and the temperature gradient logs were taken from a water filled borehole on the campus of the University of Western Ontario (Conway and Beck,[19]) The borehole is 592m deep, water filled, and cased to a depth of 441m. Features of the borehole and the core material were described by Beck and Judge [9]. Continuous analog temperature logs were obtained from the borehole. Analog temperature logs are rapidly and simply obtained but lack precision and resolution due largely to neglect of probe time constant. As the probe is lowered down the borehole it is not in thermal equilibrium with its surroundings; thus the measured borehole temperature profile does not accurately represent the actual profile. The application of suitable deconvolution and smoothing operators to the temperature record output will produce an

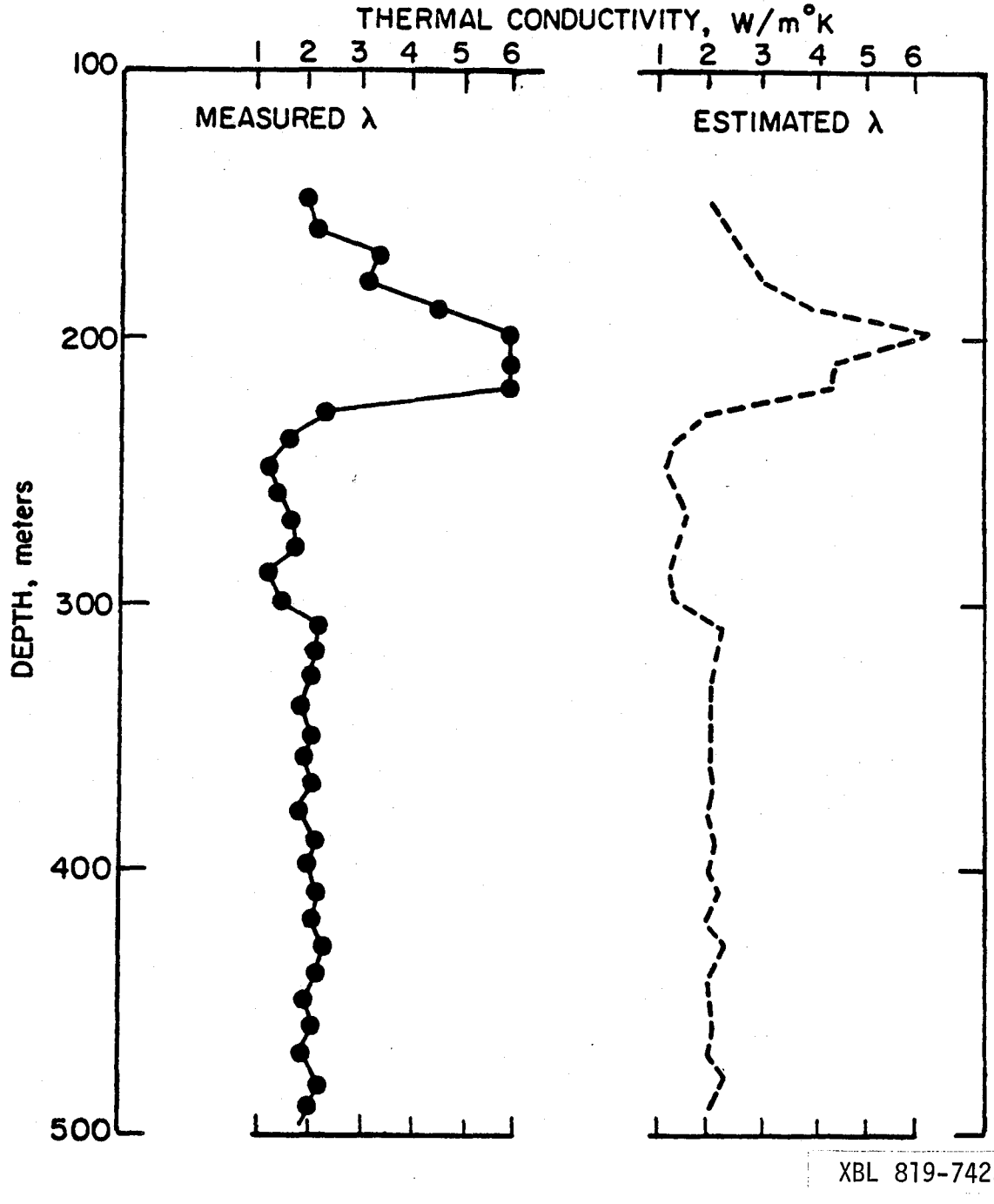

FIG. 34 THERMAL CONDUCTIVITIES FROM THE UWO BOREHOLE
(From Conaway and Beck, [19])

accurate borehole temperature profile. The application of a simple derivative or gradient operator to this temperature profile will produce a high-precision, high-resolution temperature log. Details of the development and application of suitable operators are presented by Conaway [18].

In applying the above method, first the temperature gradient taken from the borehole on the campus of the University of Western Ontario is plotted against the depth of the borehole. Three values of measured thermal conductivity values of cores at intermediate, high, and low temperature log values, reported by Beck, et al., [9], are used to estimate the formation thermal conductivity for every ten meters depth interval from the temperature gradient log. By using the linear relationship $\lambda_i/\lambda_j = (\partial T/\partial z)_j / (\partial T/\partial z)_i$ and the temperature gradient versus depth plot, thermal conductivities of the formations along the borehole are obtained from the three known thermal conductivity values of the formation. The estimated thermal conductivities were found to match very well the measured thermal conductivities in the regions of high or low values of the temperature log if the measured thermal conductivity value was selected at a low or high temperature gradient log value. However, in the regions in which temperature gradient log values were in the intermediate range, the estimated thermal conductivity values are higher than the measured values. On the other hand, if a measured thermal conductivity was selected in the intermediate temperature

gradient log value to calculate the estimated thermal conductivities, the results are matched very well in the regions which exhibit intermediate temperature gradient log value but give relatively lower values for other regions. In Figure 34, two measured thermal conductivity values are used to calculate the estimated thermal conductivities from the temperature gradient log, one for the intermediate temperature log value regions and one for the high and low temperature log value regions. Excellent agreement between estimated thermal conductivities and measured thermal conductivities is shown on Figure 34. The mean value using the temperature log is about 2.51 w/m°K compared to about 2.44 w/m°K for experimental values.

Another set of data used for comparison is provided by Amoco Production Company. This information is taken from a well in Tulsa, Oklahoma. Data for the borehole and the available core material includes temperature gradient logs, lithology, electrical resistivity, and spontaneous potential logs. Temperature gradient is measured carefully, recorded to a precision of 0.001°F. Thermal conductivities of the core are not available but are predicted from the geophysical well log parameters available. The following relations taken from Somerton, et. al., [62] and Anand [2] are used for predicting thermal conductivities:

$$\lambda = \lambda_d \left[1.0 + 0.3\left(\frac{\lambda_l}{\lambda_g} - 1.0\right)^{0.33} + 4.57\left(\frac{\phi}{100 - \phi}\ \frac{\lambda_l}{\lambda_g}\right)^{0.48m} x \right.$$

$$\left. \frac{\rho_b}{\rho_d}\right]^{-4.3} , \qquad (4.13)$$

and $$\lambda_{S_w} = \lambda_d + (\lambda_{S_w=1} - \lambda_d)\, S_w^{1/3} , \qquad (4.14)$$

where λ = thermal conductivity,

ρ = density,

ϕ = porosity in percent,

S_w = fractional brine saturation,

and subscripts d, l, g stand for dry rock, saturating liquid and gas respectively; m is the cementation factor.

Porosity and saturation are estimated from the resistivity, spontaneous potential logs and information given in the lithology logs. Details of procedure for estimating these parameters are presented in Schlumberger Log Interpretation Series (1972). In the regions where more than one type of rock are present, a simple arithmetic average was used to calculate the effective value of thermal conductivity,

$$\lambda_{eff} = \sum_{i=1}^{n} (\phi_i \lambda_i) . \qquad (4.15)$$

From Figure 35 it can be seen that agreement between predicted and estimated values is not as good as in the

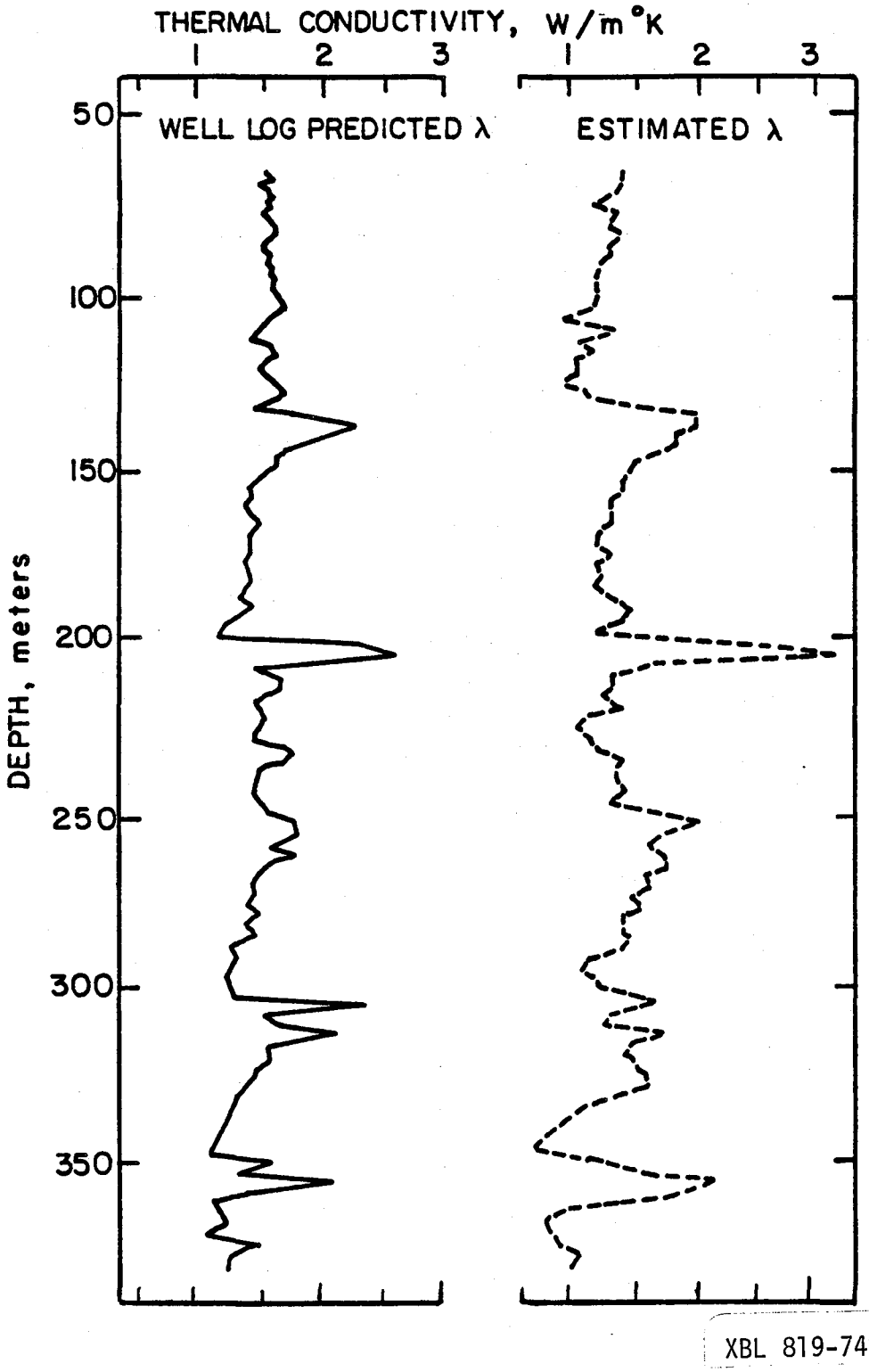

FIG. 35 THERMAL CONDUCTIVITIES FROM THE TULSA WELL
(From Amoco Production Co.)

previous comparison. The mean value using the temperature gradient log appears to be lower than the one using well log parameters, about 1.38 w/m°K compared to 1.67 w/m°K. However, agreement between predicted and estimated trends is quite good. The discrepancy is probably due to the inaccuracy in the estimated thermal conductivity values because of lack of information.

From the results of this study, in-situ values of thermal conductivity and thermal diffusivity can be estimated from temperature measurements in wells. Although laboratory methods can measure thermal conductivities with accuracy as high as one per cent for an individual specimen it is doubtful how far this represents the conductivity of the rock in-situ and it cannot take into account the effect of veins or open joints in the rock which may well be important in the calculation of heat flux. This suggests that a method for measuring conductivities in-situ which is accurate to within 5 to 10 percent would be more useful than the high precision laboratory values. Values of in-situ thermal conductivity can be useful for the following purposes:

(1) Determining terrestrial heat flow in the earth so that the distribution and relationship of the heat flux to surface and subsurface features can be obtained.

(2) Calculating heat lossses from wellbores in any production or injection process in petroleum or geothermal operations. The resultant heat losses between surface and the injection or production interval could be very

important in the success or failure of these processes.

(3) Differentiating oil-bearing or gas-bearing formations from water-bearing formations, since the rock's effective thermal conductivity varies drastically depending on whether the saturant fluid is water, oil or gas.

(4) From the correlations of thermal conductivity with other geophysical well log parameters, in-situ thermal conductivity values may also be useful in the estimation of other physical properties such as type of formation, its porosity,as well as it fluid content.

CHAPTER V

SUMMARY AND CONCLUSIONS

A mathematical model has been developed to study the effect of variable thermal conductivity of the formations and wellbore characteristics on the fluid temperature behavior inside the wellbore during injection or production and after shut-in.

During the injection or production period the wellbore fluid temperature is controlled mainly by the flow rate and heat lost to the formation. Variable thermal conductivities of the formations have little effect on the fluid temperature profile. However, the change with time of fluid temperature in the wellbore is related to the formation thermal conductivities via heat lost from the fluid to the formation.

During early shut-in times, the wellbore fluid temperature is a function of the rate of heat conduction and convection in the fluid and the rate of heat lost which is a complex function of the formation thermal conductivity. There exist negative gradients in the wellbore fluid temperature profile where the formation thermal conductivity changes abruptly from a smaller value to a larger value. As the shut-in time increases, the fluid temperature profile inside the wellbore is strongly affected by differences in formation thermal conductivities. This effect is very apparent after four hours of shut-in. The rate of return of

the fluid temperature to the geothermal is proportional to the magnitude of the formation thermal conductivity. If the well is shut-in for a long period of time, the fluid temperature gradients approach the geothermal gradients, and the values of these temperture gradients are inversely proportional to the values of formation thermal conductivities.

An estimation of the values of formation thermal conducvity can be obtained by applying a modified heat source concept to the fluid temperature record during the transient period of injection or production and early shut-in times. This involves plotting the fluid temperature versus time on log-log paper and matching with the theoretical curves.

If a well is injected into or produced for a short period of time and the shut-in time is long so that thermal equilibrium conditions prevail, values of the formtion thermal conductivities along a wellbore can be estimated by using a continuous temperature gradient log and by measuring the thermal conductivity of the formation at a few selected wellbore locations. In applying this method, two values of thermal conductivity of the formation corresponding to the locations where the temperature gradient log exhibits high and intermediate values, are measured by standard techniques, laboratory or in-situ. This along with the temperature gradient log may be used to estimate the thermal conductivity of the formations along the wellbore by applying the relationship $\lambda_1 = \lambda_2 \, (\partial T/\partial z)_2/(\partial T/\partial z)_1$. These methods are operationally simple since only a temperature measuring device must be lowered down the borehole and only thermal conductivity of the

formation at few selected locations must be known.

From the results of this study, in-situ values of thermal conductivity can be estimated from temperature measurements in wells. Although laboratory methods can measure thermal conductivities with accuracy as high as one per cent, it can only represent the value of an individual specimen. A method for measuring conductivities in-situ which is accurate to within 5 to 10 per cent would be more useful than the high precision laboratory values for many purposes. Values of in-situ thermal conductivity can be useful for the determination of terrestrial heat flows in the earth, heat losses from the wellbores in thermal recovery processes, and in differentiating oil-bearing or gas-bearing formations from water-bearing formations. They may also be useful in the estimation of other physical properties such as type of formation, its porosity, as well as its fluid content.

REFERENCES

1. Ames, W. F., Numerical Methods for Partial Differtial Equations, Academic Press, New York, 1977.

2. Anand, J., "Thermal Conductivity of Fluid Saturated Rocks at Elevated Pressures and Temperatures," M.S. Thesis, University of California, Berkeley, 1971.

3 Anand, J., Somerton, W. H., and Gomaa, E., "Predicting Thermal Conductivities of Formations from Other Known Properties," SPE Journal, Vol. 13, No. 9, 1973, P.267.

4. Anousch, G., "A Model for Predicting Thermal Conductivity of Rock - Fluid Systems," Ph.D. Dissertation, University of California, Berkeley, 1980.

5. Beck, A. E., "Techniques of Measuring Heat Flow on Land," in Terrestrial Heat Flow, Editor W.H.K.Lee, Chapter 3, American Geophysical Union Monograph, No. 8., 1965.

6. Beck, A.E., "The use of Thermal Resistivity logs in Stratigraphic Correlation," Geophysics, Vol.41, No.2, 1976, P.300.

7. Beck, A.E., Jaeger, J.C., and Newstead, G.N., "The Measurement of the Thermal Conductivities of Rocks by Observations in Boreholes," Australian Journal of Physics, Vol.9, No. 2, 1956, P.286.

8. Beck, A.E., and Beck, J.M., "On the Measurement of the Thermal Conductivities of Rocks by Observations on a Divided Bar Apparatus," Transactions of American Geo physical Union, Vol.39, No.6 , 1958, P.1111.

9. Beck, A.E., and Judge, A.S., "Analysis of Heat Flow Data - I. Detailed Observations in a Single Borehole," Geophysical Journal Vol. 18, No.2 , 1969, P.145.

10. Beck, A.E., Anglin, F.M., and Sass, J.H., "Analysis of Heat Flow Data -In-Situ Thermal Conductivity Measurements,"Canadian Journal of Earth Sciences, Vol.8, No. 1, 1971, P.1.

11. Blackwell, J.,H., "A Transient Heat Flow Method for Determination of Thermal Constants of Insulating Material in Bulk," Journal of Applied Physics, Vol.25, No. 2, 1954,P.137.

12. Blackwell, J.H., "The Axial Flow Error in the Thermal Conductivity Probe," Canadial Journal of Physics, Vol.34, 1956, P.41.2

13. Boberg, T.C., "Thermal Recovery Methods Course-Traveling Lecture Series, "Society of Petroleum Engineers of AIME, 1971.

14. Bullard, E.C., "The Time Necessary for a Borehole To Attain Temperature Equilibrium, "Monthly Notices Royal Astronomical Society, Geophysical Supplement, No.5, 1947. P. 127.

15. Carnahan, B., Luther, H.A., Wilkes, J.O., Applied Numerical Methods, John Wiley and Son, New York, 1969.

16. Carslaw, H.S., and Jaeger, J.C., Conduction of Heat in Solids, Claredon, Oxford.

17. Clark, S.P.Jr., Handbook of Physical Constants, Geological Society of America, New York, 1966.

18. Conaway, J.G., "Deconvolution of Temperature Gradient Logs," Geophysics, Vol.42, No. 4, 1977, P.823.

19. Conaway, J.G., and Beck, A.E., "Fine Scale Correlation between Temperature Gradient Logs and Lithology," Geophysics, Vol.42, No. 7, 1977, P.1401.

20. Conaway, J.G., and Beck, A.E., "Continuous Logging of Temperature Gradients," Tectonophysics, Vol. 41, 1977, P. 1.

21. Crosby, G.W., "Prediction of Final Temperature," Geothermal Reservoir Engineering Workshop, Stanford, Dec. 15-17, 1975.

22. Dakhnov, V.N., and Kjakonlv, D.J., "Thermal Investigation of Fissures," Moscow (in Russian), cited in Karl, "Physical Rock Parameters Wave Velocity, Thermal Conductivity," Freiberger Forschungshefte, Series C, Vol. 197, Sec. 2.1.3., 1965, P. 7.

23. De Vries, D.A., and Peck A.J., "On the Cylindrical Probe Method of Measuring Thermal Conductivity with Special Reference to Soils," Australian Journal of Physics, Vol. 11, 1958, P.255.

24. Diment, W.H, "Thermal Regime of a Large Diameter Borehole: Instability of the Water Column and Comparison of Air and Water -Filled Conditions, Geophysics, Vol. 32, No.4, 1967, P.720.

25. Donaldson, I.G., "Free Convection in a Vertical Tube with a Linear Wall Temperature Gradient," Australian Journal of Physics, Vol 4, 1961, P.529.

26. Dowdle, W.L., and Cobb, W.M. "Static Formation Temperature From Well-Logs - An Empirical Method," Journal of Petroleum Technology, Sept. 1975, P.1326

27. Edwards, D.K., and Catton, I., "Prediction of Heat Transfer by Natural Convection in Closed Cylinders Heated From Below," International Journal Heat Mass Transfer, Vol. 12, 1969, P.23.

28. Edwardson, M.J., Girner, H.M., Parkinson, , H.R., Williamson, C.P., and Matthews, C.S., "Calculation of Formation Temperature Disturbances Caused by Mud Circulation,Journal of Petroleum Technology, April 1962, P.416.

29. Elder, J.W., "Laminar Free Convection in a Vertical Slot," Journal of Fluid Mechanics,Vol.23, Part I, 1965, P.77.

30. Edler, J.W., "Turbulent Free Convection in a Vertical Slot," Journal of Fluid Mechanics, Vol.23, Part I., 1965, P.99.

31. Evans, L.B., and Reid, R.C., "Transient Natural Convection in a Vertical Cylinder," A.I.Ch.E. Journal, Vol.14, No.2, 1968, P.251.

32. Gebhart, B. "Natural Convection Flows and Stability," Advances in Heat Transfer, Vol.91, 1973, P.273.

33. Goss, R., and Combs, J., "Thermal Conductivity Measurement and Prediction from Geophysical Well Log Parameters with Borehole Application," Institute for Geosciences, The University of Texas at Dallas, Preprint, 1975.

34. Hellums, T.D., and Churchill, S.W., "Computation of Natural Convection by Finite Difference Methods," International Heat Transfer Conference at University of Colorado, Boulder, Colorado, Aug. 1961.

35. Hoang, V.T., "Estimation of In-situ Thermal Conductivities from Temperature Gradients Measurements," M.S. Research Report, University of California, Berkeley, 1978.

36. Horai, K.I., "Thermal Conductivity of Rock Forming Minerals," Journal of Geophysical Research, Vol.76, No. 5, 1971, P.278.

37. Horai, K.I., and Nur, A., "Relationship among Terrestrial Heat Flow, Thermal Conductivity and Geothermal Gradient," Journal of Geophysical Research, Vol. 75, No. 11, 1970, P.1985.

38. Jaeger, J.C., "Numerical Values for the Temperature in Radial Heat Flow," Journal of Mathematical Physics, Vol.34, No. 4, 1956 P.321.

39. Jaeger, J.C., "Conduction of Heat in an Infinite region Bounded Internally by a Circular Cylinder of a Perfect Conductor," Australian Journal of Physics, Vol.91, 1956, P. 176.

40. Jaeger, J.C., "Applied Theory of Heat Conduction", in Terrestrial Heat Flow, Editor W.H.K. Lee, Chapter 2, American Geophysical Union Monograph, No.8., 1965.

41. Karl, R., "Physical Rock Parameters, Wave Velocity, Thermal Conductivity," Freiberger Forschungshefte, (in German), Series C, Vol. 197, 1965, P. 7.

42. Kays, W.M., "Convective Heat and Mass Transfer," McGraw-Hill, New York, 1966.

43. Kersten, M.S., "Thermal Properties of Soils," University of Minnesota Engineering Experimental Station, Bulletin No.28.

44. Lachenbruch, A.H., and Brewer, M.C., "Dissipation of the Temperature Effect in Drilling in a Well in Artic Alaska,"U.S.G.S. Bulletin, No. 1083-C, 1959 p.73.

45. Larewerier, H.A., "The Transport of Heat in an Oil Layer Caused by the Injection of Hot FLuid," Applied Science Research, Sec. A, Vol. 5, 1955, P. 145.

46. Marx, J.M., and Langenheim, R.H., "Reservoir Heating by Hot Fluid Injection," Petroleum Transaction, AIME, Vol.216, 1959, P.312.

47. Messer, P.H., "Estimation of Static Reservoir Temperature During Operation," Geothermal Reservoir engineering Workshop, Stanford, Dec.15-17, 1975.

48 Miller, C.W., "Effect of a Conducting Wall on a Stratified Fluid in a Cylinder," AIAA Progress in Astronautics and Aeronautics: Heat Transfer and Thermal Control System, Vol. 60, 1977.

49 Miller, C.W., "Numerical Model of Transient Two-Phase Flow in a Wellbore," Report No. LBL 9056, University of California, Berkeley, Lawrence Berkeley Laboratory, Oct. 1979.

50 Moiseyenko, V.I., Doroginitskays, L.M., Leont'er, Ye.I., and Sokolova, L.S., "Dependence of the Heat Conductivity of the Elastic Rocks of the West Siberian Lowlands on other Physical Parameters," In Methods of Determining the Thermal Properties of Rocks:Akademy Nauk SSR Sibirsk, Otedeleniye Geologiy, Geofizika (in Russian), No. 2, 1970 P.106.

51 Murphy, H.D., and Lawton, R.G., "Downhole Measurements of Thermal Conductivity in Geothermal Reservoirs," Journal of Pressure Vessel Technology, Trans, ASME, Vol. 99, 1977, P.607.

52. Nowak, T.J., "The estimation of Water-Injection Profiles from Temperature Survey," Trans. AIME, Vol.198, 1953, P.203.

53. Pirson, S.J., "Oil Reservoir Engineering," McGraw Hill, New York, 1958.

54. Ramey, H.J.Jr., "Wellbore Heat Transmission," Journal of Petroleum Technology, Sept.1962, P.427.

55. Raymond, L.R., "Temperature Distribution in a Circulating Drilling Fluid," Journal of Petroleum Technology, March 1969, P.333

56. Richtmyer, R.D., and Morton, K.W., "Difference Methods for Initial-Value Problems," John Wiley and Son, New York, 1957.

57. Rohsenow, W.M., Choi, H.Y., Heat, Mass, and Momentum Transfer, Prentice Hall, New Jersey, 1961.

58 Sass, J.H., Lachenbruch, A.H., and Munroe, R.J., "Thermal Conductivity of Rocks from Measurements on Fragments and Its Application to Heat Flow Determinations," Journal of Geophysical Research, Vol.76, No. , 1971, P.3391.

59. Schoeppel, R.J., and Gilarranz, S., "Use of Well Log Temperatures to Evaluate Regional Geothermal

Gradients," Journal of Petroleum Technology, June 1969, P.667.

60. Sibbit, W.L.., Dodson, J.G., and Tester, J.W., "Thermal Conductivity of Crystalline Rocks Associated with Energy Extraction from Hot Dry Rock Geothermal Systems," Journal of Geophysical Research, Col.84, No.,B3, 1979, P.1117.

61. Smith, R.C., and Steffensen, R.J., "Interpretation of Temperature Profiles in Water-Injection Wells," Journal of Petroleum Technology, June 1975, P.777.

62. Smith, R.C., personal commuincation, 1980.

63. Somerton, W.H., "Thermal Properties of Hydrocarbon Bearing Rocks at High Temperatures and Pressures," Final Report, A.P.I. Research Project No. 117, University of California, Berkeley, Jan. 1973.

64. Somerton, W.H., "Thermal Properties of Partially Liquid-Saturated Rocks at Elevated Temperatures and Pressures," Final Report, A.P.I. Research Project No. 155, University of California, Berkeley, Mar. 1975.

65. Spillette, A.G., "Heat Transfer During Hot Fluid Injection into an Oil Reservoir," Journal of Canadian Petroleum Technology, 1965, P.213.

66. Squier, D.P. Smith, D.D., and Dougherty, E.L., "Calculated Temperature Behavior of Hot-Water Injection Wells" Journal of Petroleum Technology, April 1962, P. 436.

67. Thomas, G.W., Principles of Hydrocarbon Reservoir Simulation, Tapir, Norway, 1977.

68. Tien, C.L., Lienhard, J.H., Statistical Thermodynamics, Holt, Rinehart and Winston, New York, 1971.

69. Tikhomirov, V.M., "The Thermal Conductivity of Rocks and Its relationship to Density, Moisture Content, and Temperature," Neftianve Khoziaistvo (in Russian) Vol.46 1968, P.36.

70. Van der Held, E.F.M., and Van Drumen, T.G., "A Method of Measuring the Thermal Conductivity of Liquids," Physica, Vol.15, 1949,P.865.

71. Willhite, G.P., "Overall Heat Transfer Coefficients in Steam and Hot Water Injection Wells," Journal of Petroleum Technology, May 1967, P. 607.

APPENDIX A

FINITE DIFFERENCE REPRESENTATION OF THE GOVERNING EQUATIONS AND ALTERNATING DIRECTION METHOD

In this appendix the development of the finite difference approximations to the governing equations and the numerical scheme used to solve these equations will be discussed.

Partial derivatives can be approximated by finite differences in many ways. All such approximations introduce errors, called truncation errors, whose presence will be signified by employing the asymptotic 0 notation. Let the point $P_{i,j}$ form a discrete approximation for domain D with spacings Δz and Δr. A simple approximation for $\partial T/\partial z\big|_{i,j}$ will be developed, where the notation $T_{i,j} = T(i\Delta z, j\Delta r)$ will be employed for the discrete approximation.

Development of the Taylor series for $T(z-\Delta z)$ about z gives

$$T(z - \Delta z) = T(z) - \frac{\partial T}{\partial z}(\Delta z) + \frac{1}{2!}\frac{\partial^2 T}{\partial z^2} - 0\left[(\Delta z)^3\right], \qquad \text{(A-1)}$$

where all derivatives are evaluated at (z). Upon division by Δz one finds the relation

$$\frac{\partial T}{\partial z}\Big|_{i,j} = \frac{1}{\Delta z}\left[T_i - T_{i-1}\right] + 0[\Delta z] \qquad \text{(A-2)}$$

which, upon suppression of the truncation error, yields a backward difference approximation of first order in truncation error.

As an alternative to the backward difference approximation, a forward difference is obtained in similar fashion:

$$T(z + \Delta z) = T(z) + \frac{\partial T}{\partial z}(\Delta z) + \frac{1}{2!}\frac{\partial^2 T}{\partial z^2}(\Delta z)^2 + 0\left[(\Delta z)^3\right] . \qquad (A-3)$$

Division by Δz results in the relation:

$$\left.\frac{\partial T}{\partial z}\right|_{i,j} = \frac{1}{\Delta z}(T_{i+1} - T_i) + 0\left[\Delta z\right] . \qquad (A-4)$$

Approximation for the second derivatives are obtainable from the Taylor series of Equations (A-1) and (A-3). Addition of Equations (A-1) and (A-3) results in

$$\left(\frac{1}{\Delta z^2}\right)\left\{T(z + \Delta z) - 2T(z) + T(z - \Delta z)\right\} = \frac{\partial^2 T}{\partial z^2} + 0\left[(\Delta z)^2\right] . \qquad (A-5)$$

In index notation one would write

$$\left.\frac{\partial^2 T}{\partial z^2}\right|_{i,j} = \frac{T_{i+1,j} - 2T_{i,j} + T_{i-1,j}}{(\Delta z^2)} - 0\left[(\Delta z)^2\right] . \qquad (A-6)$$

Equation (A-6) has a second order truncation error.

In a completely similar way, the corresponding first order and second order partial derivatives in cylindrical coordinates are obtained in the forms:

$$\frac{\partial T}{\partial r} = \frac{T(r+\Delta r) - T(r-\Delta r)}{2\Delta r} - 0[(\Delta r)^2] \quad . \tag{A-7}$$

$$\frac{\partial^2 T}{\partial r^2} = \frac{T(r+\Delta r) - 2T(r) + T(r-\Delta r)}{(\Delta r)^2} + 0\ [(\Delta r)^2] \tag{A-8}$$

Or

$$\left.\frac{\partial T}{\partial r}\right|_{i,j} = \frac{T_{i,j+1} - T_{i,j-1}}{2\Delta r} + 0\ [(\Delta r)^2] \quad . \tag{A-9}$$

$$\left.\frac{\partial^2 T}{\partial r^2}\right|_{i,j} = \frac{T_{i,j+1} - 2T_{i,j} + T_{i,j-1}}{(\Delta r)^2} + \quad 0\ [(\Delta r)^2] \quad . \tag{A-10}$$

Having developed the basic finite difference approximation for the first and second order partial derivatives, it remains to derive the finite difference representation of the governing equations. The governing equation for the transient, one dimensional heat convection in a vertical cylinder with heat lost through the wall of the cylinder by conduction has the form:

$$\rho c \pi r_w^2\ u\frac{\partial T}{\partial z} + \rho c \pi r_w^2 \frac{\partial T}{\partial t} = 2\pi r_w \lambda \left.\frac{\partial \theta}{\partial r}\right|_{r_w} \quad . \tag{A-11}$$

The term $2\pi r_w \lambda \left.\frac{\partial \theta}{\partial r}\right|_{r_w}$ represents heat lost from the fluid inside the cylinder to the surroundings, per unit depth, and can be expressed as

$$2\pi r_w \lambda \left.\frac{\partial \theta}{\partial r}\right|_{r_w} = 2\pi r_w^2\ U_T\ (\theta_{r_w} - T) \quad . \tag{A-12}$$

Substitute (A-12) into Equation (A-11), and upon division by $\rho c \pi r_w^2$, Equation (A-11) has the form:

$$u \frac{\partial T}{\partial z} + \frac{\partial T}{\partial t} = \frac{2 U_T}{\rho c} \frac{(\theta|_{r_w} - T)}{r_w} \quad . \tag{A-13}$$

In finite difference from, Equation (A-13) is written as:

$$u(z) \frac{T(t + \Delta t, z) - T(t + \Delta t, z - \Delta z)}{\Delta z} + \frac{T(t + \Delta t, z) - T(t, z)}{\Delta t}$$

$$= \frac{2U_T}{\rho c} \frac{[\theta(t, 1, z) - T(t + \Delta t, z)]}{r_w} + 0[\Delta z] + 0\ [\Delta t] \quad . \tag{A-14}$$

In index notation it becomes

$$T_i^{n+1} - T_i^n = -U_i \left(\frac{\Delta t}{\Delta z}\right)\left(T_{i-1}^{n+1} - T_i^{n+1}\right) + \frac{2U_T \Delta t}{\rho c r_w}\left(\theta_{i,1}^n - T_i^{n+1}\right), \tag{A-15}$$

where superscript (n) represents the present time step and (n+1) represents the next time step.

Equation (A-15) is an approximation to the true partial differential equation (A-13) with a truncation error of the order (Δz) and (Δt). The solution of the algebraic Equation (A-15), with one unknown T_i^{n+1}, is straightforward.

The governing equation for the transient, two dimensional heat conduction bounded internally by a circular cylinder and for the case where thermal conductivity varies with the z coordinate, has the form:

$$\rho c\frac{\partial\theta}{\partial t} - \lambda(z)\frac{1\partial}{r\partial r}\left(r\frac{\partial\theta}{\partial r}\right) - \frac{\partial}{\partial z}\left(\lambda(z)\ \frac{\partial\theta}{\partial z}\right) = 0 \quad . \tag{A-16}$$

Upon division by ρc, Equation (A-16) can be cast in the form:

$$\frac{\partial\theta}{\partial t} - \alpha(z)\ \frac{1}{r}\frac{\partial}{\partial r}\left(r\ \frac{\partial\theta}{\partial r}\right) - \frac{\partial}{\partial z}\left[\alpha(z)\ \frac{\partial\theta}{\partial z}\right] = 0, \tag{A-17}$$

where $\alpha(z) = \lambda(z) / \rho c.$

Applying the finite difference approximation, implicit method, for the first order derivative in t and second order derivatives in r and z to Equation (A-17) yields:

$$\frac{\theta(t + \Delta t,r,z) - \theta(t,r,z)}{\Delta t} = \alpha(z)\ \frac{\theta(t + \Delta t,\ r + \Delta r,z) - \theta(t + \Delta t,\ r - \Delta r,z)}{2r(\Delta r)}$$

$$+ \alpha(z)\ \frac{\theta(t + \Delta t,\ r + \Delta r,z) - 2\theta(t + \Delta t,r,z) + \theta(t + \Delta t,\ r - \Delta r,z)}{(\Delta r^2)}$$

$$+ \frac{\alpha(z + \Delta z)\ \theta(t + \Delta t,r,z + \Delta z) - 2\alpha(z)\ \theta(t + \Delta t,r,z)}{(\Delta z)^2}$$

$$+ \frac{2\alpha(z - \Delta z)\ \theta(t + \Delta t,r,z - \Delta z)}{(\Delta z)^2}$$

$$+ 0\left[(\Delta r)^2\right] + 0\left[(\Delta z)^2\right] + \ 0\left[(\Delta t)^2\right] \quad . \tag{A-18}$$

In index form, Equation (A-18) can be simplified as:

$$\frac{\theta^{n+1}_{i,j} - \theta^{n}_{i,j}}{\Delta t} = \alpha_i \frac{\theta^{n+1}_{i,j+1} - \theta^{n+1}_{i,j-1}}{2r_j(\Delta r)} + \alpha_i \frac{\theta^{n+1}_{i,j+1} - 2\theta^{n+1}_{i.j} + \theta^{n+1}_{i,j-1}}{(\Delta r)^2}$$

$$+ \alpha_{i-1} \frac{\theta^{n+1}_{i+1,j} - 2\alpha_i \theta^{n+1}_{i,j} + \alpha_{i-1} \theta^{n+1}_{i-1,j}}{(\Delta z^2)} \quad . \tag{A-19}$$

This scheme is second order accurate in both time and space. In case of non-uniform grid variation in the radial direction the second and third terms in Equation (A-19), after a few algebraic manipulations, can be combined and expressed as follows:

$$\frac{1}{r}\frac{\partial \theta}{\partial r} + \frac{\partial^2 \theta}{\partial r^2} \simeq \frac{1}{r_{j+1} - r_{j-1}} \left(r_{j+\frac{1}{2}} \frac{\theta_{i,j+1} - \theta_{i,j}}{r_{j+1} - r_j} - r_{j-1/2} \frac{\theta_{i,j} - \theta_{i,j}}{r_j - r_{j-1}} \right) \tag{A-20}$$

where: $r_{j+1} = r_j + \alpha \Delta r$

$r_{j-1} = r_j - \beta \Delta r$

α, β are constants,

and

$$r_{j+1/2} = \frac{r_{j+1} + r_j}{2} \quad ,$$

$$r_{j-1/2} = \frac{r_j + r_{j-1}}{2} \quad .$$

By substituting (A-20) into Equation (A-19), the resulting equation has the form:

$$\frac{\theta^{n+1}_{i,j} - \theta^{n}_{i,j}}{\Delta t} - \frac{2\alpha_i}{r_{j+1} - r_{j-1}} \left\{ r_{j+1/2} \frac{\theta^{n+1}_{i,j+1} - \theta^{n+1}_{i,j}}{r_{j+1} - r_j} - r_{j-1/2} \frac{\theta^{n+1}_{i,j} - \theta^{n+1}_{i,j-1}}{r_j - r_{j-1}} \right\}$$

$$- \frac{\alpha_{i+1}\theta^{n+1}_{i+1,j} - 2\alpha_i\theta^{n+1}_{i,j} + \alpha_{i-1}\theta^{n+1}_{i-1,j}}{(\Delta z)^2} = 0 \quad . \tag{A-21}$$

This leads to a matrix problem of the type

$$\vec{A\theta} = \vec{d} \quad . \tag{A-22}$$

A is a pentadiagonal matrix and will be of order $N_z M_r$ which is very difficult to handle and time consuming. An alternative approach is the fractional step method of Peaceman and Rachford (1955) known as the Alternating Direction Implicit (ADI) method. The main idea is to consider a multi-dimensional problem as a collection of one-dimensional problems, each of which is solved over a fraction of a time step. The associated matrix problems are always tridiagonal, which are much easier to solve.

In this method, instead of using Equation (A-21), one of the coordinate direction is expressed implicitly leaving the other explicit and considering that time is advanced over half a time step. Then the roles of the implicit and explicit parts are interchanged to complete the time step. Thus, if the spatial derivative with respect to r is evaluated implicitly the resultant equation becomes:

$$\frac{\theta^{n+\frac{1}{2}}_{i,j}-\theta^{n}_{i,j}}{\frac{1}{2}\Delta t} - \frac{2\alpha_i}{r_{j+1}-r_{j-1}}\left[r_{j+\frac{1}{2}}\frac{\theta^{n+\frac{1}{2}}_{i,j+1}-\theta^{n+\frac{1}{2}}_{i,j}}{r_{j+1}-r_j} - r_{j-\frac{1}{2}}\frac{\theta^{n+\frac{1}{2}}_{i,j}-\theta^{n+\frac{1}{2}}_{i,j-1}}{r_j-r_{j-1}}\right]$$

$$-\frac{\alpha_{i+1}\theta^{n}_{i+1,j} - 2\alpha_i\theta^{n}_{i,j}+\alpha_{i-1}\theta^{n}_{i-1,j}}{(\Delta z)^2} = 0 \quad , \tag{A-23}$$

and

$$\frac{\theta^{n+1}_{i,j}-\theta^{n+\frac{1}{2}}_{i,j}}{\frac{1}{2}\Delta t} - \frac{2\alpha_i}{r_{j+1}-r_{j-1}}\left[r_{j+\frac{1}{2}}\frac{\theta^{n+\frac{1}{2}}_{i,j+1}-\theta^{n+\frac{1}{2}}_{i,j}}{r_{j+1}-r_j} - r_{j-\frac{1}{2}}\frac{\theta^{n+\frac{1}{2}}_{i,j}-\theta^{n+\frac{1}{2}}_{i,j-1}}{r_j-r_{j-1}}\right]$$

$$-\frac{\alpha_{i+1}\theta^{n+1}_{i+1,j} -2\alpha_i\theta^{n+1}_{i,j} + \alpha_{i-1}\theta^{n+1}_{i-1,j}}{(\Delta z)^2} = 0 \quad , \tag{A-24}$$

where the spatial derivative with respect to z is evaluated implicitly. Equations (A-23) and (A-24) lead to matrix problems of the form

$$\vec{\theta}^{n+\frac{1}{2}} = \vec{d}_z \quad , \tag{A-25}$$

and

$$V\vec{\theta}^{n+1} = \vec{d}_r \quad . \tag{A-26}$$

Each step is of first order accuracy and not unconditionally stable. However, the combined scheme is of second order accuracy and unconditionally stable. $\vec{d}_z$ contains all terms in (A-23) evaluated at time level n, while $\vec{d}_r$ contains those in (A-24) at time level n+1/2. Equations (A-25) and (A-26) are readily solved by the Gaussian elimination

technique known as the Thomas algorithm. Solution of (A-25) for $\vec{\theta}^{n+\frac{1}{2}}$ is used to evaluate $\vec{d}_r$ in Equation (A-26). Consequently, alternately solving (A-25) and (A-26) repeatedly enables one to advance the solution in time.

APPENDIX B

DETERMINATION OF THE WELLBORE FLUID TEMPERATURE DURING INJECTION OR PRODUCTION USING HEAT SOURCE CONCEPT

The governing equations for the system of wellbore fluid and formation, at any depth during injection or production, can be cast in the form

$$q' + \frac{M}{2}\frac{\partial T_D}{\partial t} = \lambda \left.\frac{\partial \theta_D}{\partial r}\right|_{r_w} , \tag{B-1}$$

$$\frac{\partial^2 \theta_D}{\partial r^2} + \frac{1}{r}\frac{\partial \theta}{\partial r} = -\frac{1}{\alpha(z)}\frac{\partial \theta_D}{\partial t} . \tag{B-2}$$

These equations are subject to the initial and boundary conditions:

$$T_D = \theta_D = 0 \quad , t = 0 \tag{B-3}$$

$$\lambda \frac{\partial \theta_D}{\partial r} = U_T (\theta_D - T_D) \quad , r = r_w \tag{B-4}$$

$$\theta_D \text{ is bounded as } r \to \infty \tag{B-5}$$

The following La Place transforms are introduced:

$$L(T_D) = \bar{T} = \int_o^\infty e^{-pt} T_D(t)\, dt = \bar{T}(p) , \tag{B-6}$$

$$L(\theta_D) = \bar{\theta} = \int_o^\infty e^{-pt}\theta_D(r,t)\,dt = \bar{\theta}(p,r) \quad , \tag{B-7}$$

where p is the transform variable.

La Place transformation of the differential equations and boundary conditions with respect to time results in the subsidiary equations and boundary conditions:

$$\frac{d^2\bar{\theta}}{dr^2} + \frac{1}{r}\frac{d\bar{\theta}}{dr} = \frac{1}{q^2}\,\theta \quad , \tag{B-8}$$

$$-\lambda\frac{d\bar{\theta}}{dr} = \frac{q'}{p} - \frac{Mp}{2}\bar{T} \quad , \; r=r_w \tag{B-9}$$

$$= U_T\,(\,\bar{\theta}-T\,) \quad , \; r=r_w \tag{B-10}$$

$$\bar{\theta} \text{ is bounded as } r \longrightarrow \infty \tag{B-11}$$

where $q^2 = \rho/\alpha$.

Solutions of Equations (B-8) and (B-9) subjected to Equations (B-10) and (B-11) give

$$\bar{T} = \frac{2r_w q\,\Delta}{p\,[r_w\rho\Delta + 2\lambda K_1(qr_w)]} \quad , \tag{B-12}$$

$$\bar{\theta} = \frac{2r_w q\,K_o(qr)}{p[r_w\rho\Delta + 2\lambda k_1(qr_w)]} \quad , \tag{B-13}$$

where, $\Delta = \frac{1}{qr_w}K_o(qr_w) + (\frac{\lambda}{r_w U_T})K_1(qr_w)$. (B-14)

$K_o(z)$, $K_1(z)$ are modified Bessel functions of the second kind and zero and first order, respectively.

From the Inversion Theorem of the La Place transformation $T_D(t)$ and $\theta_D(t,r)$ can be obtained by:

$$T_D(t) = \frac{1}{2\pi i}\int_{\gamma-i\infty}^{\gamma+i\infty} \bar{T}(p)e^{pt}dp, \tag{B-15}$$

$$\theta_D(t,r) = \frac{1}{2\pi i}\int_{\gamma-i\infty}^{\gamma+i\infty} \bar{\theta}(p,r)e^{pt}dp. \tag{B-16}$$

Exact evaluation of integrals in Equations (B-15) and (B-16) as real infinite integrals is straightforward. These solutions are quite complicated and unsuitable, however, for the present purpose, i.e., deduction of thermal conductivity and thermal diffusivity from a temperature time record, and an approximate solution for T is developed below.

If the time considered is large enough, as will be discussed later, the following method introduced by Carslaw and Jaeger [16] can be employed. The transform $\bar{T}$ is expanded formally in ascending powers of p and Equation (B-13) is evaluated term by term. Inserting the ascending series expansions for the modified Bessel functions in Equation (B-12) and simplifying, one obtains

$$\bar{T} \simeq \frac{-r_w q'}{2\lambda}\left[\frac{1}{p}\ln\left(\frac{\beta p}{w}\right) + \frac{r_w^2}{4\alpha}\left\{2\ln(\beta p) - \ln^2(\beta p) - 2\right\}\right.$$

$$\left. + \frac{r_w M}{4\lambda}\ln^2\left(\frac{\beta p}{w}\right) + 0(p)\right], \tag{B-17}$$

where $\beta = e^{2\gamma r_w^2/4\alpha}$; $1nw = 2\lambda/r_w U_T$

γ = is Euler's constant = 0.5722.

By integrating term by term on the Bromwich contour B_2 (Figure 36) using the following results,(Carslaw and Jaeger,[16]),

$$\frac{1}{2\pi i}\int_{Br_2} Ce^{pt}dp = 0 \quad , \tag{B-18}$$

$$\frac{1}{2\pi i}\int_{Br_2} \frac{1}{p} \ln(Cp) e^{pt} dp = -\left[\ln\left(\frac{t}{c}\right) + \gamma\right] \quad , \tag{B-19}$$

$$\frac{1}{2\pi i}\int_{Br_2} \ln(Cp) e^{pt} dp = -1/t \quad , \tag{B-20}$$

$$\frac{1}{2\pi i}\int_{Br_2} \ln^2(Cp) e^{pt} dp = \frac{2}{t}\ln\left[\frac{t}{c} + \gamma\right], \tag{B-21}$$

(where C is a real positive constant) one obtains

$$T(t) \simeq \frac{r_w q'}{2\lambda}\left[\ln 4\left(\frac{\alpha t}{r_w^2}\right) - \gamma + \frac{2\lambda}{U_T r_w} + \frac{1}{\left(\frac{2\alpha t}{r_w^2}\right)}\left\{\ln 4\left(\frac{\alpha t}{r_w^2}\right) - \gamma + 1.0 - \frac{(\rho c)_w}{2(\rho c)}\left[\ln 4\left(\frac{\alpha t}{r_w^2}\right) - \frac{2\lambda}{U_T r_w}\right]\right\}\right] + 0\left(\frac{1}{t^2}\right) . \tag{B-22}$$

Rigorous mathematical justification of the formal process described above has not yet been made. However, for typical rock, with a wellbore of suitable size, a few hours must elapse before the term of $0(1./\alpha t/r_w^2)$ can be neglected without introducing appreciable error;

on the other hand, if the term of $O(1./\alpha t/r_w^2)$ is included, a relatively small minimum $(\alpha t/r_w^2)$ can be tolerated (Blackwell, [11]; Murphy, et. al., [50]).

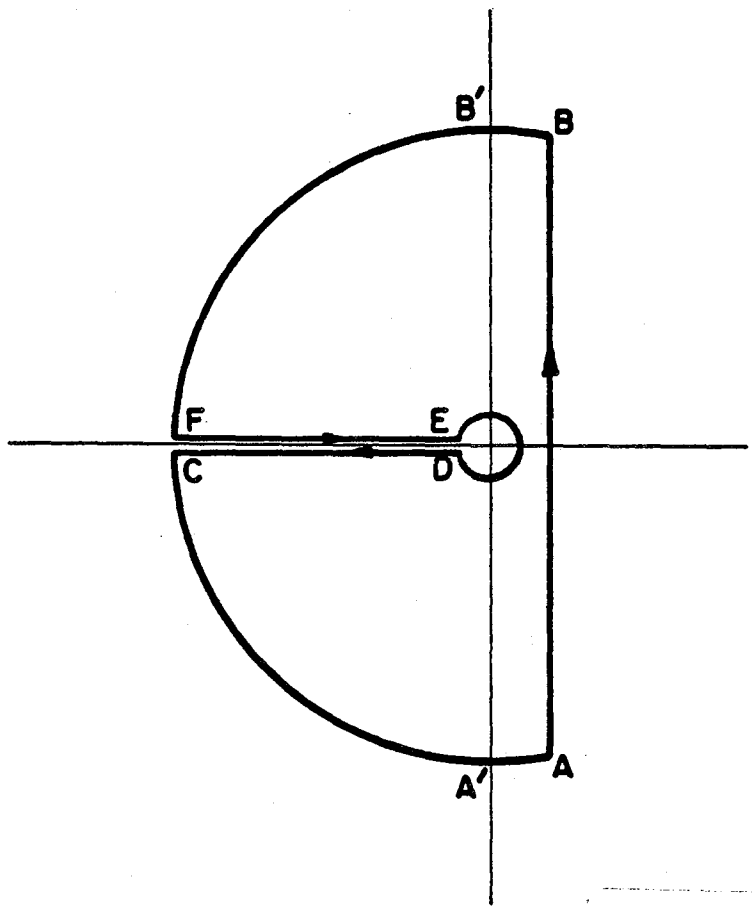

XBL 819-7425

FIG. 36 BROMWICH CONTOUR (Br_2)

APPENDIX C

LISTING OF COMPUTER PROGRAMS

```
C*****P R O G R A M   T E M P 1 *****
      PROGRAM TEMP1(FILM,INPUT,OUTPUT,TAPE6=OUTPUT,TAPE5=INPUT,TAPE7,
     1PUNCH)
C**********************************************************************
C     I N J E C T I O N/P R O D U C T I O N   W E L L   P R O B L E M
C     PROGRAM USED FOR CALCULATING TEMPERATURES OF THE FLUID AND THE
C     SURROUNDING FORMATION DURING INJECTION/PRODUCTION.
C**********************************************************************
      DIMENSION T(200),T2(200),TRES(200,200),ALAMDA(200),ALPHA(200)
      DIMENSION HCOEF(200),RT(200),TEMP(200)
      DIMENSION A(200),B(200),C(200),D(200),              BETA(200)
      DIMENSION TME(1000),TEM(1000),YY(200)
      DIMENSION RHO(200),U(200)
      DIMENSION TINT(200)
      DIMENSION TINI(90,200)
      PI=3.14159
      INDEX=0
      JDEX=0
      MAX=20
      MAXR=10
      MAXRM=MAXR-1
      MAXM=MAX-1
      AK=1.2
      DNO=.25
      DN=0.1
      TIME=0.0
      DT=60.
C       SPECI Y CHARACTERISTICS
C**********************************
CCCCC THE VARIABLES ARE DEFINED.RW IS THE RADIUS OF THE WELL.ALENGH IS
C     THE LENGTH OF THE WELL.CP IS THE HEAT CAPACITY OF THE FLUID IN THE
C     WELL.ALPHA IS THE DIFFUSIVITY OF THE FORMATION
C     HCOEF IS THE HEAT TRANSFER COEFFICIENT FROM THE FLUID IN THE WELL
C     TO THE RESERVOIR
CCCCC ROCP IS THE DENSITY TIMES THE HEAT CAPACITY OF THE FLUID
      RW=.08
      ALENGH=1000.
      DX=ALENGH/MAX
      DXSQ=DX*DX
      DELT=4.0
      CV=4270.
      ROCPRE=2.35E6
      TINJEC=150.0
      UR=2.5
      FLOW=695./60.
      CONST=FLOW/(PI*RW*RW)
      A1=-.4716676E-3
      B1=.11421303
      C1=-2.996214
      D1=27.5958
      DO 1 I=1,4
    1 ALAMDA(I)=1.2
      ALAMDA(5)=2.0
      DO 2 I=6,9
    2 ALAMDA(I)=2.8
```

```
      ALAMDA(10)=2.3
      DO 3 I=11,14
    3 ALAMDA(I)=1.8
      ALAMDA(15)=2.7
      DO 4 I=16,20
    4 ALAMDA(I)=3.6
CCCCC INITIALILIZE TEMPERATURE
C     T2(I) IS THE NEW TEMPERATURE IN THE WELL,TINT IS THE INITIAL
C     TEMPERATURE,TRES(J,I) IS THE TEMPERATURE OF THE ROCK SURROUNDING
C     THE WELL,TINJEC IS THE INJECTION TEMPERATURE,(I=1 IS AT THE TOP,
CCCCC AND I=MAX IS AT THE BOTTOM OF THE WELL)
      TINT(1)=20.
      DO 6 I=2,MAX
    6 TINT(I)=TINT(I-1)+DELT/ALAMDA(I)
      DO 10 I=1,MAX
      T2(I)=TINT(I)
      DO 20 J=1,MAXR
   20 TRES(J,I)=TINT(I)
   10 CONTINUE
      T2(1)=TINJEC
CCCCC RADIAL GRID IN RESERVOIR
C     ****************************
C     THE VARIABLES AK,DN,DNO ARE CONSTANTS WHICH CAN BE VARIED TO
CCCCC GIVE THE DESIRED SPACING(DN=1./THE TOTAL NUMBER OF GRID POINTS)
      DO 30 I=1,MAXR
   30 RT(I)=3.*(AK**((I-1)*DN/DNO)-1.)/(AK**(1./DNO)-1.)+RW
      PRINT 31
   31 FORMAT(//,10X,'DIMENSION OF RADIAL GRIDS',//)
      PRINT 32,(RT(J),J=1,MAXR)
   32 FORMAT(4X,10E10.3)
      PRINT 499
  499 FORMAT(//,45X,'INITIAL TEMPERATURE DISTRIBUTION',//)
      DO 19 I=1,MAX
      PRINT 500,(T2(I),(TRES(J,I),J=1,MAXR))
   19 CONTINUE
  500 FORMAT(4X,11E10.3)
      DO 49 I=1,MAX
      ALPHA(I)=(5.0E-7)*ALAMDA(I)
      HCOEF(I)=UR
   49 CONTINUE
      TP=(T2(1)+273.)/1.E4
      VF=A1+B1*TP+C1*TP*TP+D1*TP**3.
      RHO(1)=1./VF
      U(1)=-CONST/RHO(1)
CCCCC REINITIALIZE TEMPERATURE,I,E. T(I) IS THE OLD TEMPERATURE WHICH
CCCCC IS SET EQUAL TO THE NEW TEMPERATURE
C     ******************************************
C     NEW TEMPERATURE OF THE FLUID IN THE WELL
C     ******************************************
   35 DO 40  I=1,MAX
      T(I)=T2(I)
   40 CONTINUE
      INDEX=INDEX+1
      TIME =TIME+DT
C  CC CALCULATE THE NEW TEMPERATURE IN THE WELL
```

```
      DO 50 I=2,MAX
      TP=(T(I)+273.)/1.E4
      VF=A1+B1*TP+C1*TP*TP+D1*TP**3.
      RHO(I)=1./VF
      U(I)=RHO(I-1)*U(I-1)/RHO(I)
      T2(I)=T(I)+DT*(-U(I)*(T(I-1)-T(I))/DX)+(HCOEF(I)*DT*(TRES(1,I)-T(I
     1))*2./RW)/(RHO(I)*CV)
   50 CONTINUE
C     ******************************************
C     TEMPERATURE OF THE SURROUNDING FORMATION
C     ******************************************
C      AT TIME LEVEL N+1/2
C     **********************
      DO 60 I=1,MAXM
      IP=I+1
      IM=I-1
      DO 70 J=2,MAXRM
      JP=J+1
      JM=J-1
      C(J)=-ALPHA(I)*(DT/2.)*(RT(JP)+RT(J))/(RT(J)*(RT(JP)-RT(JM))*(RT(
     1JP)-RT(J)))
      A(J)=-ALPHA(I)*(DT/2.)*(RT(J)+RT(JM))/(RT(J)*(RT(JP)-RT(JM))*(RT(
     1J)-RT(JM)))
      B(J)=1.-C(J)-A(J)
   70 CONTINUE
      ETA=ALPHA(I)*(DT/2.)*(RT(1)+RT(2))/(RT(1)*(RT(1)-RT(2))**2)
      B(1)=1.+DT*HCOEF(I)/((RT(2)-RT(1))*ROCPRE)+ETA
      C(1)=-ETA
      CALL AMATRX(A,B,C,BETA,MAXRM,1)
      DO 80 J=1,MAXRM
      IF(I.NE.1)GO TO 8
      D(J)=TRES(J,1)*(1.-ALPHA(1)*DT/DXSQ)+(TRES(J,2)+TINT(1))*(ALPHA(1)
     1*(DT/2.)/DXSQ)
      GO TO 80
    8 D(J)=TRES(J,I)*(1.-ALPHA(I)*  DT   /DXSQ)+(TRES(J,IP)+TRES(J,IM))*
     1(ALPHA(I)*(DT/2.)/DXSQ)
   80 CONTINUE
      D(1)=D(1)+DT*HCOEF(I)*T2(I)/(ROCPRE*(RT(2)-RT(1)))
      D(MAXRM)=D(MAXRM)+(DT/2.)*ALPHA(I)*TRES(MAXR,I)*(RT(MAXR)+RT(MAXRM
     1))/(RT(MAXRM)*(RT(MAXR)-RT(MAXR-2))*(RT(MAXR)-RT(MAXRM)))
      CALL TRIDI(D,TEMP,A,C,BETA,MAXRM,1)
      DO 75 J=1,MAXRM
   75 TRES(J,I)=TEMP(J)
   60 CONTINUE
C      AT TIME LEVEL N+1
C     ********************
      DO 90 J=1,MAXRM
      JP=J+1
      JM=J-1
      DO 100 I=2,MAXM
      IP=I+1
      IM=I-1
      C(I)=-ALPHA(I)*(DT/2.)/DXSQ
      A(I)=C(I)
      B(I)=1.-2.*C(I)
```

```
  100 CONTINUE
      C(1)=-ALPHA(1)*(DT/2.)/DXSQ
      B(1)=1.-2.*C(1)
      CALL AMATRX(A,B,C,BETA,MAXM,1)
      DO 105 I=1,MAXM
      IF(J.NE.1)GO TO 11
      EI=ALPHA(I)*(DT/2.)*(RT(2)+RT(1))/(RT(1)*(RT(1)-RT(2))**2)
      D(I)=TRES(1,I)*(1.-EI-DT*HCOEF(I)/((RT(2)-RT(1))*ROCPRE))+DT*HCOEF
     1(I)*T2(I)/((RT(2)-RT(1))*ROCPRE)+TRES(2,I)*EI
      GO TO 105
   11 EI=ALPHA(I)*(DT/2.)*(RT(JP)+RT(J))/(RT(J)*(RT(JP)-RT(JM))*(RT(JP)-
     1RT(J)))
      FI=ALPHA(I)*(DT/2.)*(RT(J)+RT(JM))/(RT(J)*(RT(JP)-RT(JM))*(RT(J)-
     1RT(JM)))
      D(I)=TRES(J,I)*(1.-EI-FI)+TRES(JP,I)*EI+TRES(JM,I)*FI
  105 CONTINUE
      D(1)=D(1)+(DT/2.)*ALPHA(1)*TINT(1)/DXSQ
      D(MAXM)=D(MAXM)+(DT/2.)*ALPHA(MAXM)*TRES(J,MAX)/DXSQ
      CALL TRIDI(D,TEMP,A,C,BETA,MAXM,1)
      DO 110 I=1,MAXM
  110 TRES(J,I)=TEMP(I)
   90 CONTINUE
C     ********************
C     RESULTS PRINT OUT
C     ********************
      IF((TIME/60.).GE.1440.) GO TO 101
      IF(INDEX.LT.10) GO TO 101
      IF(INDEX.GT.1000) GO TO 97
      IF(INDEX.EQ.(INDEX/60)*60) GO TO 101
   97 IF(INDEX.EQ.(INDEX/900)*900)GO TO 101
      GO TO 35
  101 CONTINUE
      TIME3=TIME/60.
      PRINT 102,TIME3
  102 FORMAT(//,4X,*FOR TIME OF*,F10.3,4X,*MINUTES*//)
      PRINT 103
  103 FORMAT(//,1X,*WELLBORE TEMPERATURE*,30X,*RESERVOIR TEMPERATURE*,/
     1/)
      DO 120 I=1,MAX
      PRINT 1000,(T2(I),(TRES(J,I),J=1,MAXR))
      JDEX=JDEX+1
      TME(JDEX)=TIME3
      TEM(JDEX)=T2(MAX)
  120 CONTINUE
 1000 FORMAT(11F10.3)
      IF((TIME/60.).GE.1440.) GO TO 200
      GO TO 35
  200 CONTINUE
      WRITE(7,1001)((TRES(I,J),I=1,MAXR),J=1,MAX),(T2(I),I=1,MAX)
 1001 FORMAT(11F10.3)
      DO 600 I=1,MAX
      TINT(I)=T2(I)
      DO 700 J=1,MAXR
  700 TINI(J,I)=TRES(J,I)
  600 CONTINUE
```

```
      PRINT 650,(TINT(I),I=1,MAX)
      PUNCH 650,(TINT(I),I=1,MAX)
  650 FORMAT(10F8.3)
      PRINT 750,((TINI(J,I),J=1,MAXR),I=1,MAX)
      PUNCH 750,((TINI(J,I),J=1,MAXR),I=1,MAX)
  750 FORMAT(10F8.3)
      STOP
      END
```

```
C   **S U B R O U T I N E   A M A T R X **
C     SUBROUTINE USED FOR SETTING UP TRIDIAGONAL MATRIX.
C*********************************************************************
      SUBROUTINE AMATRX(A,B,C,BETA,MAX,ISTART)
      DIMENSION A(MAX),B(MAX),C(MAX),BETA(MAX)
      J=ISTART
      BETA(J)=B(ISTART)
      J=J+1
      DO 1 I=J,MAX
    1 BETA(I)=B(I)-(A(I)*C(I-1))/BETA(I-1)
      BETA(MAX)=B(MAX)-A(MAX)*C(MAX-1)/BETA(MAX-1)
      RETURN
      END
C   **S U B R O U R I N E   T R I D I**
C     SUBROUTINE USED FOR SOLVING TRIDIAGONAL MATRIX.
C*********************************************************************
      SUBROUTINE TRIDI(D,PT,A,C,BETA,MAX,ISTART)
      DIMENSION D(MAX),PT(MAX),A(MAX),C(MAX),BETA(MAX),GAMMA(200)
      J=ISTART
      GAMMA(J)=D(J)/BETA(J)
      J=J+1
      DO 1 I=J,MAX
      GAMMA(I)=(D(I)-A(I)*GAMMA(I-1))/BETA(I)
    1 CONTINUE
      I=MAX
      PT(I)=GAMMA(I)
    2 I=I-1
      PT(I)=GAMMA(I)-C(I)*PT(I+1)/BETA(I)
      IF(I.GT.ISTART) GO TO 2
      RETURN
      END
```

```
C*****P R O G R A M   T E M P 2 *****
      PROGRAM TEMP2(INPUT,OUTPUT)
C**********************************************************************
C              S H U T - I N   W E L L   P R O B L E M
C     PROGRAM USED FOR CALCULATING TEMPERATURES OF THE FLUID AND THE
C     FORMATION DURING SHUT-IN.
C**********************************************************************
      DIMENSION TW(30,200),TRES(30,200),TINI(30,200),TINT(200)
      DIMENSION ALAMDA(200),ALPHA(200),TEMP(200)
      DIMENSION A(200),B(200),C(200),D(200),BETA(200)
      DIMENSION R(200),RT(200)
      INDEX=0
      MAX=20
      MAXR=10
      MX=20
      MR=6
      MAXM=MAX-1
      MAXRM=MAXR-1
      MXM=MX-1
      MRM=MR-1
      AK=1.2
      DN0=0.25
      DN=0.1
      TO=20.
      TIME=0.
      DT=240.
C     SPECIFY CHARACTERISTICS
C************************************
CCCCC RW IS THE RADIUS OF THE WELL, ALENGH IS THE LENGTH OF THE WELL
C     ROCP IS THE DENSITY TIMES THE HEAT CAPACITY OF THE FLUID,KAPA IS
C     THE FLUID DIFFUSIVITY, H IS THE HEAT TRANSFER COEFFICIENT FROM
C     THE FLUID TO AMBIENT.
C     ALPHA(I) IS THE FORMATION DIFFUSIVITY, HCOEF IS THE HEAT TRANSFER
CCCCC COEFFICIENT FROM THE FLUID TO THE FORMATION.
      RW=0.08
      ALENGH=1000.
      DX=ALENGH/MAX
      DXSQ=DX*DX
      ROCP=2.35E6
      H=5.0
      HCOEF=25.
      AKAPA=6.0E-8
      DO 1 I=1,4
    1 ALAMDA(I)=1.2
      ALAMDA(5)=2.0
      DO 2 I=6,9
    2 ALAMDA(I)=2.8
      ALAMDA(10)=2.3
      DO 3 I=11,14
    3 ALAMDA(I)=1.8
      ALAMDA(15)=2.7
      DO 4 I=16,20
    4 ALAMDA(I)=3.6
      DO 11 I=1,MAX
   11 ALPHA(I)=(5.0E-7)*ALAMDA(I)
```

```
C     RADIAL GRID SYSTEMS
C    **********************
CCCCC FORMATION
      DO 20 J=1,MAXR
   20 RT(J)=3.*(AK**((J-1)*DN/DNO)-1.)/(AK**(1./DNO)-1.)+RW*1.2
      PRINT 21
   21 FORMAT(//,15X,*DIMENSION OF THE RADIAL GRIDS IN THE FORMATION*,
     1////)
      PRINT 22,(RT(J),J=1,MAXR)
   22 FORMAT(4X,10F12.5)
CCCCC WELLBORE
      R(1)=.3*RW
      R(2)=.55*RW
      R(3)=.75*RW
      R(4)=.85*RW
      R(5)=.93*RW
      R(6)=.99*RW
      PRINT 24
   24 FORMAT(//,15X,*DIMENSION OF THE RADIAL GRIDS IN THE WELLBORE*,////
     1)
      PRINT 25,(R(J),J=1,MR)
   25 FORMAT(4X,6F12.5)
C     INITIALIZE TEMPERATURES
C    *************************
CCCC* TW(J,I) IS THE NEW TEMPERATURE IN THE WELL,TINT(I) IS THE FLUID
C     TEMPERATURE AT THE END OF THE INJECTION PERIOD(I=1 IS AT THE TOP
C     ,AND I=MAX AT THE BOTTOM OF THE WELL)
C     TRES(J,I) IS THE TEMPERATURE OF THE SURROUNDING FORMATION.
CCCCC TINI(J,I) IS THE FORMATION TEMPERATURE JUST AFTER SHUT-IN.
      READ 45,(TINT(I),I=1,MX)
   45 FORMAT(10F8.3)
      READ 46,((TINI(J,I),J=1,MAXR),I=1,MAX)
   46 FORMAT(10F8.3)
      DO 47 I=1,MX
      DO 48 J=1,MR
   48 TW(J,I)=TINT(I)
   47 CONTINUE
      DO 49 I=1,MAX
      DO 44 J=1,MAXR
   44 TRES(J,I)= TINI(J,I)
   49 CONTINUE
      PRINT 410
  410 FORMAT(//,20X,*INITIAL FLUID TEMPERATURE DISTRIBUTION*,////)
      PRINT 415,((TW(J,I),J=1,MR),I=1,MX)
  415 FORMAT(4X,6F12.5)
      PRINT 420
  420 FORMAT(//,40X,*INITIAL FORMATION TEMPERATURE DISTRIBUTION*,////)
      PRINT 425,((TRES(J,I),J=1,MAXR),I=1,MAX)
  425 FORMAT(4X,10F12.5)
   35 INDEX=INDEX+1
      TIME=TIME+DT
C    ***************************************
C     TEMPERATURE OF THE FLUID IN THE WELL
C    ***************************************
C      AT TIME LEVEL N+1/2
```

```
C     ********************
      DO 50 I=1,MXM
      IP=I+1
      IM=I-1
      DO 51 J=2,MRM
      JP=J+1
      JM=J-1
      IF(J.GT.4) GO TO 510
      C(J)=-3.*AKAPA*(DT/2.)*(R(JP)+R(J))/(R(J)*(R(JP)-R(JM))*(R(JP)-R(J
     1)))
      A(J)=-3.*AKAPA*(DT/2.)*(R(J)+R(JM))/(R(J)*(R(JP)-R(JM))*(R(J)-R(JM
     1)))
      GO TO 511
  510 C(J)=-AKAPA*(DT/3.)*(R(JP)+R(J))/(R(J)*(R(JP)-R(JM))*(R(JP)-R(J)))
      A(J)=-AKAPA*(DT/6.)*(R(J)+R(JM))/(R(J)*(R(JP)-R(JM))*(R(J)-R(JM)))
  511 B(J)=1.-A(J)-C(J)
   51 CONTINUE
      A(1)=0.
      C(1)=-3.*AKAPA*(DT/4.)*(R(1)+R(2))/(R(1)*(R(1)-R(2))**2)
      B(1)=1.-C(1)
      ETA=AKAPA*(DT/6.)*(R(MR)+R(MRM))/(R(MR)*(R(MR)-R(MRM))**2)
      B(MR)=1.+(DT/2.)*HCOEF*2./((R(MR)-R(MRM))*ROCP)+ETA
      A(MR)=-ETA
      CALL AMATRX(A,B,C,BETA,MR,1)
      DO 52 J=1,MR
      IF(J.GT.2) GO TO 533
      IF(I.NE.1) GO TO 53
      D(J)=(1.-AKAPA*(DT/2.)/DXSQ-(DT/2.)*H/(DX*ROCP))*TW(J,1)+(AKAPA*(
     1DT/2.)/DXSQ)*TW(J,2)+((DT/2.)*H/(DX*ROCP))*TO
      GO TO 52
   53 D(J)=(1.-2.*(DT/2.)*AKAPA/DXSQ)*TW(J,I)+ (AKAPA*(DT/2.)/DXSQ)*
     1(TW(J,IP)+TW(J,IM))
      GO TO 52
  533 IF(I.NE.1) GO TO 534
      D(J)=(1.-3.*AKAPA*(DT/4.)/DXSQ-(DT/2.)*H/(DX*ROCP))*TW(J,1)+(3.*
     1AKAPA*(DT/4.)/DXSQ)*TW(J,2)+((DT/2.)*H/(DX*ROCP))*TO
      GO TO 52
  534 D(J)=(1.-2.*(DT/4.)*3.*AKAPA/DXSQ)*TW(J,I)+(3.*AKAPA*(DT/4.)/DXSQ)
     1*(TW (J,IP)+TW(J,IM))
   52 CONTINUE
      D(MR)=D(MR)+DT*HCOEF*TRES(1,I)/((R(MR)-R(MRM))*ROCP)
      CALL TRIDI(D,TEMP,A,C,BETA,MR,1)
      DO 54 J=1,MR
   54 TW(J,I)=TEMP(J)
   50 CONTINUE
C       AT TIME LEVEL N+1
C     ********************
      DO 60 J=1,MR
      JP=J+1
      JM=J-1
      DO 61 I=1,MXM
      IP=I+1
      IM=I-1
      IF(J.GT.2) GO TO 600
      C(I)=-AKAPA*(DT/2.)/DXSQ
```

```
      GO TO 601
  600 C(I)=-AKAPA*3.*(DT/4.)/DXSQ
  601 A(I)=C(I)
      B(I)=1.-2.*C(I)
   61 CONTINUE
      B(1)=B(1)+(DT/2.)*H/(DX*ROCP)
      CALL AMATRX(A,B,C,BETA,MXM,1)
      DO 62 I=1,MXM
      IF(J.EQ.1) GO TO 63
      IF(J.EQ.MR) GO TO 64
      IF(J.LT.5) GO TO 602
      EI=AKAPA*(DT/3.)*(R(JP)+R(J))/(R(J)*(R(JP)-R(JM))*(R(JP)-R(J)))
      FI=AKAPA*(DT/3.)*(R(J)+R(JM))/(R(J)*(R(JP)-R(JM))*(R(J)-R(JM)))
      GO TO 603
  602 EI=3.*AKAPA*(DT/4.)*(R(JP)+R(J))/(R(J)*(R(JP)-R(JM))*(R(JP)-R(J)))
      FI=3.*AKAPA*(DT/4.)*(R(J)+R(JM))/(R(J)*(R(JP)-R(JM))*(R(J)-R(JM)))
  603 D(I)=(1.-EI-FI)*TW(J,I)+TW(JP,I)*EI+TW(JM,I)*FI
      GO TO 62
   63 EI=3.*AKAPA*(DT/4.)*(R(2)+R(1))/(R(1)*(R(2)-R(1))**2)
      D(I)=(1.-EI)*TW(1,I)+TW(2,I)*EI
      GO TO 62
   64 EI=AKAPA*(DT/3.)*(R(MR)+R(MRM))/(R(MRM)*(R(MR)-R(MRM))**2)
      FI=(DT/2.)*HCOEF/((R(MR)-R(MRM))*ROCP)
      D(I)=(1.-EI-FI)*TW(MR,I)+TW(MRM,I)*EI+TRES(1,I)*FI
   62 CONTINUE
      D(1)=D(1)+(DT/2.)*H*TO/(DX*ROCP)
      D(MXM)=D(MXM)+AKAPA*(DT/2.)*TW(J,MX)/DXSQ
      CALL TRIDI(D,TEMP,A,C,BETA,MXM,1)
      DO 65 I=1,MXM
   65 TW(J,I)=TEMP(I)
      TW(J,MX)=1./2.*(TW(J,MX)+TRES(1,MAX))
   60 CONTINUE
C    ****************************************
C    TEMPERATURE OF THE SURROUNDING FORMATION
C    ****************************************
C      AT TIME LEVEL N+1/2
C     ********************
      DO 70 I=1,MAXM
      IP=I+1
      IM=I-1
      DO 71 J=2,MAXRM
      JP=J+1
      JM=J-1
      C(J)=-ALPHA(I)*(DT/2.)*(RT(JP)+RT(J))/(RT(J)*(RT(JP)-RT(JM))*(RT(
     1JP)-RT(J)))
      A(J)=-ALPHA(I)*(DT/2.)*(RT(J)+RT(JM))/(RT(J)*(RT(JP)-RT(JM))*(RT(
     1J)-RT(JM)))
      B(J)=1.-C(J)-A(J)
   71 CONTINUE
      ETA=ALPHA(I)*(DT/2.)*(RT(1)+RT(2))/(RT(1)*(RT(1)-RT(2))**2)
      B(1)=1.+DT*HCOEF    /((RT(2)-RT(1))*ROCP   )+ETA
      C(1)=-ETA
      CALL AMATRX(A,B,C,BETA,MAXRM,1)
      DO 72 J=1,MAXRM
      IF(I.NE.1) GO TO 73
```

```
      D(J)=TRES(J,1)*(1.-ALPHA(1)*DT/DXSQ)+(TRES(J,2)+TINI(J,1))*(ALPHA
     1(1)*(DT/2.)/DXSQ)
      GO TO 72
   73 D(J)=TRES(J,I)*(1.-ALPHA(I)* DT     /DXSQ)+(TRES(J,IP)+TRES(J,IM))*
     1(ALPHA(I)*(DT/2.)/DXSQ)
   72 CONTINUE
      D(1)=D(1)+DT*HCOEF*TW(MR,I)/(ROCP  *(RT(2)-RT(1)))
      D(MAXRM)=D(MAXRM)+(DT/2.)*ALPHA(I)*TRES(MAXR,I)*(RT(MAXR)+RT(MAXRM
     1))/(RT(MAXRM)*(RT(MAXR)-RT(MAXR-2))*(RT(MAXR)-RT(MAXRM)))
      CALL TRIDI(D,TEMP,A,C,BETA,MAXRM,1)
      DO 75 J=1,MAXRM
   75 TRES(J,I)=TEMP(J)
   70 CONTINUE
C       AT TIME LEVEL N+1
C      ********************
      DO 90 J=1,MAXRM
      JP=J+1
      JM=J-1
      DO 100 I=2,MAXM
      IP=I+1
      IM=I-1
      C(I)=-ALPHA(I)*(DT/2.)/DXSQ
      A(I)=C(I)
      B(I)=1.-2.*C(I)
  100 CONTINUE
      C(1)=-ALPHA(1)*(DT/2.)/DXSQ
      B(1)=1.-2.*C(1)
      CALL AMATRX(A,B,C,BETA,MAXM,1)
      DO 105 I=1,MAXM
      IF(J.NE.1) GO TO 83
      EI=ALPHA(I)*(DT/2.)*(RT(2)+RT(1))/(RT(1)*(RT(1)-RT(2))**2)
      D(I)=TRES(1,I)*(1.-EI-DT*HCOFF   /((RT(2)-RT(1))*ROCP  ))+DT*HCOEF
     1*TW(MR,I)/((RT(2)-RT(1))*ROCP  )+TRES(2,I)*EI
      GO TO 105
   83 EI=ALPHA(I)*(DT/2.)*(RT(JP)+RT(J))/(RT(J)*(RT(JP)-RT(JM))*(RT(JP)-
     1RT(J)))
      FI=ALPHA(I)*(DT/2.)*(RT(J)+RT(JM))/(RT(J)*(RT(JP)-RT(JM))*(RT(J)-
     1RT(JM)))
      D(I)=TRES(J,I)*(1.-EI-FI)+TRES(JP,I)*EI+TRES(JM,I)*FI
  105 CONTINUE
      D(1)=D(1)+(DT/2.)*ALPHA(1)*TINI(J,1)/DXSQ
      D(MAXM)=D(MAXM)+(DT/2.)*ALPHA(MAXM)*TRES(J,MAX)/DXSQ
      CALL TRIDI(D,TEMP,A,C,BETA,MAXM,1)
      DO 110 I=1,MAXM
  110 TRES(J,I)=TEMP(I)
   90 CONTINUE
C     ********************
C      RESULTS PRINT OUT
C     ********************
      IF((TIME/60.).GE.11520.) GO TO 101
      IF(INDEX.LT.10) GO TO 101
      IF(INDEX.GT.1000) GO TO 97
      IF(INDEX.EQ.(INDEX/60)*60) GO TO 101
   97 IF(INDEX.EQ.(INDEX/900)*900)GO TO 101
      GO TO 95
```

```
101 CONTINUE
    TIME3=TIME/60.
    PRINT 102,TIME3
102 FORMAT(///,4X,*FOR TIME OF*,F10.3,4X,*MINUTES*//)
    PRINT 103
103 FORMAT(///,20X,*WELLBORE FLUID TEMPERATURE*,//)
    PRINT 500,((TW(J,I),J=1,MR),I=1,MX)
500 FORMAT(4X,6F12.3)
    PRINT 104
104 FORMAT(///,40X,*FORMATION TEMPERATURE*,//)
    PRINT 501,((TRES(J,I),J=1,MAXR),I=1,MAX)
501 FORMAT(4X,10F12.3)
    IF((TIME/60.).GE.11520.) GO TO 200
    GO TO 35
200 CONTINUE
    STOP
    END
```

```
C   **S U B R O U T I N E   A M A T R X **
C     SUBROUTINE USED FOR SETTING UP TRIDIAGONAL MATRIX.
C*****************************************************************
      SUBROUTINE AMATRX(A,B,C,BETA,MAX,ISTART)
      DIMENSION A(MAX),B(MAX),C(MAX),BETA(MAX)
      J=ISTART
      BETA(J)=B(ISTART)
      J=J+1
      DO 1 I=J,MAX
    1 BETA(I)=B(I)-(A(I)*C(I-1))/BETA(I-1)
      BETA(MAX)=B(MAX)-A(MAX)*C(MAX-1)/BETA(MAX-1)
      RETURN
      END
C   **S U B R O U R I N E   T R I D I**
C     SUBROUTINE USED FOR SOLVING TRIDIAGONAL MATRIX.
C*****************************************************************
      SUBROUTINE TRIDI(D,PT,A,C,BETA,MAX,ISTART)
      DIMENSION D(MAX),PT(MAX),A(MAX),C(MAX),BETA(MAX),GAMMA(200)
      J=ISTART
      GAMMA(J)=D(J)/BETA(J)
      J=J+1
      DO 1 I=J,MAX
      GAMMA(I)=(D(I)-A(I)*GAMMA(I-1))/BETA(I)
    1 CONTINUE
      I=MAX
      PT(I)=GAMMA(I)
    2 I=I-1
      PT(I)=GAMMA(I)-C(I)*PT(I+1)/BETA(I)
      IF(I.GT.ISTART) GO TO 2
      RETURN
      END
```